

RECORD 2020/13

STRATIGRAPHY, PETROGRAPHY AND STRUCTURE OF ARCHAean ROCKS IN THE ROTHsay MINING AREA, WESTERN YILGARN CRATON

by

JJ Price, TG Blenkinsop, KM Goodenough and AC Kerr



Government of Western Australia
Department of Mines, Industry Regulation
and Safety

Geological Survey of
Western Australia





Government of **Western Australia**
Department of **Mines, Industry Regulation
and Safety**

RECORD 2020/13

STRATIGRAPHY, PETROGRAPHY AND STRUCTURE OF ARCHAEOAN ROCKS IN THE ROTHSAY MINING AREA, WESTERN YILGARN CRATON

by

JJ Price¹, TG Blenkinsop¹, KM Goodenough² and AC Kerr²

¹ School of Earth & Ocean Sciences, Cardiff University, CF10 3AT, United Kingdom

² British Geological Survey, The Lyell Centre, Edinburgh, EH14 4AP, United Kingdom

PERTH 2020



**Geological Survey of
Western Australia**

MINISTER FOR MINES AND PETROLEUM
Hon Bill Johnston MLA

DIRECTOR GENERAL, DEPARTMENT OF MINES, INDUSTRY REGULATION AND SAFETY
David Smith

EXECUTIVE DIRECTOR, GEOLOGICAL SURVEY AND RESOURCE STRATEGY
Jeff Haworth

REFERENCE

The recommended reference for this publication is:

Price, JJ, Blenkinsop, TG, Goodenough, KM and Kerr, AC 2020, Stratigraphy, petrography and structure of Archaean rocks in the Rothsay mining area, western Yilgarn Craton: Geological Survey of Western Australia, Record 2020/13, 109p.

ISBN 978-1-74168-905-1

ISSN 2204-4345

Grid references in this publication refer to the Geocentric Datum of Australia 1994 (GDA94). Locations mentioned in the text are referenced using Map Grid Australia (MGA) coordinates, Zone 50. All locations are quoted to at least the nearest 100 m.

About this publication

This Record is a chapter from a PhD thesis researched, written and compiled as part of a PhD project at the University of Cardiff, UK. The scientific content of the Record, and the drafting of figures, was the responsibility of the author. No editing has been undertaken by GSWA.

Disclaimer

This product was produced using information from various sources. The Department of Mines, Industry Regulation and Safety (DMIRS) and the State cannot guarantee the accuracy, currency or completeness of the information. Neither the department nor the State of Western Australia nor any employee or agent of the department shall be responsible or liable for any loss, damage or injury arising from the use of or reliance on any information, data or advice (including incomplete, out of date, incorrect, inaccurate or misleading information, data or advice) expressed or implied in, or coming from, this publication or incorporated into it by reference, by any person whatsoever.

Published 2020 by the Geological Survey of Western Australia

This Record is published in digital format (PDF) and is available online at <www.dmirswa.gov.au/GSWApublications>.



© State of Western Australia (Department of Mines, Industry Regulation and Safety) 2020

With the exception of the Western Australian Coat of Arms and other logos, and where otherwise noted, these data are provided under a Creative Commons Attribution 4.0 International Licence. (<http://creativecommons.org/licenses/by/4.0/legalcode>)

Further details of geoscience products are available from:

Information Centre

Department of Mines, Industry Regulation and Safety

100 Plain Street

EAST PERTH WESTERN AUSTRALIA 6004

Telephone: +61 8 9222 3459 Email: publications@dmirs.wa.gov.au

www.dmirswa.gov.au/GSWApublications

Cover image: Packing up the campsite in a claypan about 5 km south of Minilya in the southern Pilbara (photo by Olga Blay)

STRATIGRAPHY, PETROGRAPHY AND STRUCTURE OF ARCHAEOAN ROCKS IN THE ROTHSAY MINING AREA, WESTERN YILGARN CRATON

Contents

Abstract.....	1
1. Introduction.....	1
2. Geological Setting	3
3. Overview of Study Area.....	6
3.1 Location.....	6
3.2 Physiography	7
3.3 Previous Work	7
3.4 Geological Overview.....	9
3.5 Nomenclature	10
4. Geological Mapping.....	11
4.1 Mapping Methods.....	11
4.2 Geological Mapping Data	12
5. Stratigraphy	16
5.1 Supracrustal Rocks	18
5.1.1 <i>Macs Well Clastics</i>	18
5.1.2 <i>Two Peaks Volcanics</i>	21
5.1.3 <i>Beryl West Volcanics</i>	24
5.1.4 <i>Mulga Volcanics</i>	25
5.1.5 <i>Willowbank Clastics</i>	27
5.2 Mafic-Ultramafic Intrusive Rocks	29
5.2.1 <i>Mountain View Sill</i>	30
5.2.2 <i>Honeycomb Gabbro</i>	31
5.2.3 <i>Rothsay Sill</i>	31
5.2.4 <i>Gardner Sill</i>	33
5.2.5 <i>Damperwah Sill</i>	36
5.2.6 <i>Dolerite Dykes</i>	38
5.3 Felsic Intrusive Rocks.....	38
5.3.1 <i>Granite</i>	38
5.3.2 <i>Pegmatites</i>	38
5.4 Intrusive Relations.....	40
6. Petrography	42
6.1 Introduction	42
6.2 General Overview of Metamorphic Features	42
6.3 Chulaar Group	46
6.3.1 <i>Aphyric volcanic rocks</i>	46
6.3.2 <i>Porphyritic volcanic rocks</i>	47
6.3.3 <i>Variolitic volcanic rocks</i>	48
6.3.4 <i>Spinifex-textured rocks</i>	50
<i>Cumulate basal units</i>	50
<i>Random acicular pyroxene spinifex</i>	52
<i>Oriented acicular pyroxene spinifex</i>	53

<i>Random platy pyroxene spinifex</i>	54
6.3.5 <i>Banded felsic volcaniclastic rocks</i>	56
6.3.6 <i>Lapilli tuffs</i>	56
6.4 Willowbank Clastics	59
6.4.1 <i>Greywacke</i>	59
6.4.2 <i>Pebbly sandstone</i>	59
6.4.3 <i>Porphyroblastic mudstone</i>	60
6.4.4 <i>Felsic volcaniclastic rocks</i>	60
6.5 Warriedar Suite	61
6.5.1 <i>Cumulate ultramafic rocks</i>	61
6.5.2 <i>Pyroxenitic rocks</i>	62
6.5.3 <i>Gabbroic/doleritic rocks</i>	65
6.5.4 <i>Quartz dioritic rocks</i>	67
6.6 Summary of Petrographic Analysis	68
7. Structure	69
7.1 Introduction	69
7.2 Bedding and Way-Up Criteria	69
7.3 D ₁ Deformation	73
7.4 D ₂ Deformation	75
7.5 D ₃ Deformation	77
7.6 D ₄ Deformation	79
7.6.1 <i>Enchanted Shear Zone (ESZ)</i>	81
7.6.2 <i>Rothsay Shear Zone (RSZ)</i>	83
7.7 D ₅ Deformation	84
7.8 D ₆ Deformation	84
8. Discussion	85
8.1 Supracrustal History	85
8.2 Intrusion of Mafic-Ultramafic Sills	88
8.3 Intrusion of Felsic Rocks	89
8.4 Deformational History	90
8.4.1 <i>Layer-Parallel Shearing</i>	91
8.4.2 <i>Fold Superposition</i>	92
8.4.3 <i>Diapirism</i>	93
8.5 Structural Model	96
9. Synthesis	98
10. Authorship Contribution	99
11. Acknowledgements	99
12. References	100
Plate A: 1:25,000 Surface Bedrock Geology of the Rothsay Mining Area, Western Australia	104
Plate B: 1:25,000 Interpreted Bedrock Geology of the Rothsay Mining Area, Western Australia	105

Figures

1. Simplified geological map of the Yilgarn Craton	3
2. Simplified map of the interpreted bedrock geology of the central Yalgoo-Singleton greenstone belt	4
3. Topographic map of the southwestern Murchison Domain	6
4. 1:250,000 scale geological map of the Rothsay Fold area	8
5. Aerial satellite imagery of the study area showing the locations of map sheets used during geological mapping	10
6. Field photographs showing the classification of rock exposure used during geological mapping	11
7. Simplified geological map of the Rothsay area	13
8. Cross section along the fence line A-B-C, drawn at 1:25,000 scale.....	14
9. Cross section along the fence line D-E-F, drawn at 1:25,000 scale	14
10. Cross section along the fence line G-H, drawn at 1:25,000 scale	14
11. Stratigraphic column for rocks in the Rothsay area, drawn at 1:20,000 scale.....	15
12. Photographs of rocks comprising the lower Macs Well Clastics	16
13. Photographs of rocks comprising the upper Macs Well Clastics.....	17
14. Photographs of rocks comprising the Two Peaks Volcanics.....	20
15. Photographs of rocks comprising the Beryl West Volcanics	22
16. Photographs of rocks comprising the Mulga Volcanics	23
17. Photographs of rocks comprising the lower Willowbank Clastics.....	26
18. Photographs of rocks comprising the upper Willowbank Clastics	27
19. Photographs of rocks comprising the Mountain View Sill	29
20. Photographs of rocks from the Honeycomb Gabbro	31
21. Photographs of rocks comprising the Rothsay Sill	32
22. Photographs of rocks comprising the Gardner Sill	34
23. Photographs of quartz diorite from the Damperwah Sill	36
24. Photographs of rocks comprising granite and pegmatite dykes in the study area	37
25. Sketch map of creek section at locality 15.037, showing the contact relations between supracrustal rocks and concordant dolerite intrusive	39
26. Sketch geological map showing the distribution of pegmatite float and outcrop in the Rothsay area	40
27. Simplified geological map of the Rothsay area, showing the locations of petrographic samples	45
28. Photomicrographs of Chulaar Group aphyric volcanic rocks	45
29. Photomicrographs of Chulaar Group porphyritic volcanic rocks	47
30. Photomicrographs and element maps of variolitic rocks comprising the Mulga Volcanics.....	49
31. Photomicrographs of cumulate basal portions of spinifex-bearing volcanic units of the Mulga Volcanics	50
32. Photomicrographs of random acicular pyroxene spinifex-textured rocks of the Mulga Volcanics	51
33. Photomicrographs of oriented acicular pyroxene spinifex-textured rocks of the Mulga Volcanics	52
34. Photomicrographs of random platy pyroxene spinifex-textured rocks of the Chulaar Group	54
35. Photomicrographs of a banded felsic volcaniclastic unit from the Macs Well Clastics	55
36. Photomicrographs of lapilli-bearing tuff of the Mulga Volcanics.....	57
37. Photomicrographs of Willowbank Clastics metasedimentary and metavolcaniclastic rocks	58
38. Photomicrographs of Warriedar Suite ultramafic cumulate rocks, from comparable Warriedar Suite sills to the northeast of the Rothsay area.	61
39. Photomicrographs of Warriedar Suite pyroxenitic rocks	63
40. Photomicrographs of Warriedar Suite gabbroic rocks	64
41. Photomicrographs of Warriedar Suite leucogabbroic and quartz dioritic rocks	66
42. Simplified geological map of the study area showing representative bedding measurements and the locations and types of way-up indicators.....	70
43. Bedding orientations and way-up criteria in the Rothsay area	71
44. Map, stereonet and field photograph of S1 layer-parallel fabric	72
45. Photographs of outcrop-scale folding in the Rothsay area	74
46. Aeromagnetic map of the study area with different generations of folding symbolised	75
47. Map, stereonet and field photograph of S3 fabric	76
48. Foliated basalt outcrop comprising an S2 fabric overprinted by an S3 spaced cleavage	77

49. Aeromagnetic map of the study area, with all major faults and shears symbolised by type and mineral lineations symbolised	78
50. Photographs of outcrops with linear fabrics	78
51. Sketch map of outcropping ferruginous siltstone and BIF at locality 13.049	80
52. Stereonet showing foliation planes and lineations proximal to the Enchanted Shear Zone	81
53. Strongly foliated banded quartzite sampled close to the Enchanted Shear Zone (loc. 12.008).	81
54. Photographs of features observed along the Rothsay Shear Zone at locality 6.124	82
55. Schematic diagrams for the stratigraphic development of rocks in the Rothsay area	85
56. Aeromagnetic map of the study area outlining the potential location of layer-parallel shears.....	90
57. Schematic diagrams illustrating the structural development of the Rothsay Fold	94, 95

Tables

1. Stratigraphic nomenclature used in this study.....	9
2. Petrographic sample details, including co-ordinates, respective locality numbers from geological mapping, the assigned stratigraphic group/unit, mapped lithology and petrographic description.....	43, 44
3. Deformational framework for the Rothsay Fold area	70

Abbreviations

YSGB; Yalgoo-Singleton Greenstone Belt

BIF; Banded Iron Formation

ESZ; Enchanted Shear Zone

RSZ; Rothsay Shear Zone

STRATIGRAPHY, PETROGRAPHY AND STRUCTURE OF ARCHAEOAN ROCKS IN THE ROTHSAY MINING AREA, WESTERN YILGARN CRATON

J.J. Price¹, T.G. Blenkinsop¹, K.M. Goodenough², A.C. Kerr¹

¹School of Earth & Ocean Sciences, Cardiff University, CF10 3AT, United Kingdom

²British Geological Survey, The Lyell Centre, Edinburgh, EH14 4AP, United Kingdom

Abstract

Greenstone belts in the Archaean Yilgarn Craton of Western Australia have long been the subject of intense geological interest, especially because they host an array of world-class gold, Ni-Cu, base metal and iron ore deposits. However, some overlooked greenstone successions in the western parts of the Yilgarn Craton have seen limited geological investigation and remain poorly understood. This study presents detailed 1:25,000 scale geological mapping of the previously unmapped and reasonably well-exposed Rothsay Fold, situated in the southwestern Murchison Domain, western Yilgarn Craton. Lithological mapping has revealed that the geology of the Rothsay Fold area consists of a ~ 6.8 km-thick greenstone succession, divided into 4.2 km of supracrustal rocks and 2.6 km of mafic-ultramafic intrusive rocks. Supracrustal rocks document a cyclic progression from sedimentation and distal felsic volcanism, to extensive mafic-ultramafic volcanism, to further sedimentation and felsic volcanism. Mafic-ultramafic rocks can be divided into five distinct layered sills, several of which demonstrate along-strike lateral continuity of >20 km, and were intruded prior to deformation. There is no evidence of significant structural repetition of stratigraphy in the Rothsay area. A six-stage model is proposed to account for the structural development of the Rothsay area. An early episode of diapirism, resulting in the development of a domal structure and a layer-parallel fabric, was followed by two shortening episodes that refolded earlier structures and formed a pervasive, regionally-extensive fabric. Subsequent displacement along two major shear zones involved a significant reverse component and was associated with lode-gold mineralisation at the historically-exploited Rothsay Au deposit. The latest stages of deformation involved two faulting episodes, one of which was coeval with intrusion of granitoids and associated pegmatite dykes, which are locally Li- and B- bearing. Detailed geological mapping and a better understanding of the deformational history in the Rothsay area may assist and promote mineral exploration in an understudied, highly prospective corner of the Yilgarn Craton.

1. Introduction

Archaean greenstone belts in the Yilgarn Craton, Western Australia, occur primarily as north-south trending linear features, broadly parallel with craton-scale transpressional shear zones (Gee et al., 1981; Swager et al., 1990). However, strong linear patterns are not as prevalent in supracrustal belts in the far west of the craton. Instead, granite-greenstone contacts in the southwestern Murchison Domain display dome and keel patterns

that closely resemble the archetypal patterns of the eastern Pilbara Craton (Van Kranendonk et al. 2004). These patterns and associated folding within greenstone belts have been explained in terms of superposition of upright, orthogonal folds (Myers & Watkins, 1985; Watkins & Hickman, 1990) and more recently by diapiric emplacement of granitic domes (Zibra et al., 2018; Clos et al., 2019).

The greenstone stratigraphy comprising the supracrustal belts in the western Yilgarn Craton is also distinct from greenstone belts across the central and eastern parts of the craton. Rocks in the southwestern Murchison domain constitute many of the oldest basement rocks in the Yilgarn Craton (c. 2.95 Ga; Wang et al., 1998), some of the oldest metasedimentary successions (Van Kranendonk et al., 2013) and an array of mafic-ultramafic intrusions, including some of the largest on Earth (Ivanic et al., 2010; Ivanic, 2019). Despite these claims, the area has not historically received much scientific study, except for recent research in the northeastern Murchison Domain (e.g., Van Kranendonk et al., 2013; Smithies et al., 2018; Lowrey et al., 2020). As such, large sections of greenstone belts in the southwest Murchison Domain remain unstudied and unmapped, other than on a regional scale.

This study investigates the lithological and structural development of the Rothsay area; a portion of supracrustal rocks located in the southwest Yalgoo-Singleton greenstone belt that has been the focus of very little previous study. The Rothsay area is one of the best exposed parts of the southwestern Murchison Domain and hosts the historical Rothsay gold mine, the Karara Fe mine and several gold prospects. Regional mapping (Baxter & Lipple, 1985) has previously indicated that the area contains a complex fold structure, at least one significant shear zone and a relatively well exposed section through most of the supracrustal stratigraphy that comprises the greenstone belt. The first detailed 1:25,000 scale geological maps of a >130 km² area surrounding the Rothsay mining centre are presented in this study. Geological mapping is accompanied by cross sections of the interpreted bedrock geology and a stratigraphic column, in addition to lithological and petrographic descriptions of supracrustal rocks and mafic-ultramafic intrusive rocks comprising the stratigraphy at Rothsay. Structural observations, measurements and mapping reveal that rocks in the Rothsay area have been subjected to a complex, six stage deformational history, and indicate that diapirism played a crucial role during early deformation. This comprehensive study of a well-exposed portion of the understudied Yalgoo-Singleton greenstone belt may better inform mineral exploration in a highly prospective and hitherto overlooked portion of the Yilgarn Craton.

2. Geological Setting

The Yilgarn Craton of Western Australia is a vast portion of Archaean crust covering an area of approximately 1,000,000 km² (Ivanic et al., 2012). The craton consists of metavolcanic and metasedimentary supracrustal rocks, in addition to mafic-ultramafic and felsic intrusive rocks formed principally between 3.05 – 2.62 Ga, but with some components as old as ~3.7 Ga (Pidgeon & Wilde, 1990; Pidgeon and Hallberg, 2000). The Yilgarn Craton has been divided into seven distinct terranes (Fig. 1). The oldest Narryer Terrane in the northwest and the highly deformed South West Terrane bound the centrally-located Youanmi Terrane, whereas the Kalgoorlie, Kurnalpi, Burtville and Yamarna terranes in the east collectively constitute the Eastern Goldfields Superterrane (Cassidy et al., 2006; Fig. 1). The Youanmi Terrane is further subdivided into the Murchison Domain in the west and the Southern Cross Domain in the east, across the anastomosing Youanmi Shear Zone (Cassidy et al., 2006).

The Murchison Domain represents an Archaean granite-greenstone terrane, with elongate, north-northwest to north-northeast trending greenstone belts bound by vast swathes of felsic intrusive rocks (Watkins and Hickman, 1990) (Fig. 1). The rocks comprising greenstone belts in the Murchison Domain record a complex and protracted history, comprising 2960-2720 Ma supracrustal successions intruded by 2820-2720 Ma mafic-ultramafic intrusive complexes and 2820-2600 Ma granitic rocks (Van Kranendonk et al., 2013). The lower part of the greenstone stratigraphy (~2960-2750 Ma) is dominated by mafic-ultramafic volcanic rocks, interleaved with banded iron formation, volcaniclastic rocks and rare metasedimentary rocks, representing periods of volcanism alternating with interludes of tectonic and volcanic quiescence (Van Kranendonk et al., 2013; Zibra et al., 2018). In contrast, the uppermost part of the greenstone stratigraphy (~2740-2720 Ma) is dominated by clastic sedimentary rocks and felsic volcanic rocks, which rest upon a regional unconformity that documents uplift and erosion of the underlying supracrustal succession (Van Kranendonk et al., 2013). Extensive greenschist to amphibolite facies metamorphism has been experienced by rocks of the Murchison Domain and as a result, the original igneous mineralogy of volcanic and intrusive units is rarely preserved (Watkins & Hickman, 1990).

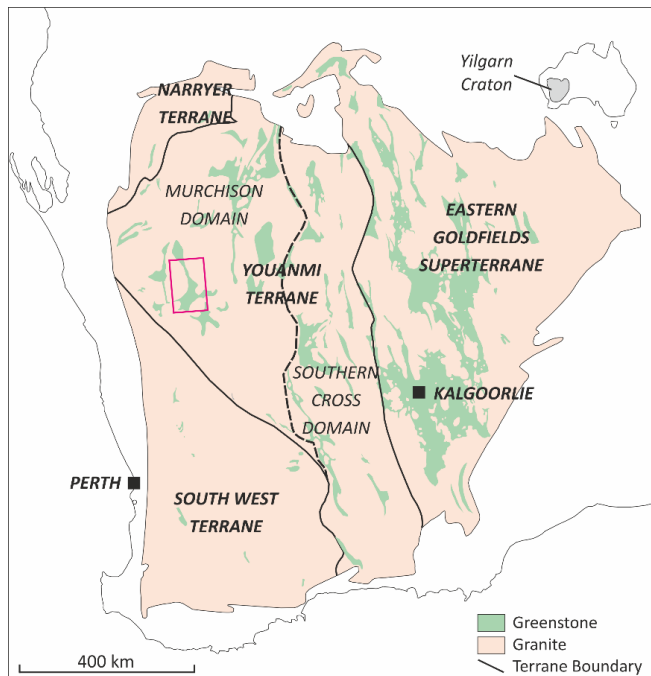


Figure 1: Simplified geological map of the Yilgarn Craton, Western Australia, outlining the distribution of greenstone belts and the location of the Rothsay study area.

Deformation in the Murchison Domain is largely heterogenous and consists of narrow zones of high strain dissecting more weakly deformed areas (Watkins & Hickman, 1990).

The Yalgoo-Singleton Greenstone Belt (YSGB) is a ~190 km, north-northwest trending, arcuate-shaped greenstone belt situated in the southwestern Murchison Domain (Fig. 1). The YSGB has been the focus of less academic study compared to the both the northeastern Murchison Domain and the eastern Yilgarn Craton, largely due to a lower endowment of discovered mineral resources, and the general scarcity of outcrop (< 5 %; Watkins & Hickman, 1990). For these reasons, the greenstone stratigraphy in the YSGB is not as well constrained as other parts of the Yilgarn Craton. Ongoing Geological Survey of Western Australia (GSPA) 1:100,000 scale regional geological mapping and associated geochronological analysis in the area is working to integrate the stratigraphy of the YSGB into the stratigraphic framework of the rest of the Murchison Domain.

The base of the exposed volcano-sedimentary succession in the YSGB is marked by a ~2.5 km thick package of felsic and intermediate volcanic and volcaniclastic rocks and minor chemical sedimentary rocks, ascribed to the ca. 2.95 Ga Gossan Hill Group (Van Kranendonk et al., 2013; Ivanic, 2019) (Fig. 2). Rocks equivalent to this group are thought to represent the basement to the greenstone succession across the Murchison Domain (Wang, 1998; Wang et al., 1998). Resting unconformably on these units is a thick <2820 Ma mafic-ultramafic volcanic package, interlayered with BIF and other interflow metasedimentary units (Watkins and Hickman, 1990). Recent mapping indicates that these units are likely equivalent to the Norie Group and/or Polelle Group rocks in the northeastern Murchison Domain (see Van Kranendonk et al., 2013), however, the extent of each of these groups is yet to be fully established. The lower greenstone succession is unconformably overlain by the Mougooderra Formation; an ~3km-thick upwards fining sequence of epiclastic sedimentary rocks including conglomerate, quartz arenite and shales, with minor chert, BIF, intermediate volcanic rocks and felsic volcaniclastic rocks (Ivanic, 2018; Watkins and Hickman, 1990). The age of the Mougooderra Formation is ambiguous, although it is inferred to be < 2746 Ma (Zibra et al., 2018; Ivanic, 2019).

The volcano-sedimentary succession underlying the Mougooderra Formation is intruded by a suite of thick mafic-ultramafic sills, occasionally in excess of ~1 km thickness, which are typically layered and comprise ultramafic basal cumulates, gabbroic centres and more highly evolved sill tops (Ivanic, 2018; Zibra et al., 2016). These sills are considered to be cogenetic and have been assigned to the intrusive Warriedar Suite (Ivanic, 2019). A further major mafic-ultramafic intrusion in the far east of the YSGB is represented by the Field's Find Igneous Complex (Fig. 2). The YSGB is surrounded by multiple generations of granitoid intrusions, many of which post-date major deformation in the belt ('post-tectonic granites'; Watkins & Hickman, 1990). However, recent structural studies of two coeval granitic intrusions in the belt, the Yalgoo Dome and Mt Mulgine Dome (Fig. 2), suggests that these intrusions were emplaced during a period of granitic diapirism (Zibra et al., 2018;

Zibra et al., 2020). The YSGB is primarily prospective for gold, in addition to base metals, W-Mo and iron ore, and is host to several major ore deposits; most notably the world-class Scuddles and Gossan Hill base-metal deposits at the Golden Grove mine, the Minjar shear-hosted lode-gold deposits and the Karara iron ore mine (Fig. 2).

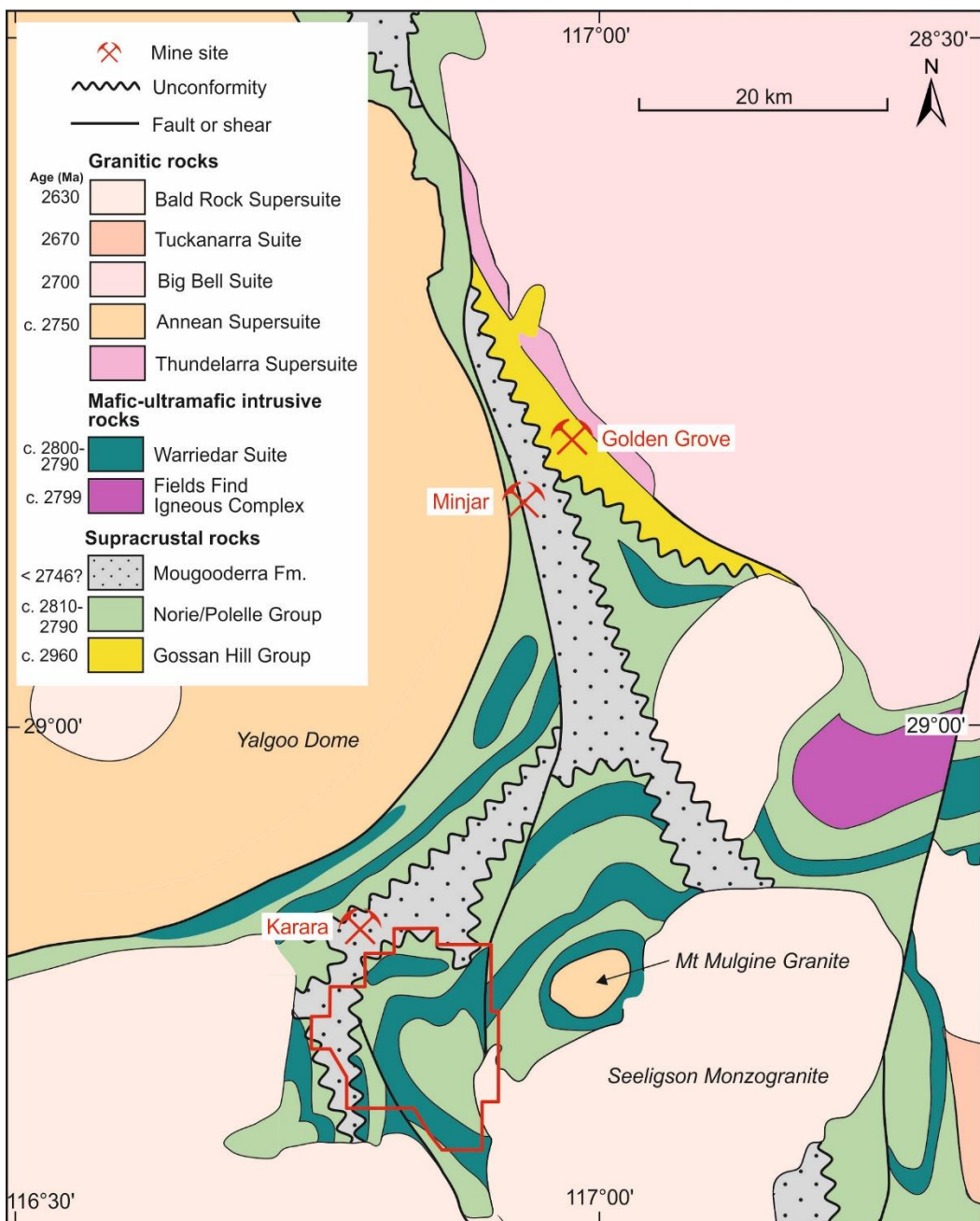


Figure 2: Simplified map of the interpreted bedrock geology of the central Yalgoo-Singleton greenstone belt, displaying named stratigraphic and magmatic units and major structures. The locations of mine sites in the area are also shown for reference and the study area is outlined in red. A more detailed geological map of the study area is shown in Figure 4. Adapted from Ivanic (2019); geology from Geological Survey of Western Australia.

3. Overview of Study Area

3.1 Location

The Rothsay Fold is located in the southwest portion of the Yalgoo-Singleton Greenstone Belt, Murchison Domain (Fig. 2). It contains the deserted historical mining settlement of Rothsay, situated 62 km northeast of Perenjori and 80 km west of Paynes Find (Fig. 3). The study area measures 14.2 km by 13.8 km and covers a total area of ~133 km², restricted to exploration and mining tenements held by Minjar Gold Pty and Egan Street Resources during the course of study. The land can be accessed from a number of exploration tracks adjoining the Warriedar-Coppermine Road (Fig. 3), however, most tracks in the area are highly vegetated and inaccessible.

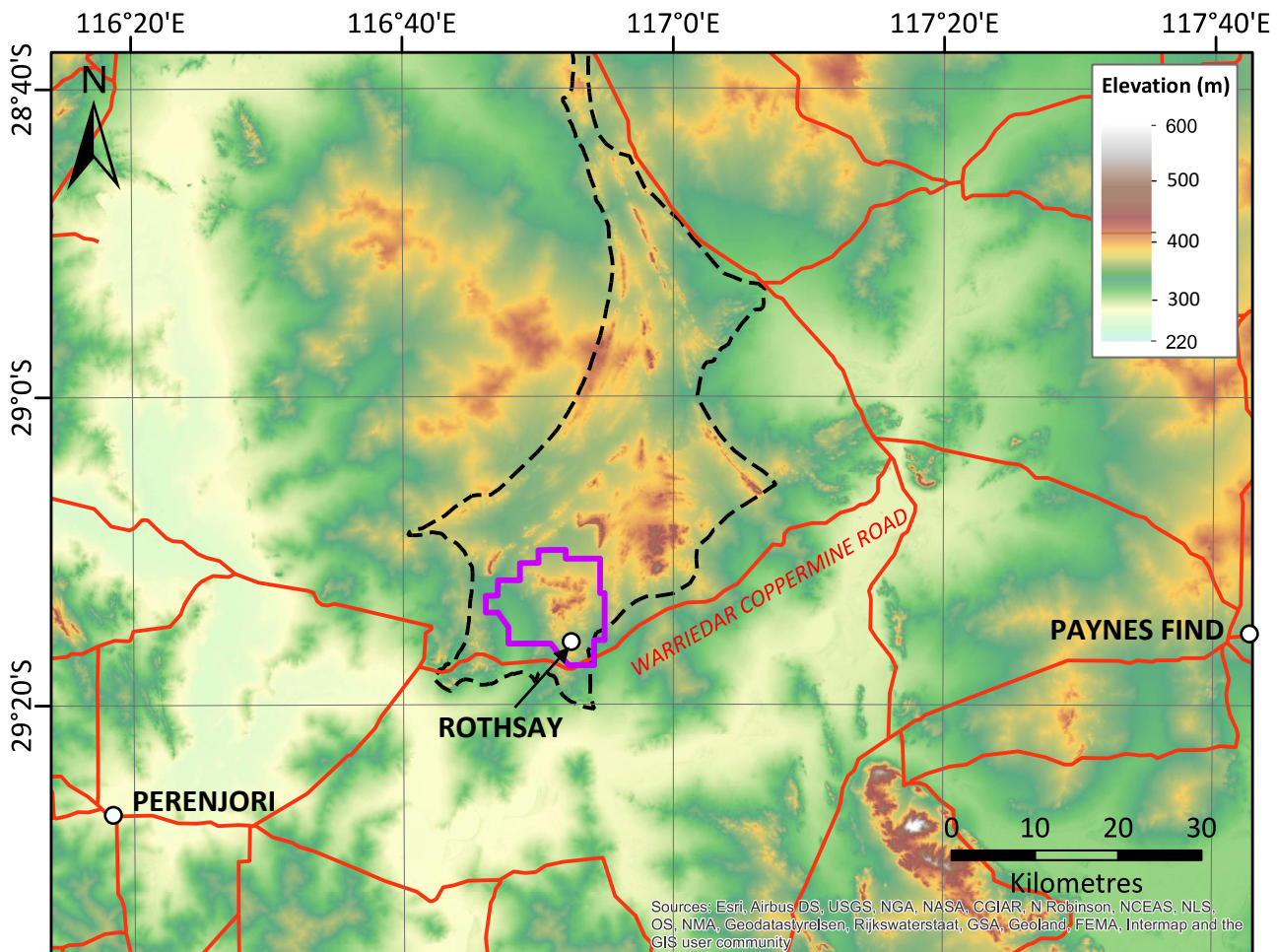


Figure 3: Topographic map of the southwestern Murchison Domain showing the location of the study area (purple) relative to nearby roads (red) and settlements. An outline of the central Yalgoo-Singleton greenstone belt is shown by the black dashed line. Basemap courtesy of ESRI.

3.2 Physiography

The topography of the area is largely flat with numerous gently sloping hills, varying in elevation from 290 m to 460 m above sea level (Fig. 3). Vegetation is dominated by mulga (acacia) bushes and eucalyptus trees. As is the case across the Murchison Domain, much of the bedrock is blanketed by superficial cover. During the Oligocene-Miocene, the Yilgarn Craton was subjected to tropical conditions, leading to the development of a deeply weathered lateritic layer overlying saprolite (Butt, 1981). Rock is now exposed either in watercourses that have dissected laterite and underlying saprolite, or in elevated areas that were originally above the duricrust laterite (Watkins and Hickman, 1990). Rock exposure is approximately 10% (outcrop + subcrop = 23 %), concentrated in the central part of the study area and greater than that found elsewhere in the region (< 5 %). Supracrustal rocks, primarily basalts, form elongate, undulating hills, whereas prominent ridges typically consist of banded iron formations and other ferruginous metasedimentary rocks. Superficial cover consists primarily of alluvial and colluvial material, in addition to laterite and locally, lateritic gravels and sands (Baxter & Lipple, 1985).

3.3 Previous Work

All previously published geological work in the Rothsay area is that of Geological Survey of Western Australia (GWSA) geologists, who have worked in the region a number of times over the last century. Clarke (1925) first documented the geology of rocks hosting mineralisation at the Rothsay mining centre, with simple geological mapping undertaken around the peripheries of the mine. Baxter and Lipple (1985) mapped the area to a 1:250,000 scale as part of regional-scale reconnaissance mapping, which remains the only published geological map of the Rothsay area to date (Fig. 4). This work was summarised by Watkins & Hickman (1990) as part of a synthesis of the geological evolution of the Murchison Domain, including some limited geochemical sampling in the study area. Since 2005, the GWSA have been undertaking a regional 1:100,000 scale mapping program of the Murchison Domain, and have remapped areas including much of the Yalgoo-Singleton Greenstone Belt (Ivanic, 2018; Ivanic et al., 2015; Zibra et al., 2017, 2016). However, the Rothsay area is yet to be remapped as part of this program.

The undergraduate theses of Price (2014) and Wickham (2014) included some 1:5,000 scale geological mapping in the northwestern part of the study area, carried out in collaboration with Minjar Gold Pty. The areas covered have been revisited and reinterpreted as part of this study.

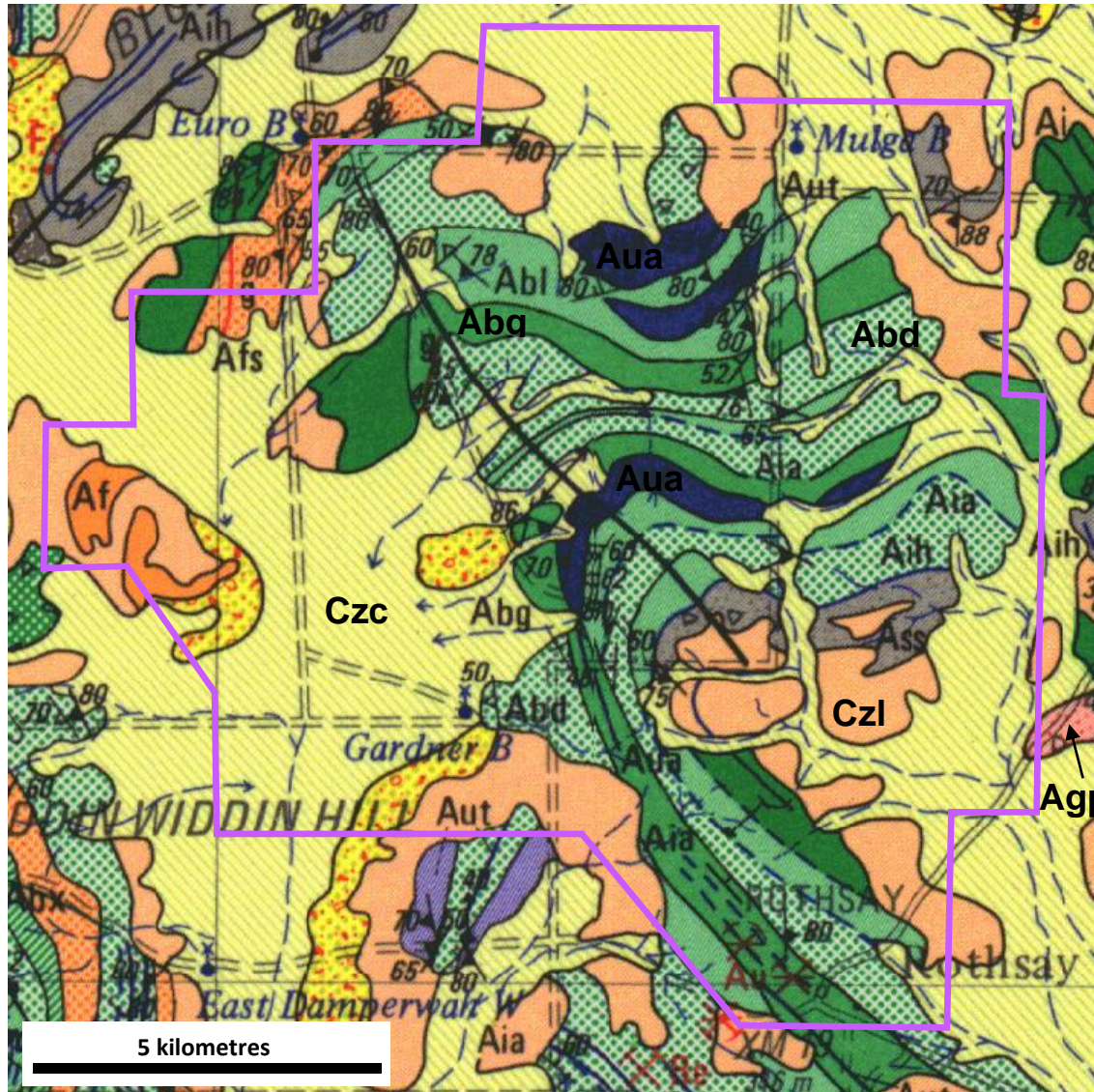
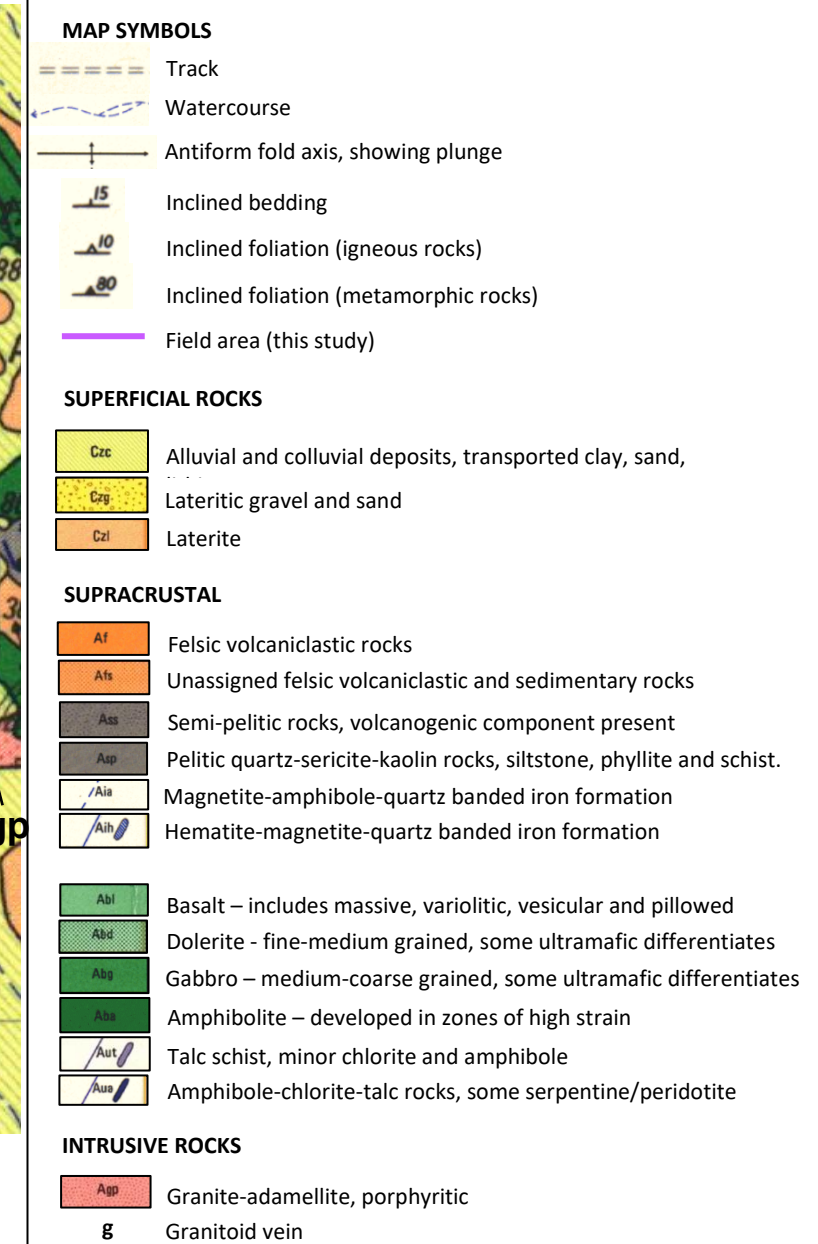


Figure 4: Geological map of the Rothsay Fold area at 1:250,000 scale, extracted from the GSWA Perenjori Map Sheet (Baxter & Lipple, 1985). The study area is outlined in purple.



3.4 Geological Overview

The geology of the Rothsay area consists of a typical Archaean supracrustal greenstone succession, comprising metavolcanics and metasedimentary rocks, intruded by a network of mafic-ultramafic layered sills (Fig. 4). A large 50 x 25 km granite, known as the Seeligson Monzogranite (Zibra et al., 2018), has intruded the succession in the southeast and supracrustal units typically dip away from granitoid contacts. The volcano-sedimentary stratigraphy has been deformed into an antiformal, ~12km wavelength fold structure, referred to herein as the Rothsay Fold. The Rothsay Fold has a northwest-plunging fold axis and a broadly upright axial plane, which separates a northeast limb from a southwest limb. In the south of the study area, a high-strain, north-northwest trending shear zone is host to historically-exploited lode-gold mineralisation at Rothsay. A significant unconformity has been identified within the volcanosedimentary succession that forms the Yalgoo-Singleton belt, at the base of the metasedimentary-dominated Mougooderra Formation (Watkins & Hickman, 1990). Recent regional-scale geological reinterpretations have suggested the southwest part of the Yalgoo-Singleton belt (within the Rothsay study area) contains an unconformable contact within the greenstone succession (e.g., Ivanic, 2019), however, it is unclear whether this represents the unconformity at the base of the Mougooderra Formation.

Felsic intrusive rocks

Walganna Suite²	Seeligson Monzogranite ²	Biotite monzogranite, K-feldspar-quartz-biotite-muscovite-(Li-B) pegmatites
-----------------------------------	-------------------------------------	---

Mafic-ultramafic intrusive rocks

Warriedar Suite¹	Damperwah Sill	Dolerite, gabbro, quartz diorite
	Gardner Sill	Peridotite, gabbro, dolerite, diorite
	Rothsay Sill	Peridotite, pyroxenite, gabbro, dolerite
	Mountain View Sill	Dolerite, gabbro, pyroxenite, quartz diorite, 'Honeycomb Gabbro'

Supracrustal rocks

Chulaar Group	Willowbank Clastics	Mudstone, greywacke, pebbly sandstone, felsic volcaniclastic rocks, conglomerate
	Mulga Volcanics	Variolitic basalt, spinifex-textured basalt, BIF, lapilli tuff
	Beryl West Volcanics	Basalt, spinifex-textured basalt
	Two Peaks Volcanics	Basalt, porphyritic dacite, BIF
	Macs Well Clastics	Quartzite, ferruginous siltstone, BIF, felsic volcaniclastic rocks

Table 1: Stratigraphic nomenclature used in this study, for felsic intrusive rocks, mafic-ultramafic intrusive rocks and supracrustal rocks in the Rothsay area. The key lithologies in each unit are also outlined. ¹Warriedar Fm after Ivanic (2019); ²Walganna Suite and Seeligson Monzogranite after Zibra et al. (2018).

3.5 Nomenclature

The geology of the Rothsay area has only previously been mapped at 1:250,000 scale and ongoing GSWA geological mapping in the region is incomplete, therefore a largely informal stratigraphy is used in this study and summarised in Table 3.1. Lithological units have been grouped into assemblages based on lithological associations, field relations and distinctive macroscopic and microscopic features. Five supracrustal assemblages have been distinguished and broadly correspond with formations in a formal stratigraphy. The lower four such assemblages have been assigned to the informal Chulaar Group, whereas the uppermost assemblage has been ascribed to the informal Willowbank Clastics. Chulaar Group rocks may correlate with Norie Group and/or Polelle Group rocks in the northeastern Murchison Domain (see Van Kranendonk et al., 2013). However, in the absence of geochemical or geochronological data, this remains to be proved. Mafic-ultramafic intrusive rocks have been divided into four mafic-ultramafic layered sills and collectively assigned to the Warriedar Suite, recently defined in the central Yalgoo-Singleton belt by Ivanic (2019). The only significant felsic intrusion in the area has previously been classified as the Seeligson Monzogranite of the regional Walganna Suite by Zibra et al. (2018).

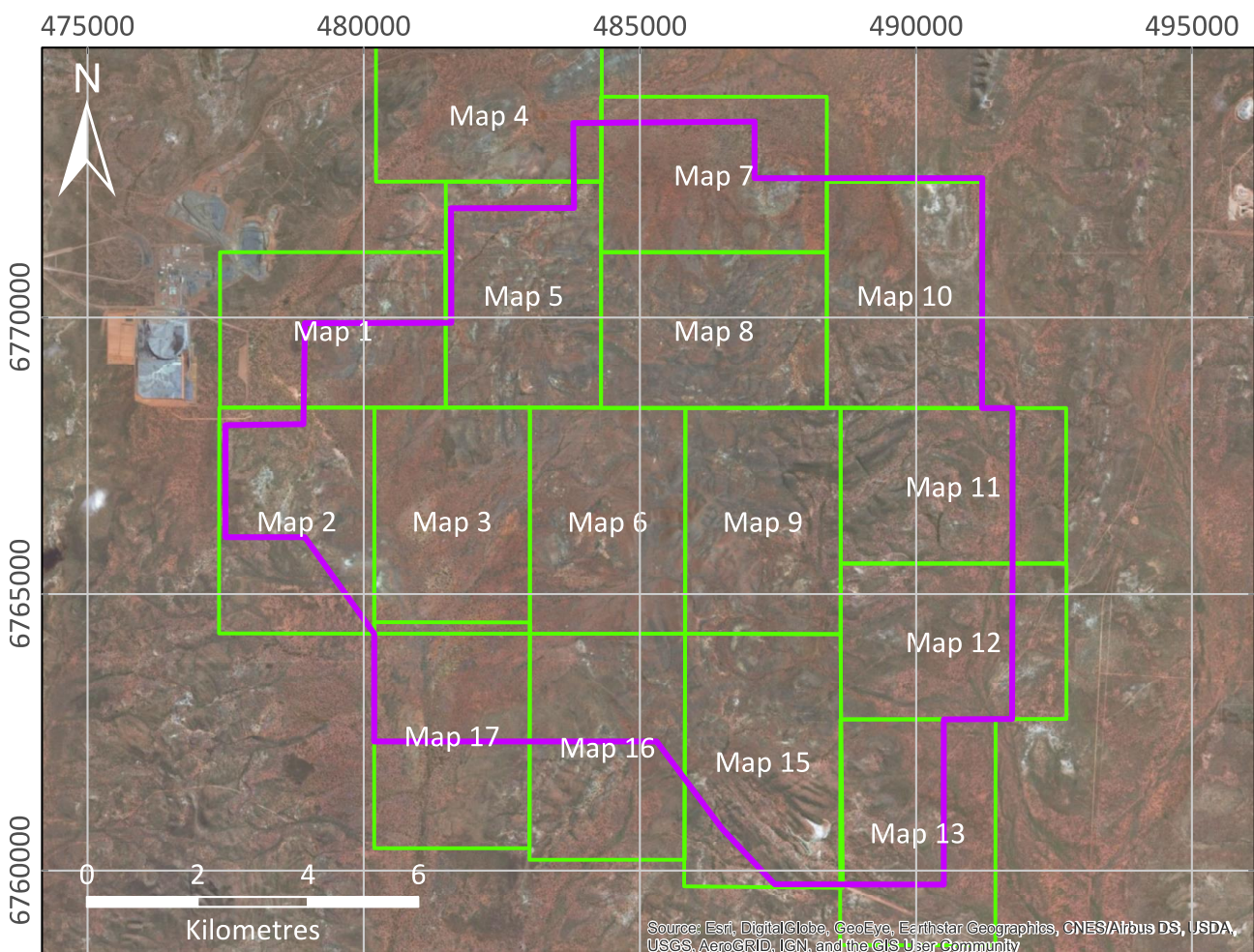


Figure 5: Aerial satellite imagery of the study area (pink) showing the locations of map sheets used during geological mapping, and the prefix used for field localities. Aerial imagery courtesy of ESRI.

The informal names ascribed to supracrustal assemblages and intrusive sills are mainly given after the names of local historical bores and wells, as well as former gold exploration targets. Several names are assigned after distinctive features exhibited by some units (e.g., Two Peaks Volcanics, Honeycomb Gabbro). Almost all rocks in the study area have been subjected to low-medium grade regional metamorphism, and most have been deformed to some degree. Where the protolith of a rock has been clearly identified, igneous or sedimentary nomenclature is used and the prefix meta- omitted. In rare instances where protoliths cannot be easily distinguished, metamorphic nomenclature is used.

4. Geological Mapping

4.1 Mapping Methods

Geological mapping was undertaken during two field seasons in July-September 2017 and July-September 2018, over a total of approximately eight weeks. The field area is divided into a total of sixteen map sheets (Fig. 5), which have each been mapped at 1:5,000 scale. Map sheets 6, 8 and 10 have been remapped after Price (2014). Map sheets 1-5 have been remapped after Wickham (2014), using a combination of original field observations and new field observations and descriptions made at revisited localities. All field observations are assigned locality numbers, which consist of a prefix referring to the sheet number, followed by the locality number within the given sheet (e.g., loc. 8.104; locality 104 on map sheet 8). The study area has a negligible magnetic declination of -0.5°.

During geological mapping, the following classification was used relative to the degree of certainty that a rock was representative of the bedrock:

- **Outcrop** – rock in situ and part of the bedrock (Fig. 6a).
- **Subcrop** – dense boulders/blocks not in situ but considered to represent underlying bedrock (Fig. 6b).

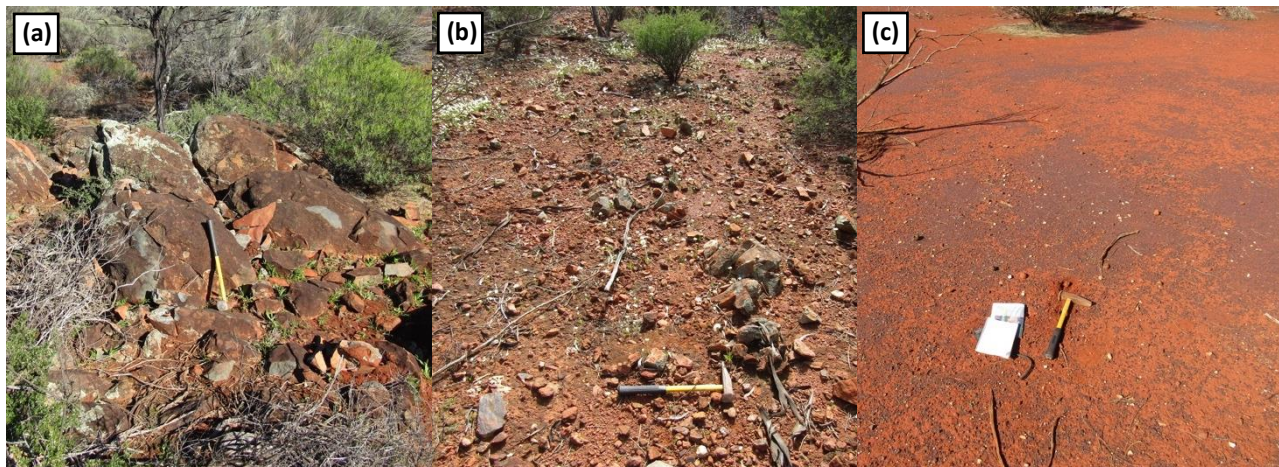


Figure 6: Field photographs showing the classification of rock exposure used during geological mapping with hammer for scale: (a) outcrop at locality 15.028; (b) subcrop at locality 16.032; (c) float at locality 17.006.

- **Float** – scattered clasts lying on superficial cover, which are less confidently representative of underlying bedrock (Fig. 6c). Float can be described as dense (>1 clast/ m^2) or sparse (<1 clast/ m^2).

In areas of little to no outcrop, a series of traverses were undertaken, typically perpendicular to the predicted strike of units. Float mapping was assisted by the recording of changes in vegetation and regolith, which proved to be very useful in areas lacking outcrop or subcrop. In areas of better subcrop/outcrop, traverses were less systematic and important contacts were followed. Aeromagnetic imagery was utilised for correlation of magnetic units, primarily BIF, serpentinised ultramafic units and dolerite dykes.

4.2 Geological Mapping Data

Two 1:25,000 scale geological maps of the Rothsay accompany this study: I) a 1:25,000 scale surface bedrock geological map of the Rothsay mining area (Plate A), based on 1:5,000 scale geological mapping and field observations in areas in which subcrop and outcrop were identified and II) a 1:25,000 scale interpreted bedrock geological map of the Rothsay mining area (Plate B), using a combination of outcrop mapping, float mapping, changes in regolith and vegetation, aerial imagery and aeromagnetic imagery. A simplified interpreted geological map of bedrock in the Rothsay area is displayed in Figure 7 and shows the extent of stratigraphic units denoted in this study. Three 1:25,000 scale cross sections have been drawn along the fence lines A-B-C (Fig. 8), D-E-F (Fig. 9) and G-H (Fig. 10) represented on the interpreted bedrock map in Plate B, in order to illustrate the interpreted sub-surface geology. Furthermore, a 1:20,000 scale stratigraphic column constructed from the exposed stratigraphy is displayed in Figure 11.

In the electronic appendix accompanying this study, mapping GIS data is present in the form of individual shapefiles, including bedrock geology, structures, planar and linear structural measurements, and localities visited during mapping, for reference. This data is also provided in the form of an ArcGIS layer package (for use on ArcMap 10.7 or later), which preserves symbology.

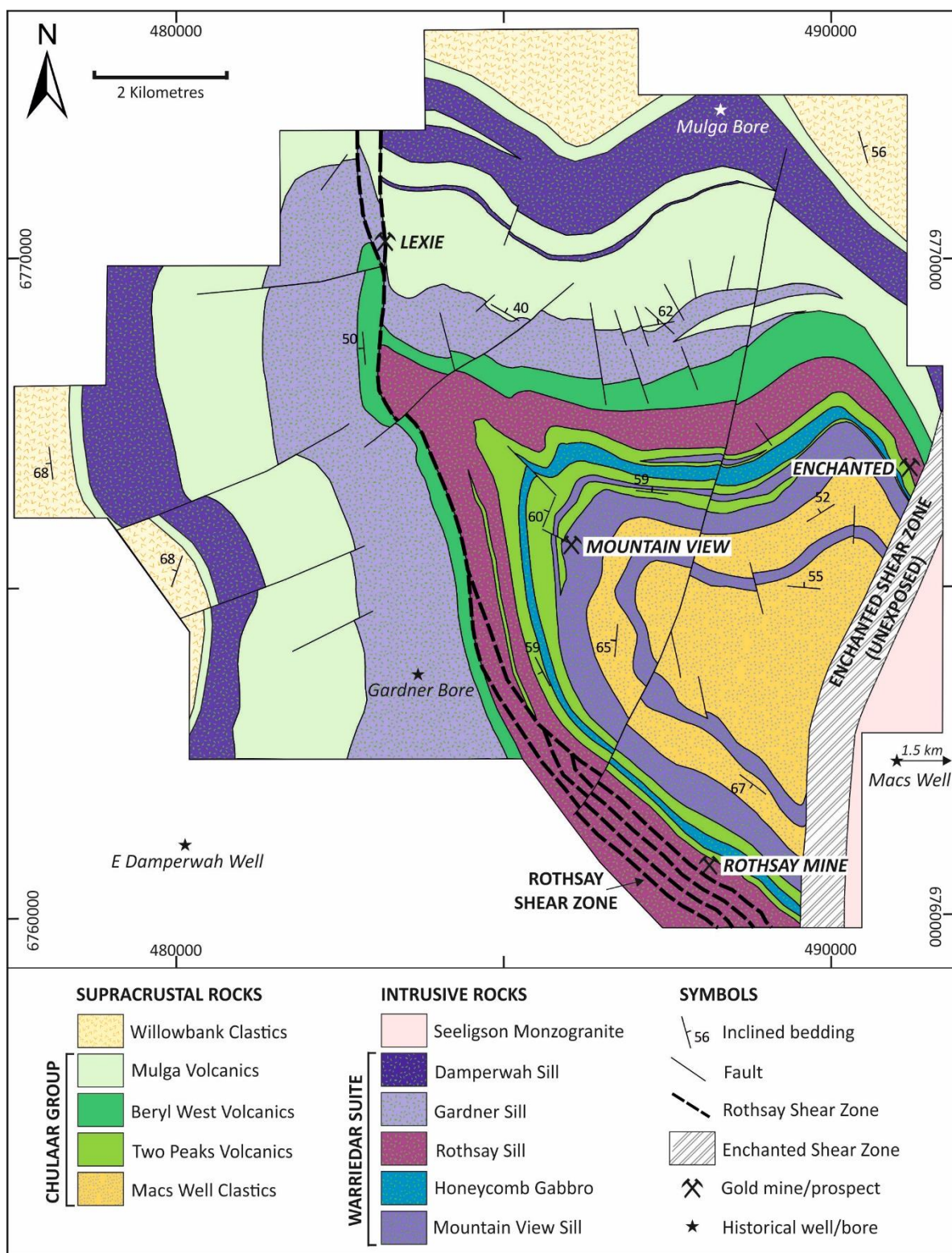


Figure 7: Simplified geological map of the Rothsay area the supracrustal units and intrusive rocks described in this study, in addition to major structures, representative bedding measurements, notable gold mines and prospects and historical wells/bores.

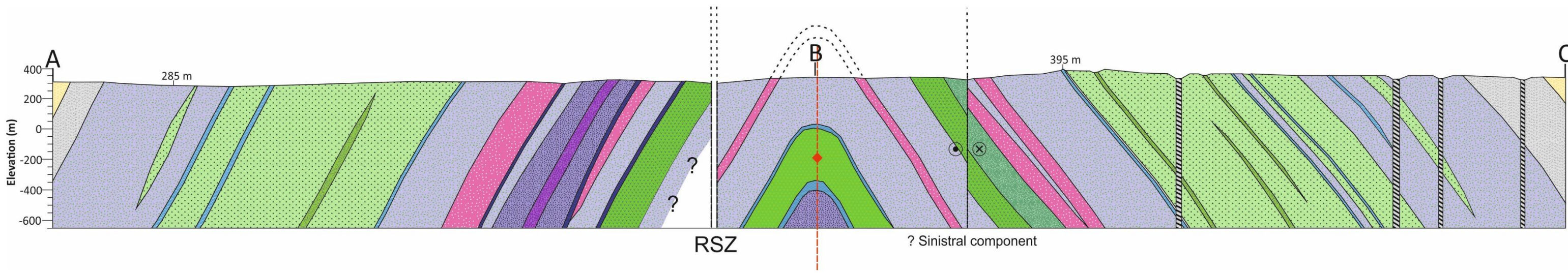


Figure 8: Cross section along the fence line A-B-C, drawn at 1:25,000 scale with no vertical exaggeration. RSZ = Rothsay Shear Zone. The highest and lowest topographic points along the section are labelled.

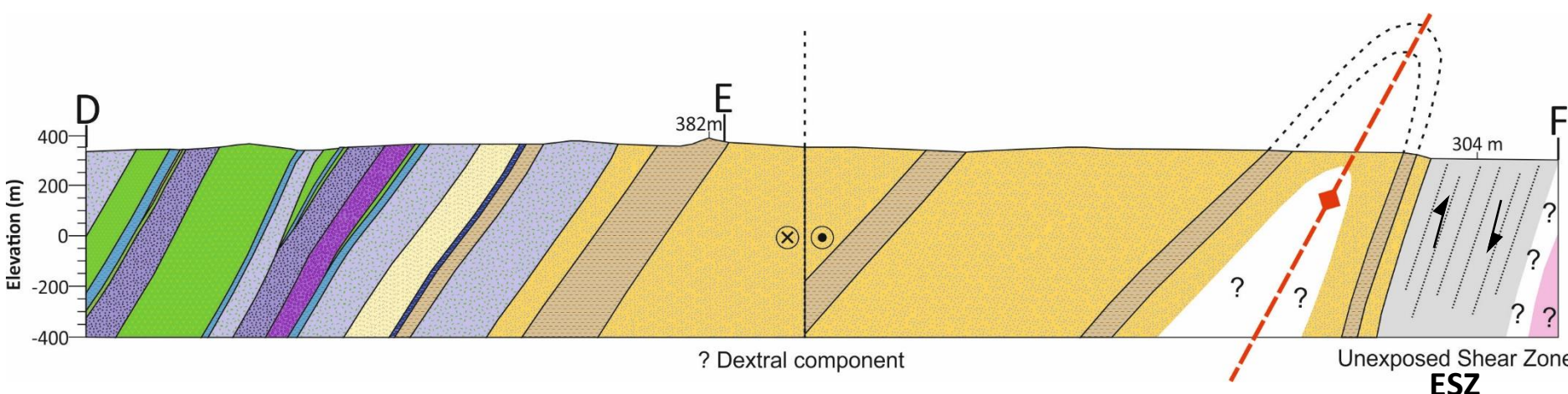


Figure 9: Cross section along the fence line D-E-F, drawn at 1:25,000 scale with no vertical exaggeration. ESZ = Enchanted Shear Zone. The highest and lowest topographic points along the section are labelled.

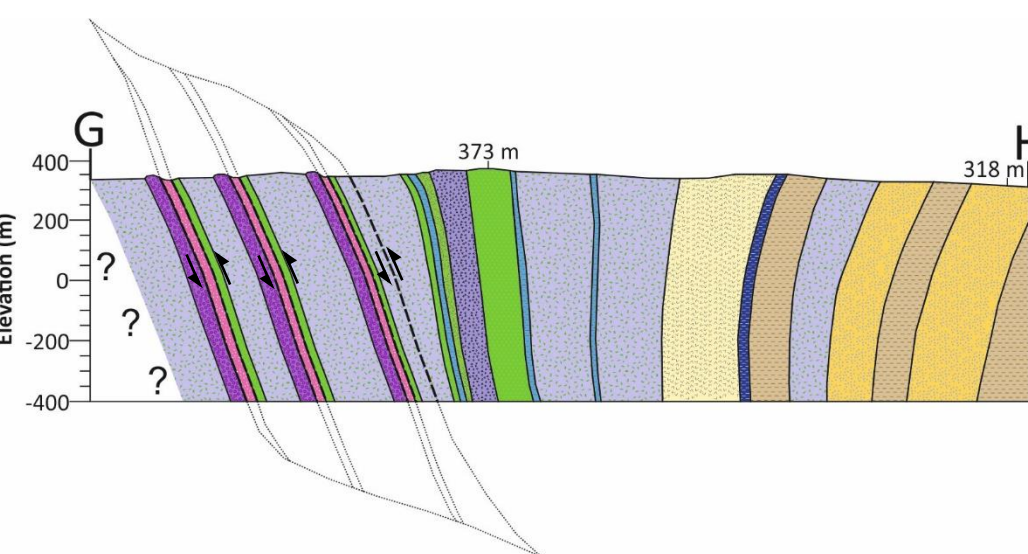
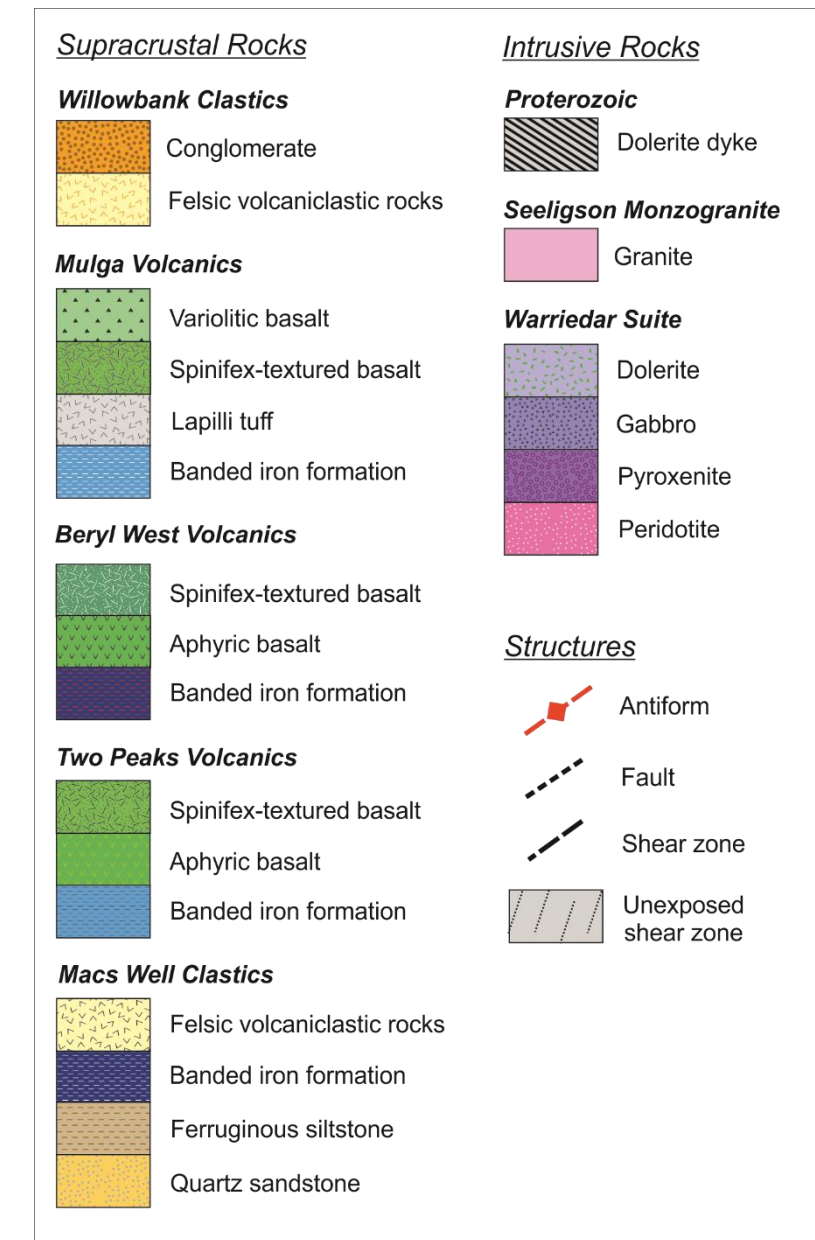


Figure 10: Cross section along the fence line G-H, drawn at 1:25,000 scale with no vertical exaggeration. The highest and lowest topographic points along the section are labelled.



SUPRACRUSTAL ROCKS

MAFIC-ULTRAMAFIC INTRUSIVE ROCKS

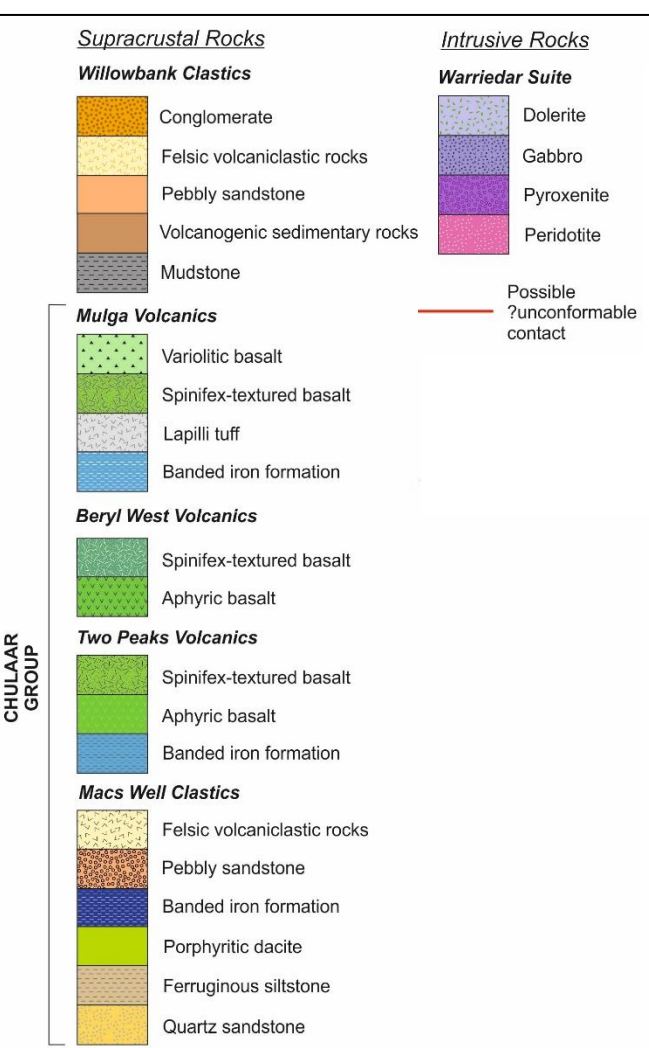
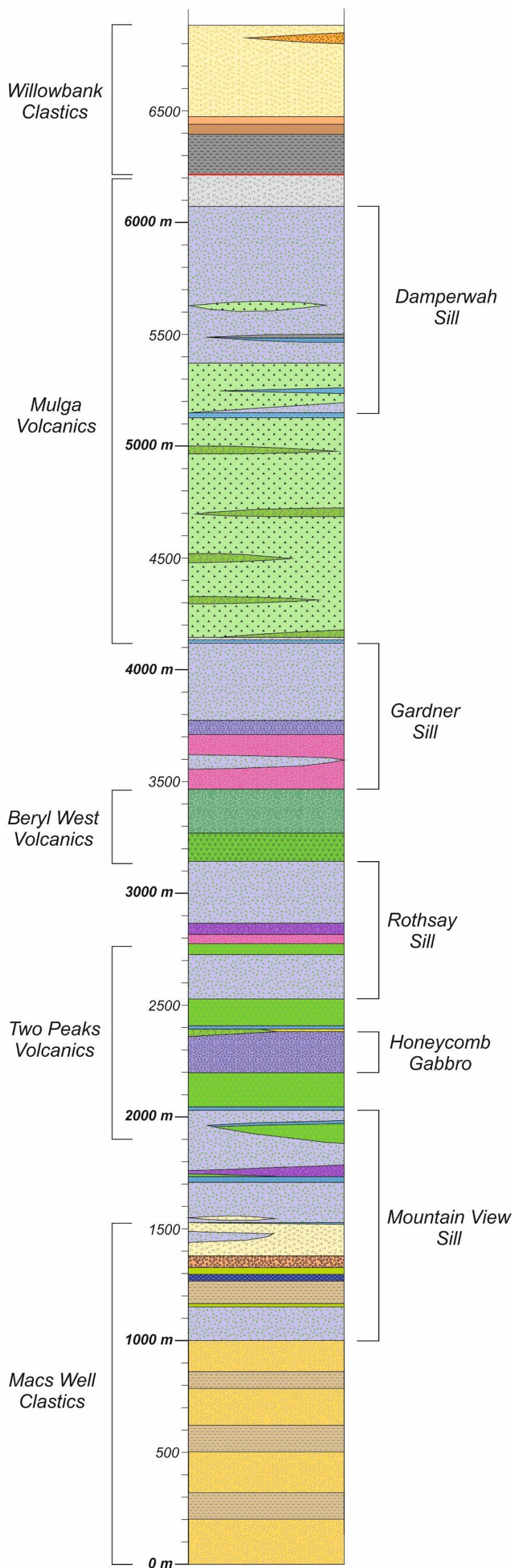


Figure 11: Stratigraphic column for rocks in the Rothsay area, drawn at a scale of 1:20,000 (1 mm = 20 m). The names ascribed to groups of supracrustal rocks and mafic-ultramafic intrusive rocks are shown on the left and right sides of the column, respectively. Note the different scale used here compared to accompanying 1:25,000 scale geological maps and cross sections – used in this instance to better show thin (<10 m) units. The red line denotes a potential unconformable/disconformable contact at the base of the Willowbank Clastics, which does not outcrop in the study area but is observed elsewhere in the Yalgoo-Singleton belt. The stratigraphic column has been drawn the right way-up according to multiple way-up criteria presented in Section 6.2. Most of the stratigraphic column (all units underlying and including the Damperwah Sill) has been constructed based on a N-S transect across the northeast limb of the Rothsay Fold. The uppermost part of the column comprising the upper Mulga Volcanics and overlying Willowbank Clastics was constructed using a transect in the far western part of the field area, due to a lack of exposure elsewhere, with the exception of laterally discontinuous conglomeratic units, which were added based on units outcropping in the far northeast. The stratigraphic column has been drawn according to the true thicknesses of units, which have been calculated using apparent thicknesses from geological mapping and the average dip measurements of bedding in metasedimentary units and the layer-parallel foliation in metagneous units along the transects described above. Features such as lenses within layered sills and units that pinch out along strike are represented on the column and the broad direction in which they pinch out has been included, with the right-hand side of the column broadly corresponding to the northeast and the left hand-side broadly corresponding to the southwest.

5. Stratigraphy

In this section, the supracrustal rocks and mafic-ultramafic intrusions present in the Rothsay area are described, starting at the base of the succession according to the stratigraphic column (Fig. 11) and stratigraphic map (Section 4.2.) Way-up criteria supporting the younging direction of the supracrustal succession are presented in Section 3.5.2 and include graded bedding, spinifex branching and igneous-



Figure 12: Photographs of rocks comprising the lower Macs Well Clastics. (a) Non-magnetic, fine grained ferruginous siltstone, with bedding evident (loc. 12.030); (b) Finely bedded ferruginous siltstone, magnetite and minor 1-2 mm quartzite bands (loc. 12.051a); (c) Interbedded ferruginous siltstone and 1-3 cm quartzite beds (loc. 12.019); (d) Typical exposure of ferruginous siltstone as a low lying ridge, facing west (loc. 12.068); (e) Banded unit of grey fine-grained quartzite and cream medium-grained quartzite (loc. 12.008); (f) Contrasting wildflower abundance on Fe-rich ferruginous siltstone (left; loc. 13.046) and Fe-poor quartzite-dominated units (right; loc. 12.040).

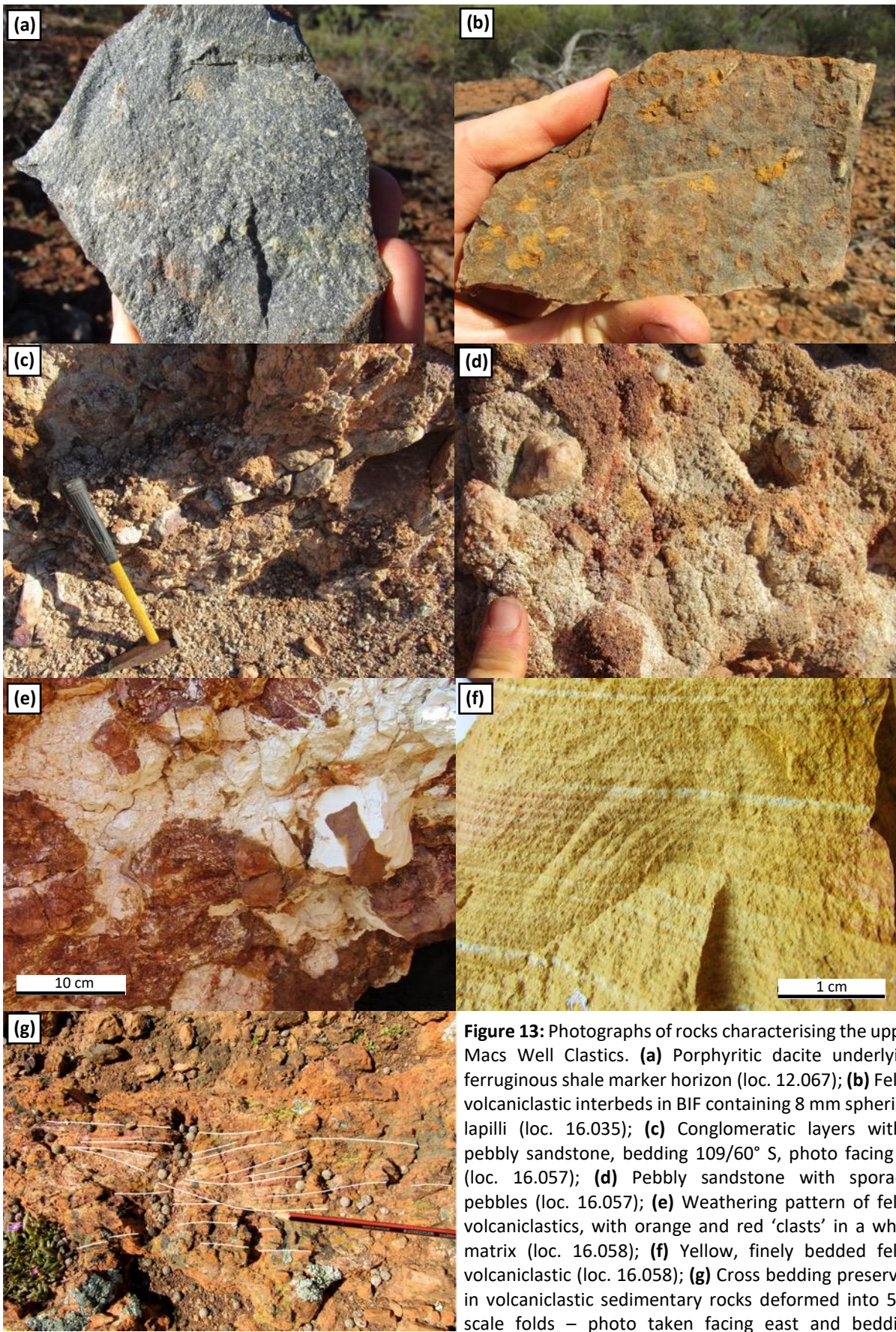


Figure 13: Photographs of rocks characterising the upper Macs Well Clastics. **(a)** Porphyritic dacite underlying ferruginous shale marker horizon (loc. 12.067); **(b)** Felsic volcaniclastic interbeds in BIF containing 8 mm spherical lapilli (loc. 16.035); **(c)** Conglomeratic layers within pebbly sandstone, bedding 109/60° S, photo facing W (loc. 16.057); **(d)** Pebby sandstone with sporadic pebbles (loc. 16.057); **(e)** Weathering pattern of felsic volcaniclastics, with orange and red 'clasts' in a white matrix (loc. 16.058); **(f)** Yellow, finely bedded felsic volcaniclastic (loc. 16.058); **(g)** Cross bedding preserved in volcaniclastic sedimentary rocks deformed into 5m-scale folds – photo taken facing east and bedding oriented 350/70° E (loc. 11.082).

differentiation. Contact relations between supracrustal rocks and intrusive rocks are also outlined.

5.1 Supracrustal Rocks

5.1.1 Macs Well Clastics

The Macs Well Clastics are a ~1.4 km-thick package of sedimentary rocks and lesser volcaniclastic rocks, situated at the base of the supracrustal succession exposed in the Rothesay Fold area. The Macs Well Clastics also represents the lowermost formation in the Chular Group exposed in the area and is named after the historical locality Macs Well (Fig. 11), located 4 km southeast of the type locality. The lowermost ~1 km of the Macs Well Clastics are characterised by alternations between ferruginous siltstone interbedded on a cm-scale with banded iron formation (BIF) and quartzite, and quartzite-dominated units. There are three units, 50-120 m in thickness, dominated by ferruginous siltstone, which consists of a finely laminated, dark brown, and fine-grained matrix (Fig. 12a). The siltstones are typically non-magnetic to weakly magnetic, however, where interbedded with BIF comprising millimetre-scale magnetite bands, the rocks are highly magnetic (Fig. 12b). Minor quartzite beds up to several centimetres in thickness are also locally interbedded (Fig. 12c). These ferruginous units are typically poorly exposed and where present, form low lying platforms or ridges that are often deeply weathered and ferruginised (Fig. 12d). Intervening quartzite-dominated units are largely unexposed and have only been identified from exploratory drill chips, float mapping and rare exposures along waterways. One such exposure near the base of the package consists of fine-grained (<0.5 mm), grey quartzite bands alternating with medium grained (1-2 mm) light yellow quartzite on a 0.5-1 cm centimetre scale (Fig. 12e). Further up sequence, quartzites are fine to medium grained (0.5-2 mm) with a sugary texture, some displaying red-pink staining indicative of iron oxide content. The abundant layering, principally bedding, present in both quartzite and ferruginous siltstones has allowed preservation of folding on a decimetre to decametre scale.

Distinguishing contacts with minimal exposure available was greatly assisted by recognising changes in vegetation, particularly the wildflowers that bloom in the area in early spring. Wildflowers were found to grow preferentially on Fe-bearing units, and so were used to map the contacts between ferruginous siltstone/BIF, where the wildflowers were abundant, and quartzite, where flowers were scarce (Fig. 12f). These contacts closely match the trends of aeromagnetic anomalies in localities where highly magnetic BIF was interbedded with ferruginous siltstone.

The stratigraphic top of the interbedded siltstone and quartzite units is intruded by a ~150 m-thick dolerite sill concordant to the stratigraphy (see Section 5.2.1). This sill is overlain by a thin, ~10 m porphyritic dacite unit, comprising a light grey, crystalline, fine grained groundmass with tabular 2-4 mm plagioclase phenocrysts (Fig.

13a), representing the lowermost volcanic rock in the supracrustal succession. Overlying the dacite is a further ~120 m-thick unit composed of interbedded ferruginous siltstone and BIF, with subordinate 1-2 mm interbeds of quartzite. Unlike those further down sequence, this unit is very well exposed, forming a near continuous, elevated ridge up to 30 m in height that can be traced along strike for over 10 km. The unit becomes more magnetic towards its top, grading into a highly magnetic, dark red-black, magnetite-hematite-quartz BIF for the top 30 m. Immediately beneath this highly magnetic horizon, interbedded orange-brown, fine to medium grained clastic units containing rounded 8 mm oxidised spherules are present, interpreted as lapilli-bearing felsic volcanioclastic horizons (Fig. 13b). In turn, the highly magnetic BIF is succeeded by a 30 m-thick layer of a fine grained, aphyric volcanic rock of andesitic composition.

The upper portion of the Macs Well Clastics is generally poorly exposed, however, a coherent stratigraphy can be constructed from several good outcrops. The andesite described above is overlain by a poorly exposed (< 100 m) thickness of non-magnetic ferruginous siltstone, above which a ~50 m broadly fining upward sequence of pebbly sandstone with conglomeratic layers occurs. The latter are locally concentrated near the base of the unit and occur as decimetre-scale layers of a clast-supported, poorly to moderately sorted, polymict conglomerate that define the orientation of bedding (Fig. 13c). Clasts vary in size from 2 mm to 30 cm and are primarily composed of quartz, with lesser pebbly sandstone autoliths. The conglomeratic portions grade into laterally continuous poorly-bedded pebbly sandstone, comprising moderately sorted, sub-rounded to sub-angular clasts, typically 0.5-2 mm but up to 5-7 mm in size, with sporadic ~5 cm pebbles (Fig. 13d). Clasts are composed primarily of quartz, in addition to lesser chert, of similar appearance to that in underlying BIF, and fine grained, crystalline, cream-coloured clasts, possibly felsic volcanic in origin. Bright white alteration indicates a possible volcanogenic component to the matrix.

Pebby sandstone grades upwards into a bedded felsic volcanioclastic unit that varies in thickness from 80-180 m and marks the top of the Macs Well Clastics. This unit is typified by an orange-brown, fine grained, friable matrix, showing bedding on a 1-3 mm scale (Fig. 13f; Section 6.3.5). It also locally shows a peculiar weathering pattern; a raised platform of bright white material contains orange-brown mottling in which a bedded volcanioclastic unit is evident and the margins of which are altering to the bright white material (Fig. 13e). In the far northeast, felsic volcanioclastics are interbedded with oxidised ferruginous sediment (possibly BIF) and display signs of sedimentary reworking in the form of cross bedding (Fig. 13g), however, the outcrop is significantly deformed and so cannot be used as a way-up criterion. This volcanioclastic unit can be traced along strike for over 8 km, however, exposure is not continuous along its strike length. This may be a consequence of the generally poor exposure or may instead signify localised deposition and accumulation of the described volcanioclastics. Dolerite intrudes this unit locally, predominantly at the fold nose and in the southern part of the southwest limb. The upper margin of the Macs Well Clastics is intruded by the Mountain View Sill (Section

5.2.1). Minor 5 m lenses of a fine grained, orange felsic volcaniclastic unit are present in the lower, doleritic portion of this intrusive sill.

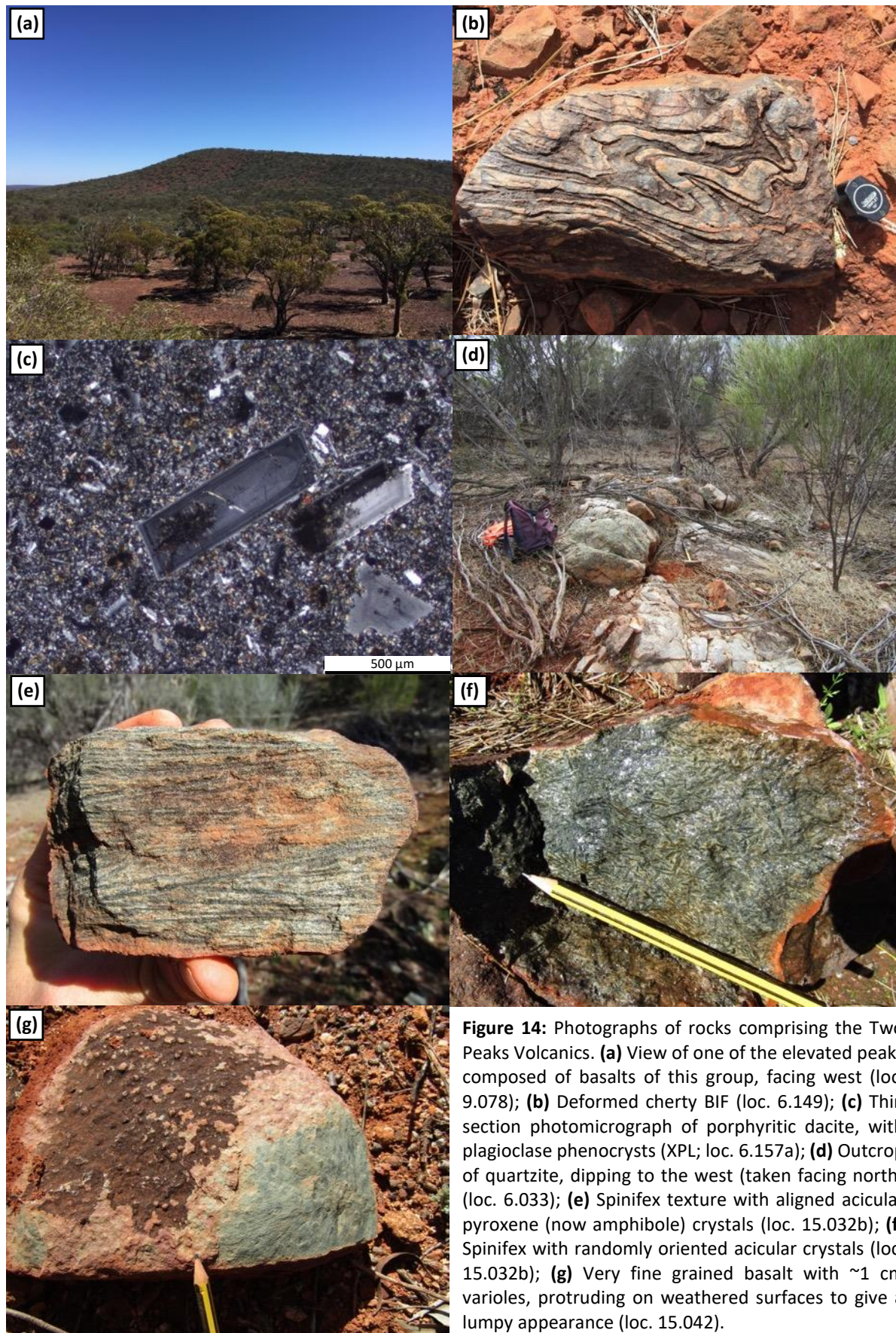


Figure 14: Photographs of rocks comprising the Two Peaks Volcanics. **(a)** View of one of the elevated peaks composed of basalts of this group, facing west (loc. 9.078); **(b)** Deformed cherty BIF (loc. 6.149); **(c)** Thin section photomicrograph of porphyritic dacite, with plagioclase phenocrysts (XPL; loc. 6.157a); **(d)** Outcrop of quartzite, dipping to the west (taken facing north) (loc. 6.033); **(e)** Spinifex texture with aligned acicular pyroxene (now amphibole) crystals (loc. 15.032b); **(f)** Spinifex with randomly oriented acicular crystals (loc. 15.032b); **(g)** Very fine grained basalt with ~1 cm varioles, protruding on weathered surfaces to give a lumpy appearance (loc. 15.042).

5.1.2 Two Peaks Volcanics

The Two Peaks Volcanics are a 400-450 m-thick succession characterised by aphyric mafic volcanic rocks and interflow BIF, with minor porphyritic and spinifex-textured volcanic rocks. The group is named after the two most prominent peaks in the area, which are composed of basalt from this succession (Fig. 14a). The Two Peaks Volcanics conformably overlie the Macs Well Clastics, however, the contact between the two has been intruded by the Mountain View sill. As a result, multiple discontinuous horizons of Two Peaks Volcanics are preserved within this intrusive sill, including some thin (<10 m) horizons of aphyric basalt directly above and below BIF. Above the Mountain View sill, a 10 m-thick, moderately magnetic unit of red-black-white cherty BIF is present, containing 1-2 cm banding and preserving intense folding in some outcrops (Fig. 14b). This is overlain by a 120-150 m-thick, very well exposed mafic volcanic unit that forms the local topographic highs, elevated ~80 m higher than surrounding flat-lying areas (Fig. 14a). The unit thickens to ~320 m in the fold hinge and thins towards the northeast, likely a consequence of the intrusion of sills. The volcanic pile consists mainly of aphyric, featureless and very fine to fine grained basalt, some of which break into elongate shards and make a high-pitched noise when struck with a hammer. Other portions are coarser, with crystals reaching 1 mm in size and a glittery appearance, potentially representing more slowly cooled, thicker flows. No discernible pillow structures are identified. Near the base of the unit, a thin (<1m), more evolved porphyritic dacite is present, containing 0.2-2.5 mm euhedral phenocrysts of plagioclase and amphibole (Fig. 14c) (Section 6.3.2).

The top of this basalt pile is intruded by the Honeycomb Gabbro, associated with the mafic-ultramafic network of sills (Section 5.2.2). Above this intrusive is a key stratigraphic marker horizon, consisting of two discontinuous supracrustal units overlain by a red-grey-black BIF. On the northeast limb and at the fold hinge, a thin (5 m) layer of massive quartzite is present, consisting of white-pink, medium-grained (0.5-1 mm) crystalline quartz with a sugary texture (Fig. 14d). The quartzite is only exposed at one locality (Loc. 6.033) but is present as subcrop and float along most of its length. The outcrop shows bedding surfaces parallel to the stratigraphy and patches of iron oxide, demonstrating contained Fe content. Thinning of this quartzite to the south coincides with the appearance of the second marker horizon on the southwest limb that is absent on the northeast limb; a poorly exposed pyroxene spinifex-bearing volcanic unit up to 25 metres in thickness (type locality: 15.032). Elongate, acicular crystals of pyroxene (now amphibole) up to 5 cm in length are strongly aligned in some parts of the outcrop (Fig. 14e), and randomly orientated in others (Fig. 14f). Outcrop is not contiguous enough to distinguish individual flows, however, this difference in alignment likely represents the various zones of spinifex-textured lava flows. This unit was originally mapped as a komatiite, but subsequent geochemistry has indicated that it is of basaltic composition.

The overlying red-grey-black BIF is 15 m in thickness and is highly magnetic, hosting 0.5-1 cm bands of magnetite. Intervening chert varies from grey to red in colour, and though typically planar, this unit is significantly deformed close to the Rothsay Fold hinge. In turn, this is overlain by a further 120 m of aphyric basalt that is generally poorly exposed, forms low-lying ground and locally contains 1-2 mm tremolite needles. The top of the Two Peaks Volcanics is intruded by the Rothsay mafic-ultramafic layered sill (Section 5.2.3). Within this sill, a thin (< 50 m), discontinuous horizon of very fine grained basalt with faint variolitic structures is present (Fig. 14g) and marks the top of the Two Peaks Volcanics.

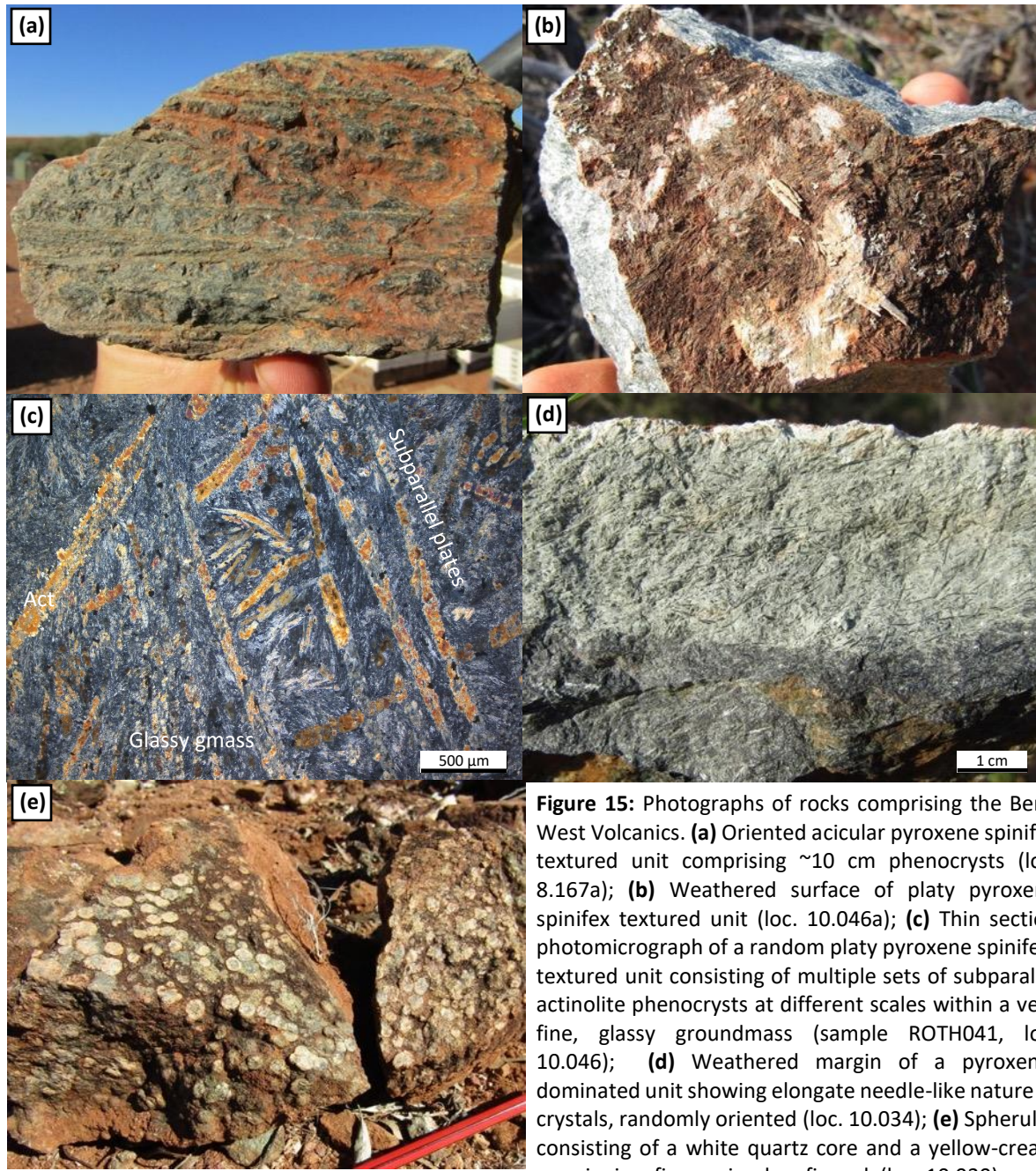


Figure 15: Photographs of rocks comprising the Beryl West Volcanics. **(a)** Oriented acicular pyroxene spinifex textured unit comprising ~10 cm phenocrysts (loc. 8.167a); **(b)** Weathered surface of platy pyroxene spinifex textured unit (loc. 10.046a); **(c)** Thin section photomicrograph of a random platy pyroxene spinifex-textured unit consisting of multiple sets of subparallel actinolite phenocrysts at different scales within a very fine, glassy groundmass (sample ROTH041, loc. 10.046); **(d)** Weathered margin of a pyroxene-dominated unit showing elongate needle-like nature of crystals, randomly oriented (loc. 10.034); **(e)** Spherules consisting of a white quartz core and a yellow-cream margin, in a fine-grained mafic rock (loc. 10.030).

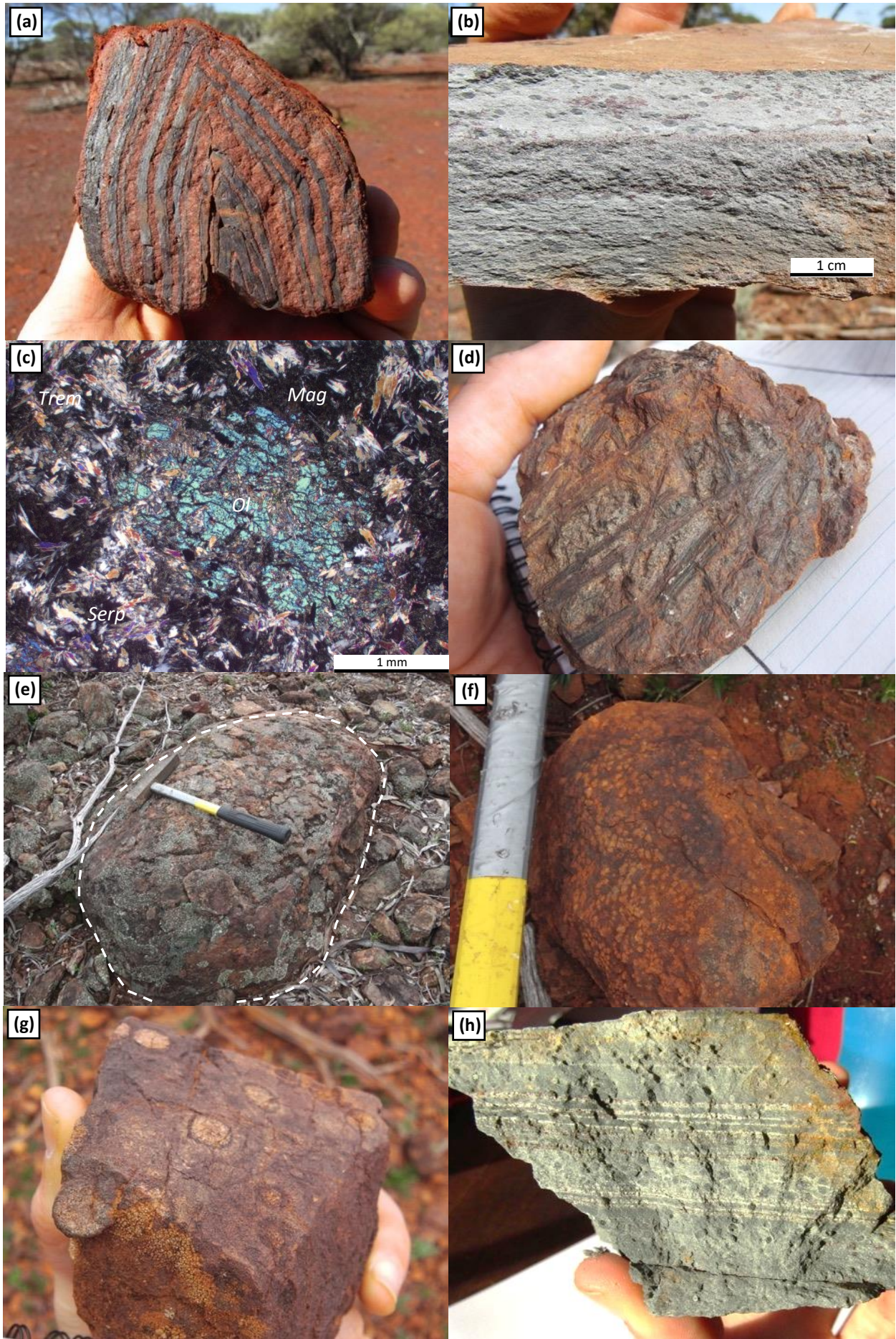


Figure 16 (previous page): Photographs of rocks comprising the Mulga Volcanics. **(a)** Folded red-black BIF with 4-8 mm magnetite bands (loc. 8.186); **(b)** Andesitic lapilli tuff with rounded to oblate lapilli concentrated on some horizons, some of which show an angular clast at their core (loc. 8.184); **(c)** Photomicrograph of ultramafic cumulate taken in cross polarised light, showing fragmented original olivine crystals, surrounded by serpentine, tremolite and magnetite (loc. 8.185); **(d)** Pyroxene spinifex-textured unit interleaved with basalt (loc. 8.076); **(e)** Metre-scale pillow structure composed of aphyric basalt (loc. 8.134); **(f)** Variolitic basalt with rounded varioles 1-2 mm in size (loc. 8.116); **(g)** Variolitic basalt with 1-1.2 cm varioles, which preferentially stick out on weathered surfaces (loc. 8.116); **(h)** Finely bedded grey tuff with lapilli concentrated on some bedding horizons, and white, quartz-rich horizons (loc. 2.084);

5.1.3 Beryl West Volcanics

The Beryl West Volcanics are a ~320 m-thick sequence of aphyric and spinifex-textured volcanic rocks situated between intrusive rocks of the Rothsay and Gardner mafic-ultramafic layered sills. The sequence takes its name after a historical beryl mine located adjacent to its constituent rocks to the south of the study area and comprises the lowermost supracrustal units to be dissected by the Rothsay Shear Zone. Rocks of the Beryl West Volcanics are generally poorly exposed and outcrops are low-lying and patchy, not elevated like other volcanic packages.

The stratigraphic base of the succession consists of aphyric and featureless basalt, which progresses upwards into a spinifex-textured volcanic rock comprising randomly orientated, needles of amphibole (pseudomorphing pyroxene) 2-6 mm in length amongst a fine-grained groundmass. This can be found across much of the strike length of the group and in turn, progresses upwards into well-developed spinifex textured rocks, with oriented acicular pyroxene crystals up to 10 cm in length (Fig. 15a). Furthermore, multiple units comprise another form of spinifex texture, characterised by randomly oriented sets of aligned, often skeletal crystals with a platy crystal habit (Fig. 15b), remarkably similar to random platy pyroxene spinifex described by Lowrey et al. (2017) in similar rocks in the northeastern Murchison Domain. In thin section, the interstices between larger plate sets contains smaller plate sets and a very fine glassy groundmass, consistent with rapid cooling (Fig. 15c; Section 6.3.4). Such rocks are only found in the north of the field area and appear to be discontinuous towards the south, replaced instead by greater thicknesses of aphyric and proto-spinifex-textured basalts that contain small (<3 mm) elongate amphibole crystals. In this part of the stratigraphy, it is often difficult to distinguish between pyroxene spinifex-textured volcanic rocks and intrusive pyroxenitic rocks of the overlying Gardner Sill that contain elongate amphibole (after pyroxene) crystals. This is especially the case within the area of Map 10. The heavily altered margins of outcrops commonly exhibit elongate crystals of pyroxene (now pseudomorphed by amphibole) (Fig. 15d) and weathered surfaces also expose the elongate nature of crystals. In one instance, these units are host to unusual spherulitic structures consisting of quartz and feldspar in a finer grained groundmass (Fig. 15e), 0.7-1.2 mm in diameter and similar in shape to spherules in basalts of the overlying Mulga Volcanics. These spherules are associated with 1-3 cm diameter quartz veining which cross cuts host rocks.

5.1.4 Mulga Volcanics

The Mulga Volcanics are a 1.4 km-thick succession dominated by variolitic, pillowed and spinifex-textured basalts, with minor interflow BIF and lapilli-bearing tuff. The succession is underlain by the Gardner mafic-ultramafic layered sill and overlain by the Damperwah Sill. The Mulga Volcanics take their name from a historical local bore (Mulga Bore; Fig. 11) and the native mulga (acacia) bush which is often densely vegetated in areas overlying basalts of this group. Mulga Volcanics rocks are much better exposed on the northeast limb of the Rothsay Fold than they are on the southwest limb, where they are typically blanketed by transported cover occupying a large drainage channel.

The base of the Mulga Volcanics is marked by a 10 m-thick moderately well exposed cherty BIF, with a distinctive red-black to red-gold appearance (Fig. 16a). The unit contains magnetite bands on a 1-10 mm scale, with localised development of the fibrous Fe-amphibole grunerite. An overlying 5 m wide unit of lapilli-bearing tuff also acts as a crucial marker horizon and along with the BIF unit, characterises the base of the succession. Despite its poor exposure, it is frequently found as float and has a very distinctive spotted appearance (Fig. 16b). The tuff is characterised by 5-15 mm beds dominated by fine, grey ash, comprising alternations between fine to medium grained quartz-bearing units, and very fine-grained lapilli-bearing units. Lapilli are rounded, 0.2-3 mm in size, often contain an angular fragment at their centres and are concentrated on bedding horizons (Section 6.3.6). The beds also exhibit graded bedding and erosive bases to some beds, demonstrating a degree of sedimentary reworking of volcaniclastic material and acting as way-up criteria (see Section 7.2). Overlying the tuff is a well exposed ~1.2 km mafic-ultramafic volcanic pile consisting of interleaved aphyric, variolitic and spinifex-textured volcanic rocks. On the northeast limb, the base of this pile is marked by a 20 m-thick spinifex-textured komatiitic unit comprising oriented elongate needles of amphibole (pseudomorphing pyroxene) up to 7cm in length and 1-2 mm in width, consistent with the “string-beef” spinifex classification of Arndt et al. (1977) (Section 6.3.4). This unit can be traced laterally along strike for 3 km and is associated with a 5 metre-scale highly magnetic ultramafic cumulate, directly underlying the spinifex-textured rocks and interpreted as the cumulate base to a komatiitic flow. This ultramafic unit contains a groundmass of serpentine, magnetite and tremolite, with preservation of 1-4 mm cumulate olivine crystals that are fragmented and partially serpentинised (Fig. 16c; Section 6.3.4). In the field, brown chalcedony is found proximal to this ultramafic unit.

The overlying 1.2 kilometre volcanic pile consists of similar 20-30 metre acicular pyroxene spinifex-textured units interleaved with aphyric and variolitic basalt that characterise this succession; the latter volumetrically outnumbering spinifex-textured units by approximately 6:1. Due to the less resistant nature of spinifex-textured rocks, they form a series of narrow valleys concordant to the stratigraphy within the typically elevated volcanic succession. Spinifex varies in form between randomly orientated acicular pyroxene crystals (Fig. 16d) to strongly aligned ‘sheaves’ of acicular phenocrysts, defining “string-beef” spinifex textures. Basalt units occasionally exhibit pillow structures up to 1.5 metres in diameter (Fig. 16e) and frequently contain

spherules that are spheroidal to slightly elliptical in shape and range in size from 0.5 mm to > 1 cm (Fig. 16f, Fig. 16g). Spherules are typically, but not always, concentrated around the margin of pillows (Section 6.3.3). The volcanic rocks are commonly foliated and present as low lying, patchy outcrop. Green talc-chlorite schist is developed locally, particularly close to major faults. Towards the top of the succession, a ~60 m dolerite is intruded and two thin (<10 m) cherty BIF units are distinguished by the presence of coincident float and magnetic anomalies. The upper portion of the Mulga Volcanics and as such, the top of the Chulaar Group, is intruded by the Damperwah mafic-ultramafic sill. In the far west of the area and overlying the Damperwah intrusion, the top of the Mulga Volcanics is marked by a ~140 m-thick unit of a grey-coloured lapilli-bearing tuff with a very similar appearance and geochemistry to the thin tuffaceous unit present at the base of the group. The uppermost unit is finely bedded to massive and is characterised by spherical lapilli typically 2-3 mm, but rarely up to 5-6 mm in size concentrated on specific bedding horizons and often exhibiting a black angular fragment at their centres. Some parts of the unit contain lighter coloured quartz-rich horizons (Fig. 16h), whereas other portions consist entirely of fine grained, grey ash. This unit is poorly exposed elsewhere in the study area, but is interpreted to be present along strike based on a small amount of float material in areas of no exposure.

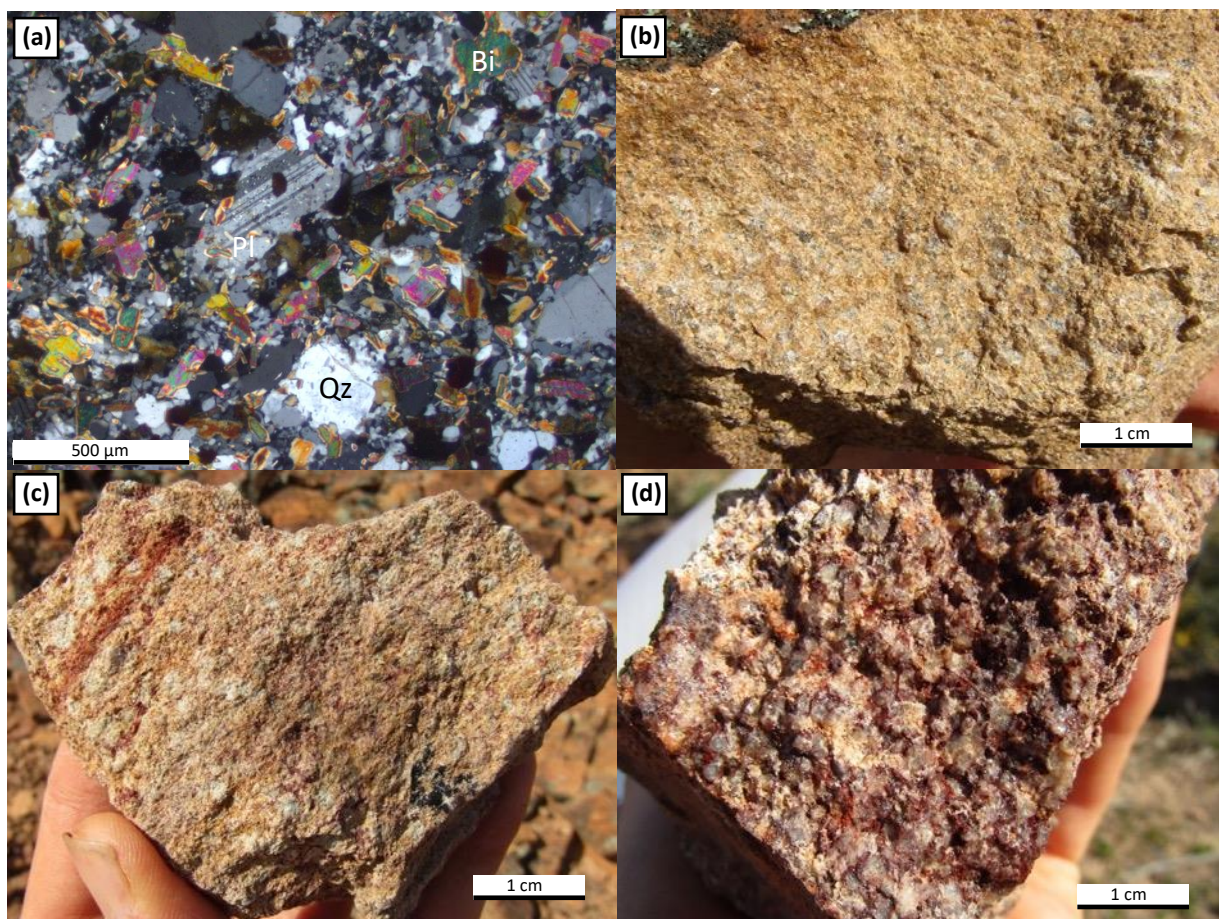


Figure 17: Photographs of rocks comprising the lower Willowbank Clastics exposed in the Rothsay area. **(a)** Thin section photomicrograph of a greywacke comprising anhedral grains of plagioclase, biotite and quartz (cross polarised light; loc. 2.088) **(b)** Volcanogenic quartz sandstone with 2-3 mm clasts (loc. 2.089); **(c)** Volcaniclastic unit with rounded, white 4-5 mm clasts and minor quartz in the matrix (loc. 2.089); **(d)** Pebby quartz sandstone with a red, iron-bearing matrix (loc. 2.090).

5.1.5 Willowbank Clastics

The Willowbank Clastics represents a sequence of sedimentary and volcaniclastic rocks that form the top of the supracrustal greenstone assemblage present in the Rothsay Fold area. The Willowbank Clastics are named after a local gold exploration target close to the type locality, overlie the Mulga Volcanics and have a minimum

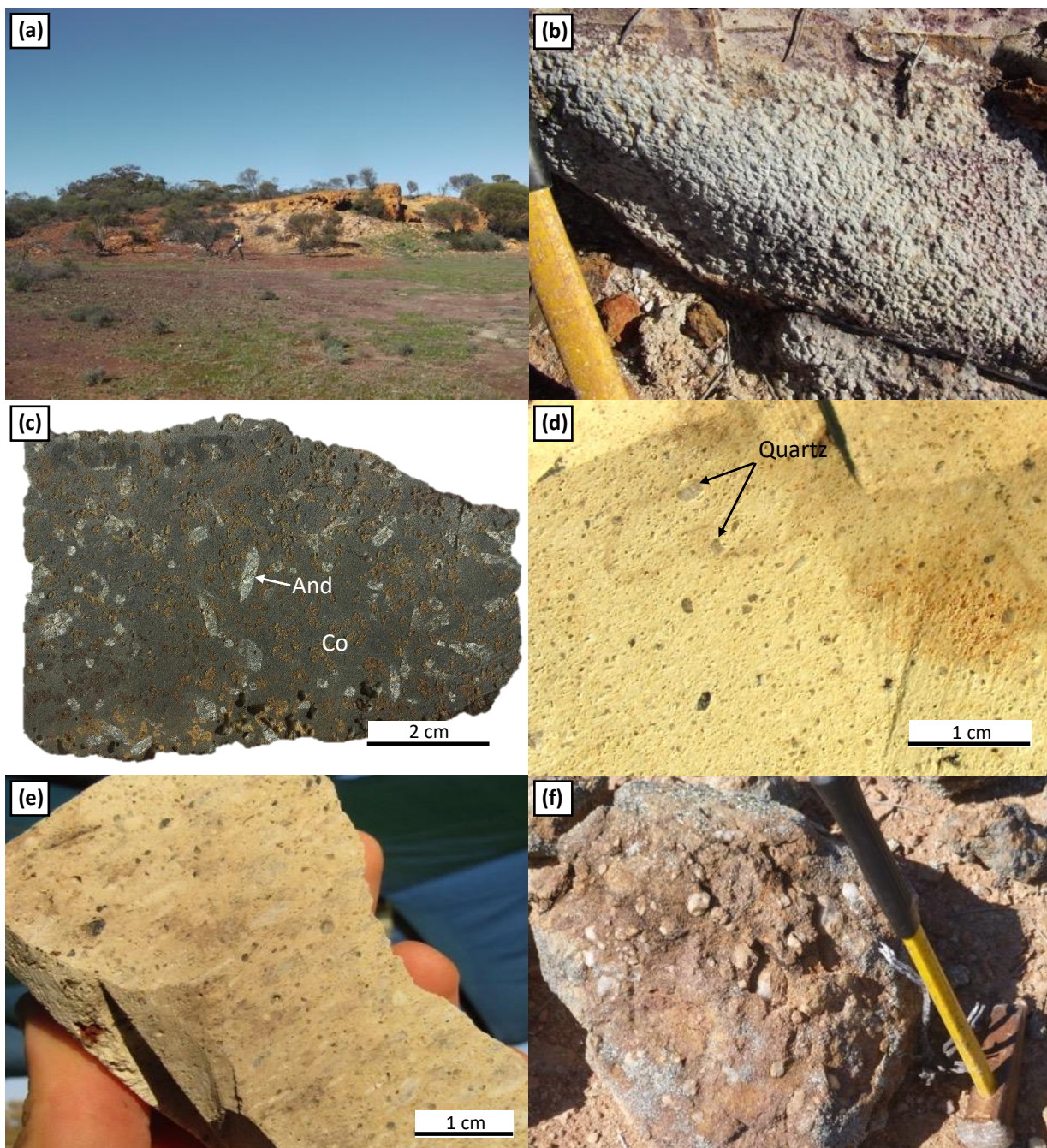


Figure 18: Photographs of rocks comprising the upper Willowbank Clastics exposed in the Rothsay area **(a)** Typical weathered exposure of felsic volcaniclastic rocks and ash beds (loc. 2.039); **(b)** Felsic volcaniclastic unit containing dense lapilli on a 20 cm horizon – hammer handle for scale (loc. 2.091); **(c)** Cut surface of a porphyroblastic metapelitic rock containing andalusite and pinitized cordierite porphyroblasts – note the cavities around the margin of the sample representing the removal of cordierite alteration products (loc. 2.091; sample ROTH053); **(d)** Cut surface of a felsic volcaniclastic rock, containing angular quartz crystals, minor rounded lithic clasts and some black clasts (potentially volcanic glass), in a fine-grained matrix (loc. 10.093); **(e)** Cut surface of a coarser grained felsic volcaniclastic rock containing quartz crystals, and larger 4-5 mm lithic fragments. The rock possesses a fabric that could be primary (loc. 10.095); **(f)** Conglomerate outcrop containing rounded pebbles of quartz up to 10 cm in size (loc. 10.107).

preserved thickness of 600 m. The true exposed thickness could be as much as 1 km; however, this is difficult to corroborate due to very patchy exposure and attenuation of units into the Enchanted Shear Zone in the east (Fig. 11). The base of the Willowbank Clastics is very poorly exposed, however, several small m-scale outcrops of a red-brown, fine-grained and non-magnetic mudstone are present in the west. This mudstone has an apparent thickness of about 180 m, before progressing into a coarsening upwards sedimentary sequence. The base of this sequence is marked by a 30 m-thick unit of an immature, fine to medium grained (0.1-1 mm) micaceous greywacke, comprising clasts of muscovite, feldspar and quartz (Fig. 17a; Section 6.4.1). In turn, greywacke grades into a well exposed, 15 m-thick unit of medium-grained, volcanogenic quartz sandstone, containing 1-3 mm sub-rounded quartz clasts (Fig. 17b). Volcanogenic content is represented by a yellow-brown, ashy matrix (Section 6.4.2). This coarsens upwards into a 5 m-thick volcaniclastic rock unit containing lithic clasts up to 8 mm in size amongst a red-grey ashy matrix, with some quartz clasts (Fig. 17c). This unit and the underlying volcanogenic sandstone form an elevated ~5 metre ridge in an otherwise flat terrain. The volcaniclastic layer is overlain by a 35 m-thick unit of a clast-supported, moderately sorted, monomict pebbly quartz sandstone, containing quartz clasts 3-6 mm in size and a red-pink matrix, indicative of contained Fe (Fig. 17d). This unit has a similar appearance to the pebbly sandstone near the top of the Macs Well Clastics lower in the supracrustal succession.

Overlying the pebbly sandstone, a 125 m-thick succession of intermediate to felsic volcaniclastic rocks occurs, dominated by grey, bedded, lapilli-bearing tuffs, with interbedded white-cream felsic volcaniclastic rocks. The lower ~20 m of this succession is exposed as an elevated ~5 m platform of friable, grey-white ash containing clasts of multiple lithologies, demonstrating a distinctive weathering pattern similar to that of felsic volcaniclastics in the Macs Well Clastics (Fig. 18a). This ash bed encloses horizons containing dense lapilli as clasts (Fig. 18b) and another less-common clast lithology consists of a fine-grained, porphyroblastic metasedimentary rock containing euhedral andalusite crystals up to 1 cm in size and rounded, 1-2 mm pinitized cordierite porphyroblasts (Fig. 18c; Section 6.4.3).

The upper portion of the exposed Willowbank Clastics is typified by felsic volcaniclastics, identified only in the far northeast of the study area. These rocks comprise poorly bedded clastic units composed of a white-cream coloured, fine grained quartzofeldspathic groundmass and clasts of quartz from 0.5mm to 2mm in size (Fig. 18d; Section 6.4.4). Some beds contain lithic clasts up to 8 mm in size that are elongate and define a fabric that may represent a primary feature (Fig. 18e). Rare lapilli-bearing horizons and interbeds of a darker grey ashy volcaniclastic rock are also present. This unit is characterised at the surface by milky quartz float, including in areas where the unit does not outcrop. Towards the top of the package, laterally discontinuous lenses of conglomerate occur within the felsic volcaniclastics. Conglomerates are poorly sorted, polymict and contain sub-angular to sub-rounded clasts of quartz varying in size from < 1cm to 12+ cm in size, in a grey to red, finer-grained matrix (Fig. 18f). At the contacts, there is a clear gradation on a 10-metre scale from volcaniclastic rocks with minor quartz clasts, to volcanogenic sandstone, to quartz sandstone and then into conglomerate. The conglomeratic lenses within felsic volcaniclastic rocks marks the top of the supracrustal stratigraphy

present in the Rothsay Fold area.

5.2 Mafic-Ultramafic Intrusive Rocks

The Warriedar Suite of mafic-ultramafic layered intrusive sills intrudes the supracrustal stratigraphy in the Rothsay area and can be broadly separated into four sill complexes, based primarily on lithological evolution and their geometries. These intrusions comprise the lowermost **Mountain View Sill**, the **Rothsay Sill**, the **Gardner Sill** and the uppermost **Damperwah Sill**. A further distinct, relatively thin unit, the Honeycomb Gabbro, occurs at the top of the Mountain View Sill. The rocks comprising each of these mafic-ultramafic intrusions are described below:

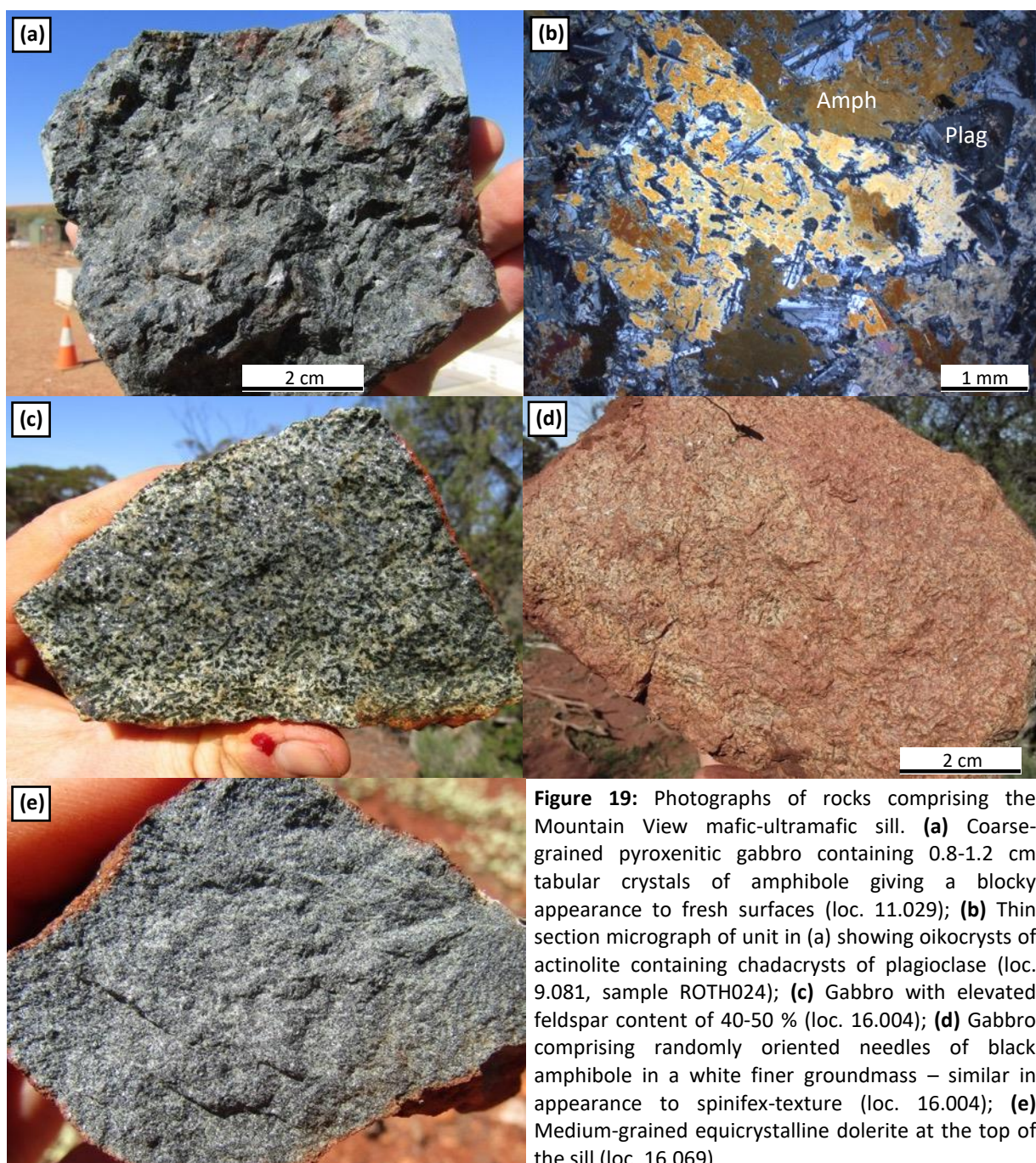


Figure 19: Photographs of rocks comprising the Mountain View mafic-ultramafic sill. **(a)** Coarse-grained pyroxenitic gabbro containing 0.8-1.2 cm tabular crystals of amphibole giving a blocky appearance to fresh surfaces (loc. 11.029); **(b)** Thin section micrograph of unit in (a) showing oikocrysts of actinolite containing chadacrysts of plagioclase (loc. 9.081, sample ROTH024); **(c)** Gabbro with elevated feldspar content of 40-50 % (loc. 16.004); **(d)** Gabbro comprising randomly oriented needles of black amphibole in a white finer groundmass – similar in appearance to spinifex-texture (loc. 16.004); **(e)** Medium-grained equicrystalline dolerite at the top of the sill (loc. 16.069).

5.2.1 Mountain View Sill

The Mountain View Sill is a dismembered 500 m-thick mafic-ultramafic intrusive complex intruded between supracrustal rocks of the Macs Well Clastics and Two Peaks Volcanics. It is named after a local gold exploration target (Fig. 11) and reflects the subdued topography of the constituent intrusive rocks relative to surrounding, elevated supracrustal units. The base of the sill is marked by a 140 m-thick unit of poorly exposed dolerite, intruded in the upper part of the Macs Well Clastics. Outcrops are rare, but where present are deeply weathered and comprise medium-grained and equicrystalline dolerite, with crystals locally reaching 3-4 mm in length. The average crystal size decreases towards the margin of the dolerite, consistent with chilled margins and an intrusive origin. Above the ~400 m-thick upper portion of the Macs Well Clastics, a further 180 m-thick poorly exposed unit of equicrystalline dolerite is present, composed of 1-2 mm crystals of plagioclase feldspar and amphibole (replacing original pyroxene). Plagioclase crystals are often stained pink – a product of alteration and a characteristic feature of this unit. Towards the top of the dolerite, amphibole crystals increase to 4-5 mm in size and are acicular in shape. In the southwest (Loc. 16.060), a 5 m-thick lens of deeply weathered and oxidised, friable felsic volcaniclastic unit is enclosed within dolerite, close to the contact with like units in the upper Macs Well Clastics.

A laterally-continuous ~40 m-thick layer of cherty BIF and minor basalt is present above a ~180 m-thick dolerite intrusion, which in turn is overlain by a ~120 metre layer of coarser grained mafic intrusive rocks. This includes a lower ~50 m unit of coarse-grained pyroxenitic gabbro, composed of 0.8-1.2 cm tabular crystals of amphibole (actinolite) and 20-30 % interstitial crystals of plagioclase (Fig. 19a). Petrographic analysis shows that actinolite crystals are in fact poikilitic with inclusions of plagioclase crystals and display a sub-ophitic texture, both examples of relic igneous textures (Fig. 19b; see Section 6.5.3). This unit occurs over 7 kilometres on the northeast limb and pinches out towards the south, and exposure is typical of that of mafic intrusive rocks in the area, occurring as mounds of large (up to 2m) rounded boulders. Pyroxenite grades upwards into a coarse gabbro, comprising 5-15 mm crystals and an increased feldspar content of 40-50 % (Fig. 19c). Some portions of the gabbro contain randomly orientated black amphibole crystals in a white groundmass, with a superficial appearance somewhat like spinifex texture (Fig. 19d). In turn, the gabbro grades upwards into a thin doleritic horizon. This dolerite is in upper contact with basalt and BIF, which is present as a discontinuous raft within the intrusive sill complex, stretching 5 km along strike and up to 100 m in thickness.

Above the basalt-BIF raft, a ~60 m-unit of equicrystalline dolerite occurs with 35-40% feldspar content (Fig. 19e). In some instances, crystals reach 4-5 mm in size and interstitial feldspar weathers preferentially, resulting in a blocky appearance to weathered surfaces. The top 15-20 m of the dolerite in contact with Two Peaks Volcanics supracrustal units comprises finer 0.5-1 mm crystals, indicative of a more quickly cooled, chilled upper margin.

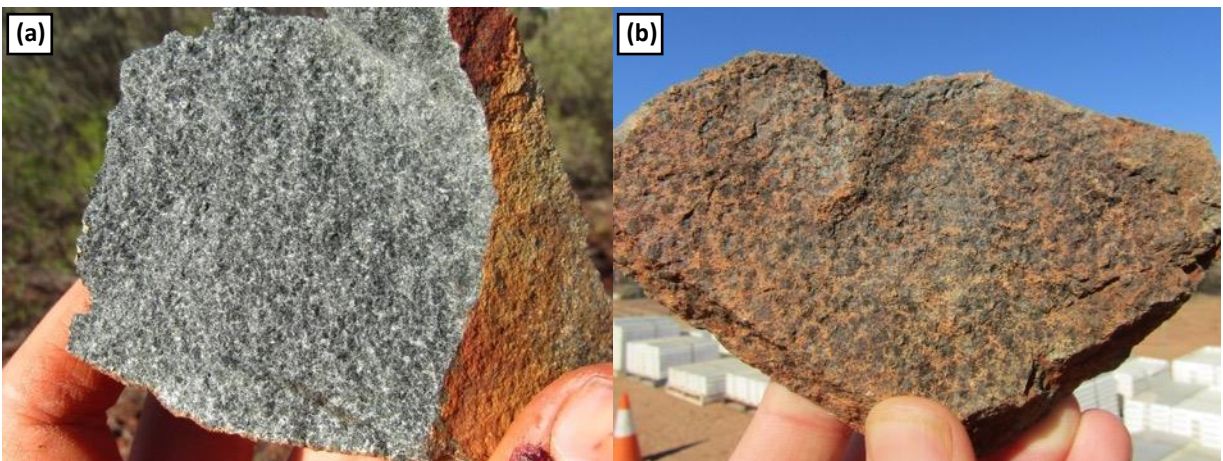


Figure 20: Photographs of rocks from the Honeycomb Gabbro. **(a)** Fresh surface showing rounded amphibole crystals in a finer grained groundmass (loc. 16.019); **(b)** Weathered surface displaying the characteristic honeycomb texture that typifies this unit (loc. 6.168).

5.2.2 Honeycomb Gabbro

The Honeycomb Gabbro is a 110-180 m-thick unit of gabbro that intrudes the upper portion of the Two Peaks Volcanics, above aphyric basalt and below the quartzite and spinifex-textured komatiite horizons. The unit represents the uppermost component of the Mountain View Sill and is composed of rounded to blocky amphibole crystals 0.8-2.5 mm in size, with finer grained interstitial plagioclase and ilmenite and minor quartz (Fig. 20a). Plagioclase content remains consistent at 25-30 % along strike of the unit. Weathered surfaces exhibit a honeycomb-like texture (Fig. 20b) that characterises and gives its name to this unit. Amphibole crystals are typically significantly deformed, and often show deformed crystallographic axes in the form of a strong undulose extinction (Section 6.5.3).

5.2.3 Rothsay Sill

The Rothsay Sill is a 550 m-thick mafic-ultramafic layered sill intruded at the contact between supracrustal rocks of the Two Peaks Volcanics and Beryl West Volcanics. The sill is named after the historical Rothsay gold deposit that is hosted by these rocks. Exposure is good in the north and in the far south but is patchy elsewhere. The base of the Rothsay Sill consists of several metres of a poorly exposed and altered unit, dominated by a fibrous mass of tremolite: likely the alteration product of an ultramafic precursor. This is overlain by a thick body of medium grained (2-4 mm) dolerite, with 30-40% feldspar, the top of which is marked by an incorporated < 50 m thick horizon of variolitic basalt.

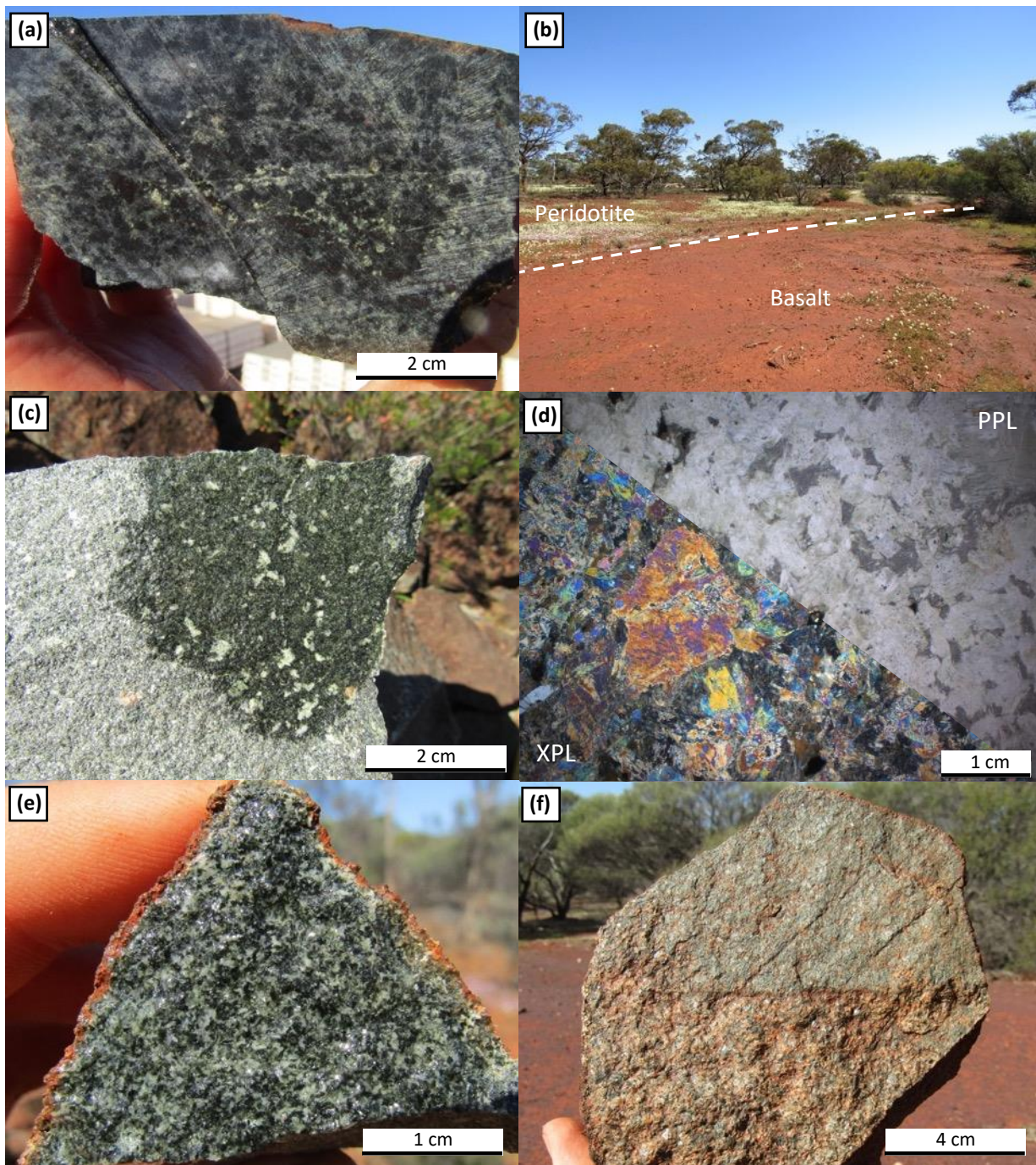


Figure 21: Photographs of rocks comprising the Rothsay mafic-ultramafic sill. **(a)** Serpentised ultramafic with carbonate alteration and a relic cumulate texture (loc. 6.140); **(b)** Contact between ultramafic peridotite and basalt marked by wildflower abundance, which grow preferentially on Fe-rich ultramafic units (loc. 16.079); **(c)** Outcrop of porphyritic pyroxenite with distinctive white phenocrysts in a dark fine-grained groundmass (loc. 16.080); **(d)** Thin section photomicrograph of porphyritic pyroxenite showing tremolite crystals displaying a relic cumulate texture (loc. 9.005a, sample ROTH007); **(e)** Evolved equigranular gabbro with 50% feldspar content towards the top of the sill (loc. 16.089); **(f)** Sharp contact between two intrusives of different crystal size and feldspar-content (loc. 15.014).

A poorly exposed ultramafic unit from 25-45 m in thickness occurs above the basaltic horizon. The ultramafic rock typically comprises a dark, fine grained and highly magnetic groundmass, subject to serpentinisation and carbonate alteration, with relict cumulate textures (Fig. 21a; see Section 6.5.1). This unit is interpreted as a

serpentinite, derived from a cumulate olivine-bearing ultramafic rock of peridotite composition. Weathered surfaces have a characteristic lumpy appearance and in highly altered areas, fibrous chrysotile veining and magnetite veinlets crosscut outcrops, and chalcedony occurs as float locally. The unit is largely continuous along strike but does pinch out in several locations. When under superficial cover, contacts with this unit were identified by vegetation and wildflower density, which was much greater above the ultramafic cumulate compared to surrounding lithologies (Fig. 21b).

A distinctive, well exposed < 40 m-thick unit of porphyritic pyroxenite overlies the ultramafic cumulate. This unit comprises a non-magnetic assemblage of 2-6 mm amphibole (tremolite) phenocrysts in an equicrystalline groundmass of 1 mm amphibole crystals and up to 10% interstitial altered feldspar (Fig. 21c) and exhibits a relict cumulate texture in thin section (Fig. 21d; see section 6.5.2). Notably, phenocrysts vary in colour from white in the southwest, to colourless-grey in the north. The amphibole-dominant mineralogy and cumulate textures suggests the protolith was a pyroxenitic cumulate rock, crystallised above the olivine-bearing cumulate immediately below. Outcrops in the south occur as prominent mounds of rounded boulders and are typified by a pitted appearance from preferential weathering of phenocrysts. In the north, porphyritic pyroxenite forms a prominent E-W trending, 40 m-elevated ridge. This cumulate-textured pyroxenite grades upwards into a coarser gabbro, with crystals up to 1-1.5 cm in size and a more leucocratic composition; over 50% feldspar content is observed in the southwest near the Rothsay mining centre (Fig. 21e). Crystal size decreases upwards to a moderately well-exposed dolerite (1-2 mm), which constitutes the upper portion of the Rothsay Sill. This distinct sequence of rocks in the upper portion of the sill – serpentinite, porphyritic pyroxenite, leucogabbro and dolerite – is fundamental for distinguishing structural repetition in the Rothsay Shear Zone (RSZ) in the far southwest, where the sequence is repeated three times. Within the upper dolerite, portions of coarser gabbroic rocks are present and some pieces of subcrop show sharp contacts between intrusions of differing crystal size (Fig. 21f). The Rothsay Sill represents the uppermost unit that is only found on the eastern side of the RSZ; all overlying rocks are dissected by the shear zone.

5.2.4 Gardner Sill

The Gardner Sill is a layered mafic-ultramafic sill intruded between the Beryl West Volcanics and the Mulga Volcanics and varies in thickness from 650 m east of the RSZ, to 950 m in the west. The Gardner Sill is the best example of a differentiated, layered mafic-ultramafic sill in the area, comprising an ultramafic, cumulate base, a gabbroic core, and an evolved leucogabbroic top. It is named after a historical bore located above constituent rocks in the southwest of the study area (Fig. 11). The sill is dissected by the RSZ and as a result, is thicker and more differentiated to the west.

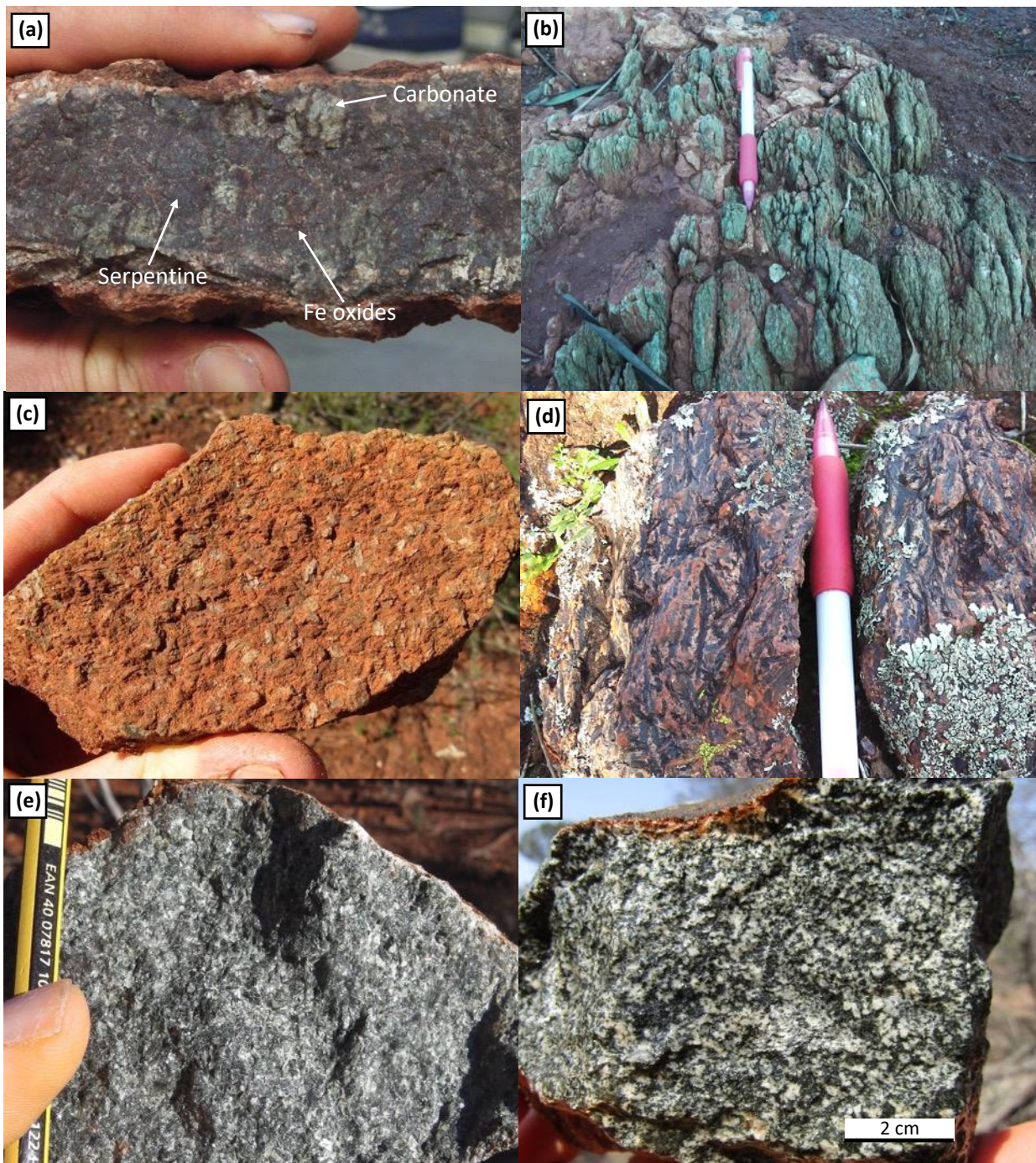


Figure 22: Photographs of rocks characterising mafic-ultramafic rocks of the Gardner Sill. **(a)** Carbonate altered serpentised ultramafic, showing green carbonate, grey serpentine and red specks of iron oxide (loc. 8.122); **(b)** Bright green talc-chlorite schist derived from altered and sheared ultramafic protolith (loc. 5.122); **(c)** Weathered surface of a blocky-textured gabbro comprising coarse amphibole crystals (loc. 5.172); **(d)** Intrusive pyroxenite with feathery, elongate crystals of amphibole, after pyroxene (loc. 5.091); **(e)** Medium-grained, equicrystalline dolerite (loc. 8.041); **(f)** Coarser-grained leucogabbro from the evolved upper portion of the intrusion (loc. 8.178).

The base of the Gardner Sill is marked by a poorly exposed ~100 m-thick unit of a dark, fine-grained, highly magnetic ultramafic cumulate, typically consisting of serpentine (after olivine), tremolite, magnetite and magnesite as a consequence of hydration and carbonation reactions (Fig. 22a). The ultramafic protolith is interpreted as the olivine-bearing cumulate at the base of the mafic-ultramafic intrusion, of peridotitic composition. Magnetite is locally present as 1-4 mm grains and mm-scale veinlets, in addition to needle-

shaped ilmenite crystals 0.1-2 mm in length. Fibrous chrysotile veinlets 2-20 mm in width crosscut outcrops in the far west. Weathered surfaces have characteristic lumpy appearance, as is the case for equivalent ultramafic cumulates in the underlying Rothsay Sill. Along its strike length, further ultramafic alteration products - chrysotile, talc and yellow-white chalcedony - are found as float on superficial cover. In more highly altered areas, the unit is associated with talcose, fibrous masses of tremolite – also derived from the ultramafic precursor. The ground overlying the unit is typically densely vegetated and feels unusually soft underfoot. Close to the RSZ, the ultramafic cumulate is represented by a highly foliated and magnetic, bright green talc-chlorite(-fuchsite) schist (Fig. 22b).

The rocks overlying this basal ultramafic unit differ on either side of the RSZ and so will be described independently below. East of the RSZ, the ultramafic unit encloses a discontinuous lens of non-magnetic dolerite up to 80 m in thickness, and is overlain by a ~60 m equicrystalline, coarse grained gabbro with crystals up to 1 cm and distinct blocky appearance (Fig. 22c). This unit grades upwards into a well exposed dolerite, with 1-2 mm crystals and 35% feldspar content (Fig. 22e). Dolerite outcrops as a series of stacks composed of large, rounded boulders subject to onion-skin weathering, the typical outcropping manner of mafic intrusive rocks in the area. The top 250 m of the intrusion reverts to a coarser grained gabbro, in which feldspar content gradually increases with stratigraphic height. The uppermost 50 m of the intrusion is leucogabbroic, with 2-5 mm crystals, ~60 % feldspar content and represents the most evolved portion of the intrusion (Fig. 22f). Intense epidote and chlorite alteration in some parts of this horizon are indicative of high fluid flow. The Gardner Sill thins to the east, possibly due to attenuation into the Enchanted Shear Zone.

To the west of the RSZ, the basal ultramafic layer is underlain by a poorly exposed dolerite and is overlain by a 100 m-thick unit composed largely of gabbro with tabular actinolite crystals 5-8 mm in size. Overlying this gabbro is a 70 m-thick pyroxenite-rich (>75%) gabbro unit, dominated by feathery pyroxene (now amphibole) crystals up to 2-4 cm in size, separated by interstitial feldspar crystals (Fig. 22d). This intrusive pyroxene-dominant unit has a similar appearance to that of spinifex texture found in supracrustal volcanic rocks of the Beryl West Volcanics and Mulga Volcanics. This layer is succeeded by a further 120 m layer of equicrystalline gabbro with an average crystal size of 4-6 mm, which in turn grades upwards into a ~100 m layer of less well exposed, medium grained (1-2 mm) dolerite. The top 20 metres of this doleritic unit, which is in upper contact with a BIF horizon, is relatively evolved and contains visible quartz crystals in one locality, thought to be primary. A second ultramafic cumulate layer is present above the dolerite and BIF, very poorly exposed but when observed, with identical characteristics and features to that of the equivalent, underlying ultramafic layer. The top of the Gardner Sill to the west of the RSZ consists of a ~300 m-thickness of medium grained dolerite, essentially unexposed other than a substantial subcrop in the far southwest. The Gardner Sill typifies a well-layered and differentiated mafic-ultramafic sill and demonstrates the lateral variation possible along strike within the individual sill complexes.

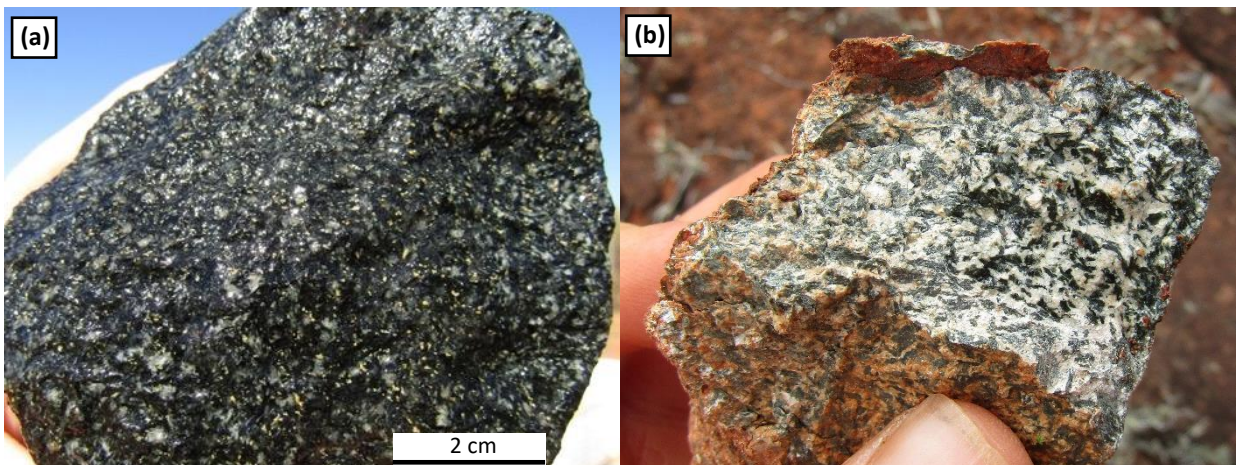


Figure 23: Photographs of quartz diorite that characterises the top portion of the Damperwah Sill. **(a)** Sample of quartz diorite with distinctive white-clear crystals of feldspar and quartz and yellow grains of leucoxene (loc. 11.053); **(b)** Sample of diorite from the upper Damperwah Sill in the far west of the study area, with highly elevated feldspar content and discernible yellow leucoxene (loc. 2.077).

5.2.5 Damperwah Sill

The Damperwah Sill is a 650-750 m-thick mafic intrusion that intrudes the upper part of the Mulga Volcanics, named after a historical well overlying constituent rocks in the southwest of the study area (Fig. 11). The sill is generally very poorly exposed and only outcrops in a small number of localities; it has otherwise been identified and characterised by float present above superficial cover. For this reason, the stratigraphy and features of this sill are not very well understood. The Damperwah Sill is essentially unexposed east of the RSZ, however, float is present that consists of dolerite with 1-3 mm crystals and also indicates the presence of multiple inclusions of fine-grained basalt within the lower part of the sill. A discontinuous <50 m-thick raft of BIF and shale is also present within the intrusive complex over a strike length of ~ 3km. The base of the sill is exposed in a 150-metre elevated outcrop in the northwest of the field area (loc. 1.034), an anomalous exposure of an otherwise poorly outcropping complex. Here, it comprises a medium grained (2-3 mm) dolerite with a feldspar content of approximately 40%, apparently more evolved than the lower portions of other intrusions. Elsewhere, further doleritic and occasional coarser-grained (4-5 mm) equivalents are found as float.

The upper portion of the Damperwah Sill is more evolved, consisting of a medium-grained intermediate-mafic rock with > 60% felsic mineral content and elongate amphibole phenocrysts up to 6 mm in length. In the east of the study area (loc. 11.053), one such subcropping unit has a mineralogy and textures consistent with a quartz diorite. The unit contains quartz crystals up to 2 mm in size, coarse and euhedral (> 0.5 mm) zircon crystals, and distinctive yellow leucoxene grains, resulting from breakdown of Ti-bearing minerals, primarily ilmenite (Fig. 23a). Petrographic analysis also reveals granophyric textures, comprising intergrowths of quartz in alkali feldspar crystals (Section 6.5.4). Similar evolved quartz dioritic rocks can be found in the upper ~200

metres of the Damperwah Sill over a strike length in excess of 20 km (Fig. 23b). In general, the Damperwah Sill appears to be more evolved than other mafic intrusive complexes in the area.

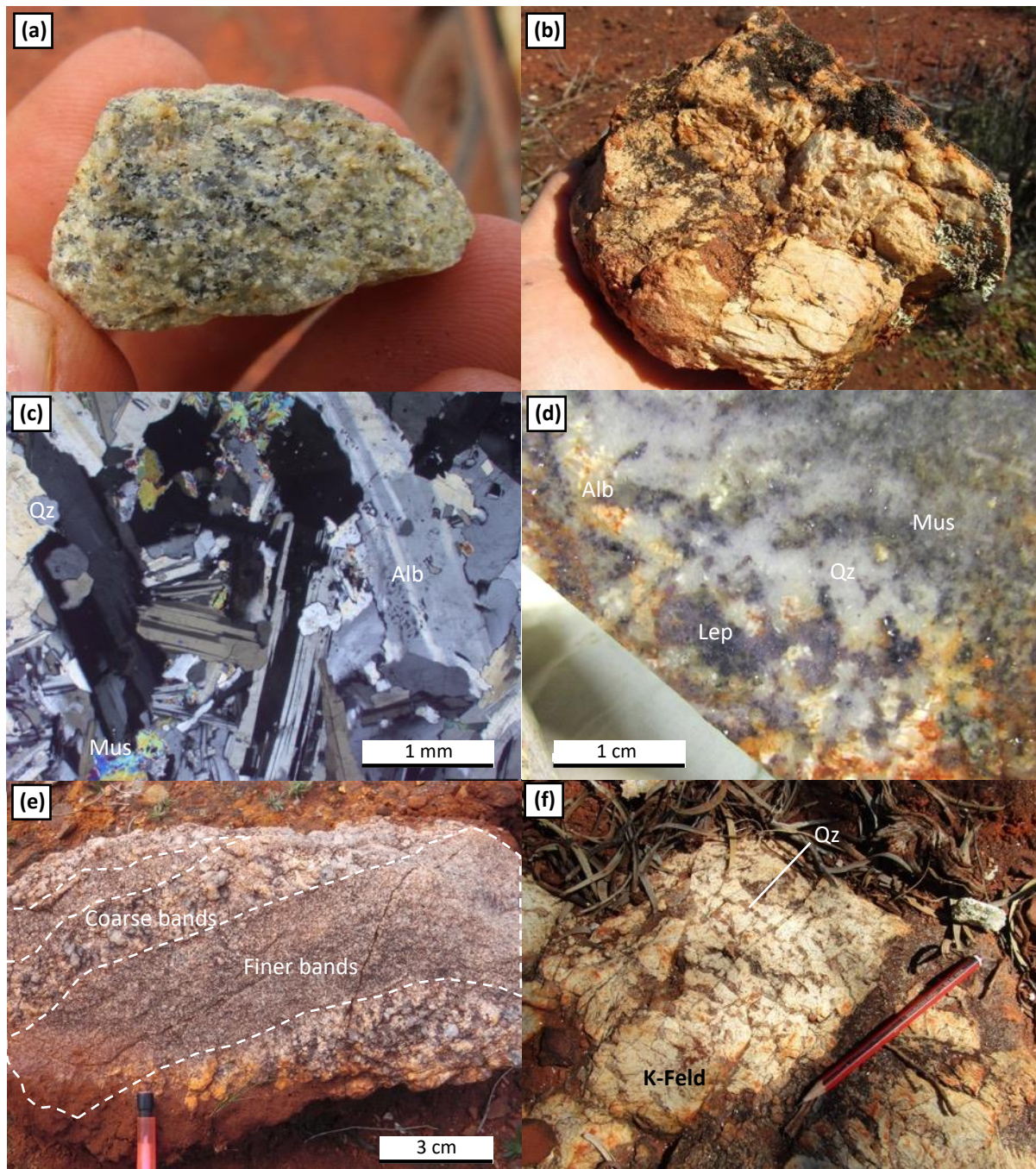


Figure 24: Photographs of rocks comprising granite (a) and pegmatite dykes (b-f) in the study area. (a) Granite identified in drill chips representing the unexposed granite in the southwest of the area (loc. 12.072); (b) Pegmatite sample containing large, euhedral feldspar crystals with muscovite and quartz (loc. 13.016); (c) Thin section photomicrograph (xpl) of a typical pegmatite sample comprising albite (Alb), quartz (Qz), muscovite (Mu) (loc. 6.052, sample ROTH014); (d) Cut surface of a Li-bearing pegmatite comprising purple lepidolite (Lep), quartz, muscovite and albite (loc. 6.052, sample ROTH014); (e) Block of pegmatite showing crystal size variation with coarser-grained bands separating finer-grained aplites (loc. 6.050); (f) Outcrop showing well-developed graphic textures, comprising intergrowths in quartz in a large >10 cm crystal of K-feldspar (K-Feld) (loc. 16.066).

5.2.6 Dolerite Dykes

Discordant dolerite dykes are very poorly exposed in the area and are often represented by highly vegetated creeks and valleys. In rare instances where float is observed at the surface, these intrusions consist of medium-grained (2-4 mm) dolerite and are undeformed and not metamorphosed. Crucially, the doleritic dykes are weakly to moderately magnetic, in contrast to the typical non-magnetic nature of most doleritic and gabbroic rocks of mafic-ultramafic sills. Consequently, the dykes are evident on aeromagnetic imagery; at least seven can be distinguished in the project area. The dykes range in thickness from a few metres to 30 m, have lengths in excess of 5-10 km and orientations typically NW-SE and NE-SW. They cross-cut both the volcano-sedimentary stratigraphy and surrounding granitoids, as well as folds, faults and shear zones, and thus are interpreted as postdating magmatism and deformation. The dykes are essentially straight along their strike length and are not affected by the topography, suggesting they are steeply dipping to vertical.

5.3 Felsic Intrusive Rocks

5.3.1 Granite

Granite is not exposed within the field area. The only evidence for the presence of felsic intrusive rocks are historical drill chips left as spoil at the surface in the far east (e.g., loc. 12.071). At these localities, a monzogranite comprising medium-grained, 1-2 mm crystals of plagioclase feldspar, K-feldspar, quartz and biotite mica is present beneath thick (>5 m) superficial cover (Fig. 24a). This corresponds to the margin of the 50 x 25 km granitic pluton, the Seeligson Monzogranite, to the southeast of the area. There is a distinct change in a sand-dominated regolith overlying areas of granitic bedrock in this area.

5.3.2 Pegmatites

Felsic pegmatite dykes discordantly intrude the supracrustal stratigraphy of the area and are well exposed in the south but only present as float and subcrop elsewhere. Pegmatites crosscut folding, faults and shear zones and invariably lack a fabric, thus are interpreted as post-deformational. Pegmatite dykes also cross-cut shear-hosted lode-gold mineralisation at the Rothsay Mining Centre. The dykes are typically 1-5 m in width and increase in abundance towards the Seeligson Monzogranite pluton to the southwest. In this area, the pegmatites are both discordant and concordant with supracrustal units and appear to be concentrated in basalts of the Two Peaks Volcanics. The mineralogy of the pegmatites is variable but composed primarily of quartz, albite and K-feldspar with minor muscovite and biotite (Fig. 24b, 3.24c). Locally, lithium-bearing lepidolite mica occurs as pink-purple rosettes (Fig. 24d) and light green apatite is present as 1-3 mm crystals with a greasy lustre. Rare occurrences of a dark green mineral are possibly beryl, as has been exploited historically from a pegmatite-hosted beryl mine located immediately south of the study area. Crystal sizes vary

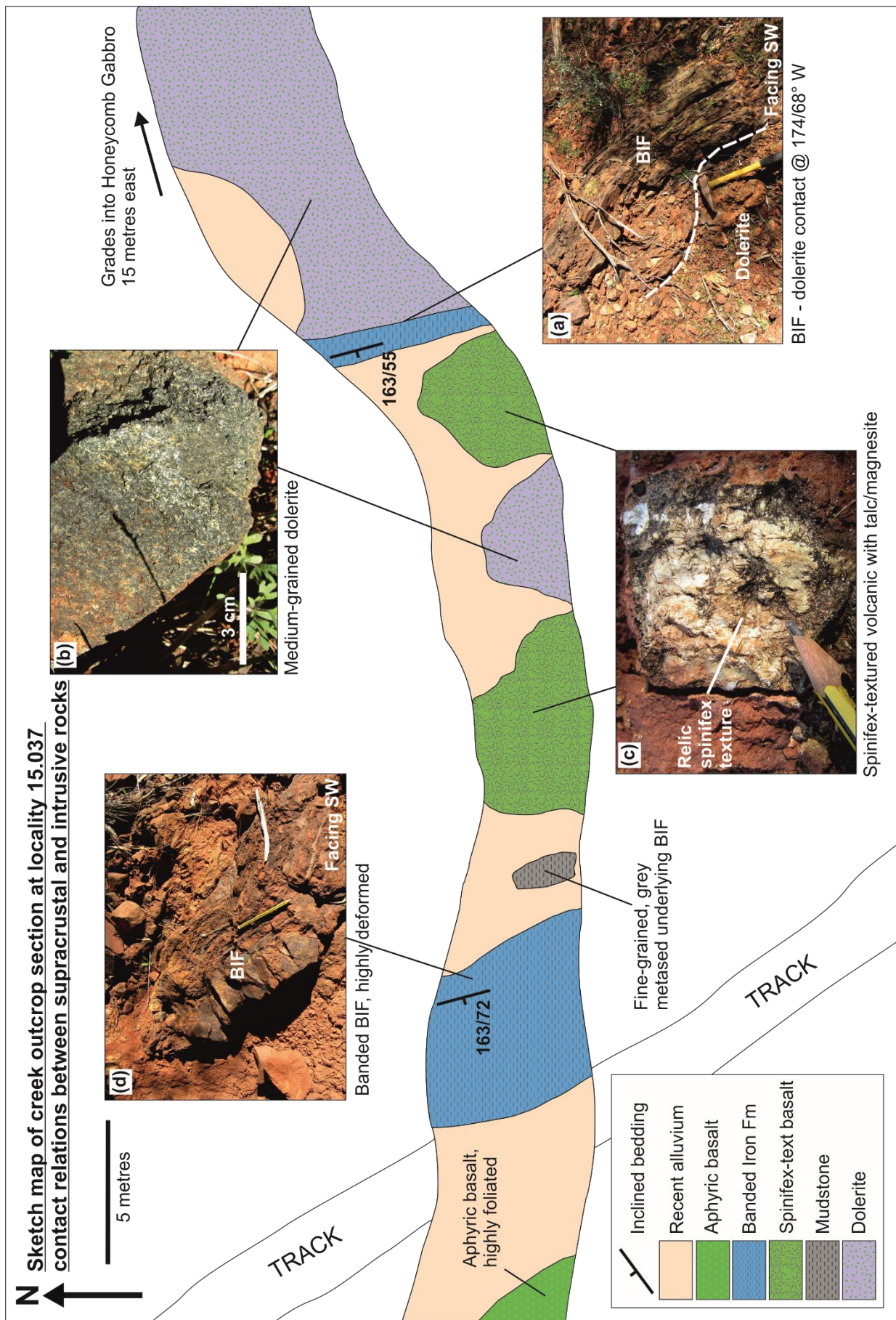


Figure 25: Sketch map of an outcrop section in a creek at locality 15.037, showing the contact relations between supracrustal rocks and concordant dolerite intrusive rocks.

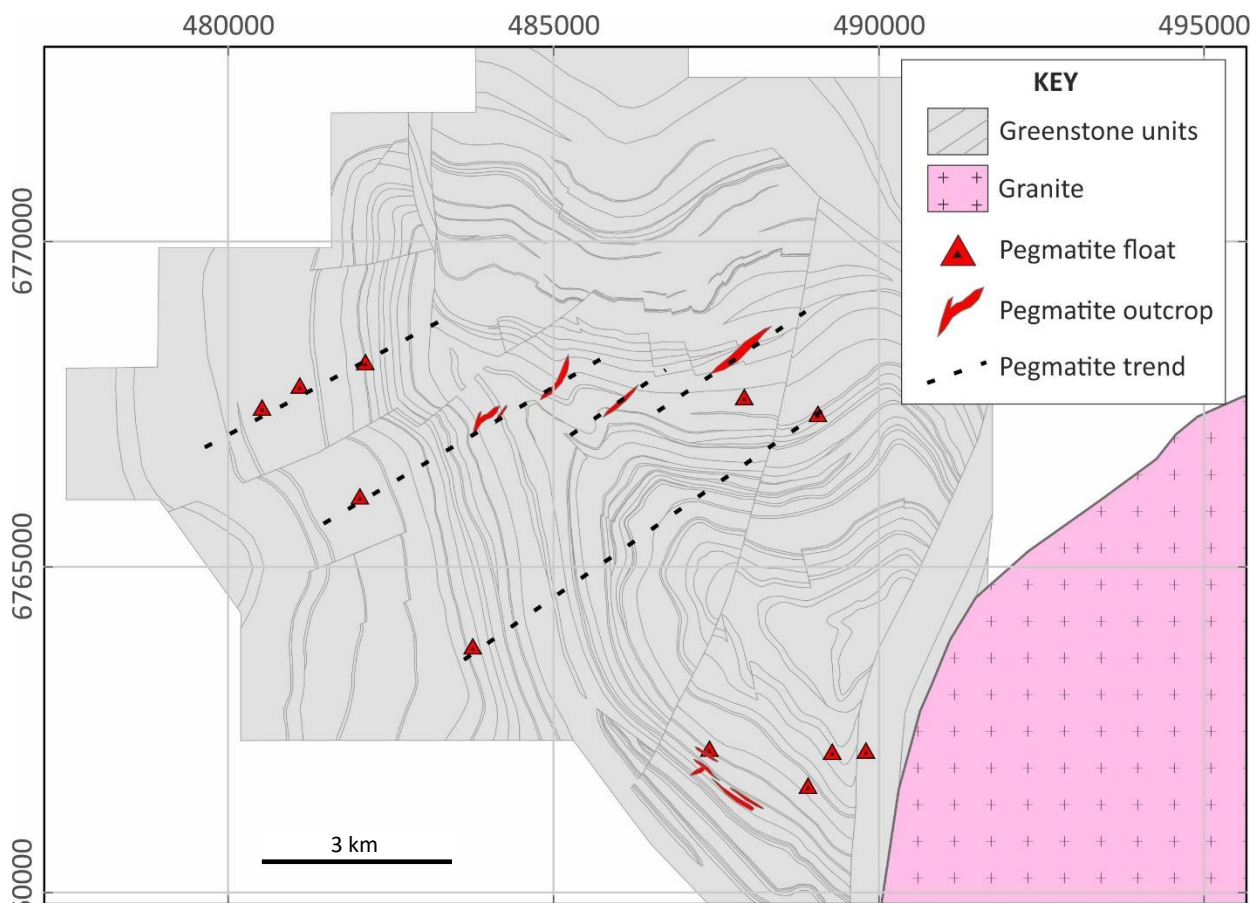


Figure 26: Sketch geological map showing the distribution of pegmatite float and outcrop in the Rothsay Fold area relative to the granite-greenstone contact. Pegmatites form at least 4 parallel dykes trending NE-SW up to 10 kilometres from the granite-greenstone contact.

considerably from 1-2 mm up to 10 cm, with some portions exhibiting a porphyritic texture, comprising coarse 1cm + crystals of feldspar in a finer-grained groundmass of mica, feldspar and quartz. Parallel banding of coarser-grained pegmatitic portions and aplitic finer portions are common in some dykes (Fig. 24e). Graphic textures are also present on a mm to 10 cm scale, comprising intergrowths of quartz in large crystals of K-feldspar (Fig. 24f).

5.4 Intrusive Relations

Contacts between supracrustal rocks and intrusive rocks are rarely observed in outcrop. However, typical contact relationships can be largely distinguished from areas of subcrop. A conspicuous feature of intrusive sills is the enclosure of multiple 'screens' of BIF observed in all mafic-ultramafic sills. These screens are often continuous for several kilometres along strike and have apparent thicknesses of up to 20 metres. Similar laterally continuous lenses of basalt are also contained within the Rothsay and Damperwah sills and can locally be distinguished from fine-grained intrusive dolerite by spherulitic features. The composite Mountain View

Sill contains two laterally discontinuous horizons of basalt and BIF up to 120 metres in thickness which thin and appear to pinch out along strike; interpreted as rafts of supracrustal units within the complex. The Mountain View Sill also contains metre scale lenses of underlying felsic volcaniclastic rocks (Macs Well Clastics) close to its base and occurs as lenses of dolerite within underlying units. These features are consistent with a pre-existing volcano-sedimentary supracrustal succession intruded by a network of mafic-ultramafic sill complexes. At one particularly good creek exposure – locality 15.037 – the contact between the Honeycomb Gabbro and overlying Two Peaks Volcanics is present in outcrop (Fig. 25). Dolerite of the former is directly overlain by a 1 m-thick BIF unit, which in turn is overlain by 20 m of spinifex-textured basalt and a further ~8 m BIF (Fig. 25). The dolerite-BIF contact is essentially parallel to bedding exhibited by both BIF units, consistent with the concordant nature of intrusions. Within the spinifex-textured unit, a 6 m-thick medium-grained dolerite is present but is not found elsewhere along strike. This ostensibly represents a minor intrusion of the more substantial Honeycomb Gabbro into overlying supracrustal rocks.

Subcrops of pegmatite dykes crosscut the volcano-sedimentary stratigraphy and are typically oriented NE-SW. When these outcrops are correlated with float occurrences, at least four parallel NE-SW trending dykes can be distinguished in the area (Fig. 26). These dykes are parallel to D₅ NNE-trending faults (Section 7.7) and increase in abundance towards the supracrustal contact with Seeligson Monzogranite, suggesting that they were emplaced during intrusion of this granitic pluton.

6. Petrography

6.1 Introduction

Petrographic analysis has been undertaken on thin sections from a suite of 46 representative samples from the major stratigraphic units identified in the Rothsay area; namely the Chulaar Group, Willowbank Clastics, and Warriedar Suite. In this section, the petrography of rocks comprising each of these stratigraphic groups is described. Details of petrographic samples are given in Table 2 and sample locations are displayed on Figure 27.

6.2 General Overview of Metamorphic Features

All supracrustal and mafic-ultramafic intrusive rocks in the Yalgoo-Singleton greenstone belt have been affected by regional metamorphism (Watkins & Hickman, 1990). Consequently, the original mineralogy of many rocks has been modified and primary minerals are frequently replaced by metamorphic minerals. In mafic extrusive and intrusive igneous rocks, metamorphic assemblages vary from actinolite-chlorite-epidote-albite to hornblende-actinolite-albite, demonstrating upper greenschist to lower amphibolite-grade metamorphism. Primary pyroxene in mafic volcanic and intrusive rocks is frequently pseudomorphed by metamorphic amphibole; most commonly actinolite although hornblende and tremolite are present in some units. Several Warriedar Suite intrusive samples contain rare relict primary clinopyroxene and orthopyroxene, however, pyroxene is no longer present in most intrusive samples and all Chulaar Group volcanic rocks. This includes pyroxene spinifex-textured volcanic rocks of the Chulaar Group, in which pyroxene phenocrysts are invariably replaced by metamorphic actinolite ± hornblende ± chlorite. In this section, the term pyroxene-spinifex will be used in reference to the original mineralogy and distinct texture of these volcanic rocks, despite pyroxene no longer being part of the mineral assemblage. Intrusive and volcanic rocks with olivine-bearing protoliths have all been subject to serpentisation and primary olivine is seldom preserved within the serpentised alteration assemblage.

Sample No.	Eastings	Northings	Locality No.	Stratigraphic Group	Stratigraphic Unit	Mapped Lithology	Petrographic Description
BAD002	495582	6791719	/	Warriedar Suite	<i>NE of study area</i>	Peridotite	Serpentinised, porphyritic ultramafic cumulate
CHU003	502841	6797811	/	Warriedar Suite	<i>NE of study area</i>	Peridotite	Serpentinised, carbonate-altered ultramafic cumulate
CHU009	505552	6799362	/	Warriedar Suite	<i>NE of study area</i>	Peridotite	Serpentinised ultramafic cumulate
ROTH009	487373	6770901	8.054	Warriedar Suite	Damperwah Sill	Dolerite-gabbro	Metadolerite
ROTH034	491580	6767737	11.053	Warriedar Suite	Damperwah Sill	Dolerite	Granophyric meta-quartz diorite
ROTH049	478983	6766916	2.078	Warriedar Suite	Damperwah Sill	Gabbro	Equicrystalline metagabbro
ROTH008	487094	6768820	8.104a	Warriedar Suite	Gardner Sill	Dolerite-gabbro	Partially sericite-clay altered metagabbro
ROTH011	486684	6768805	8.118	Warriedar Suite	Gardner Sill	Dolerite	Lineated metadolerite
ROTH019	487938	6768480	8.167a	Warriedar Suite	Gardner Sill	Gabbro	Harrisitic-textured metagabbro
ROTH035	486172	6769022	8.178	Warriedar Suite	Gardner Sill	Gabbro	Saussuritised meta-quartz diorite
ROTH007	487822	6767371	9.005a	Warriedar Suite	Rothsay Sill	Dolerite	Porphyritic metapyroxenite
ROTH029	488997	6767579	11.015	Warriedar Suite	Rothsay Sill	Gabbro	Porphyritic metagabbro
ROTH064	484912	6763970	15.020a	Warriedar Suite	Rothsay Sill	Dolerite	Foliated metadolerite
ROTH077	487091	6761347	16.080	Warriedar Suite	Rothsay Sill	Pyroxenite	Saussuritised porphyritic metapyroxenite
ROTH006	487905	6766786	9.008	Warriedar Suite	Honeycomb Gabbro	Gabbro	Porphyritic metagabbro
T2	485318	6766539	6.035	Warriedar Suite	Honeycomb Gabbro	Gabbro	Honeycomb-textured metagabbro
ROTH024	486478	6766296	9.081	Warriedar Suite	Mountain View Sill	Pyroxenite	Poikiloblastic metagabbro
ROTH067	486433	6763276	16.012	Warriedar Suite	Mountain View Sill	Dolerite-gabbro	Random acicular pyroxene spinifex textured metabasalt
ROTH044	490297	6771622	10.093	/	Willowbank Clastics	Felsic volcanioclastic rocks	Felsic volcanioclastic metasandstone
ROTH053	478122	6766769	2.093	/	Willowbank Clastics	Metasedimentary rocks	Porphyroblastic andalusite-cordierite metapelite
ROTH061	490378	6772361	10.106	/	Willowbank Clastics	Felsic volcanioclastic rocks	Felsic volcanioclastic metasandstone
ROTH080	478231	6766791	2.088	/	Willowbank Clastics	Metasedimentary rocks	Metagreywacke
ROTH081	478190	6766792	2.089	/	Willowbank Clastics	Metasedimentary rocks	Volcanogenic pebbly metasandstone
ROTH001	488853	6770342	10.021	Chulaar Group	Mulga Volcanics	Spinifex-textured basalt	Random acicular pyroxene spinifex-textured metabasalt
ROTH002	487153	6769587	8.107b	Chulaar Group	Mulga Volcanics	Basalt	Aphyric metabasalt

Table 2 (continued overleaf)

Sample No.	Eastings	Northings	Locality No.	Stratigraphic Group	Stratigraphic Unit	Mapped Lithology	Petrographic Description
ROTH003	486969	6769258	8.107a	Chulaar Group	Mulga Volcanics	Spinifex-textured basalt	Random acicular spinifex-textured metabasalt
ROTH004	486997	6769136	8.106a	Chulaar Group	Mulga Volcanics	Basalt	Weakly variolitic metabasalt
ROTH010	487133	6771278	7.070	Chulaar Group	Mulga Volcanics	Basalt	Basalt (traces of random acicular pyroxene spinifex)
ROTH012	486673	6769150	8.116	Chulaar Group	Mulga Volcanics	Variolitic basalt	Variolitic basalt
ROTH012-1	486673	6769150	8.116	Chulaar Group	Mulga Volcanics	Variolitic basalt	Variolitic basalt
ROTH012-2	486673	6769150	8.116	Chulaar Group	Mulga Volcanics	Variolitic basalt	Variolitic basalt
ROTH013	482935	6771919	5.014	Chulaar Group	Mulga Volcanics	Basalt	Meta-andesite
ROTH023	487317	6768951	8.184	Chulaar Group	Mulga Volcanics	Lapilli tuff	Thinly bedded andesitic lapilli tuff
ROTH026	486613	6768948	8.185	Chulaar Group	Mulga Volcanics	Peridotite	Ultramafic extrusive olivine cumulate
ROTH027	486554	6768974	8.188	Chulaar Group	Mulga Volcanics	Spinifex-textured basalt	Aligned acicular pyroxene spinifex-textured metabasalt
ROTH036	487728	6770392	8.045a	Chulaar Group	Mulga Volcanics	Basalt	Random platy/acicular pyroxene spinifex-textured metabasalt
ROTH050	478533	6766821	2.085	Chulaar Group	Mulga Volcanics	Lapilli tuff	Massive andesitic lapilli tuff
T1	486291	6770503	8.070	Chulaar Group	Mulga Volcanics	Spinifex-textured basalt	Random acicular pyroxene spinifex-textured metabasalt
T3	487758	6769700	8.003	Chulaar Group	Mulga Volcanics	Spinifex-textured basalt	Aligned acicular pyroxene spinifex-textured metabasalt
ROTH041	490232	6768970	10.046	Chulaar Group	Beryl West Volcanics	Spinifex-textured basalt	Random platy pyroxene spinifex-textured metabasalt
ROTH048	488770	6768532	10.030	Chulaar Group	Beryl West Volcanics	Basalt	Spherulitic basalt
ROTH005	487905	6767104	9.006	Chulaar Group	Two Peaks Volcanics	Basalt	Aphyric metabasalt
ROTH047	485732	6765490	6.157a	Chulaar Group	Two Peaks Volcanics	Porphyritic dacite	Porphyritic metadacite
ROTH068	485576	6763774	15.032b	Chulaar Group	Two Peaks Volcanics	Spinifex-textured basalt	Random acicular pyroxene spinifex-textured basalt
ROTH062	489567	6765430	12.057	Chulaar Group	Macs Well Clastics	Porphyritic dacite	Porphyritic metadacite
ROTH070	488818	6761438	13.028a	Chulaar Group	Macs Well Clastics	Felsic volcaniclastic rocks	Banded felsic volcaniclastic rock

Table 2: Petrographic sample details, including co-ordinates (GDA94/MGA Zone 50 co-ordinate system), respective locality numbers from geological mapping, the assigned stratigraphic group/unit, mapped lithology and petrographic description.

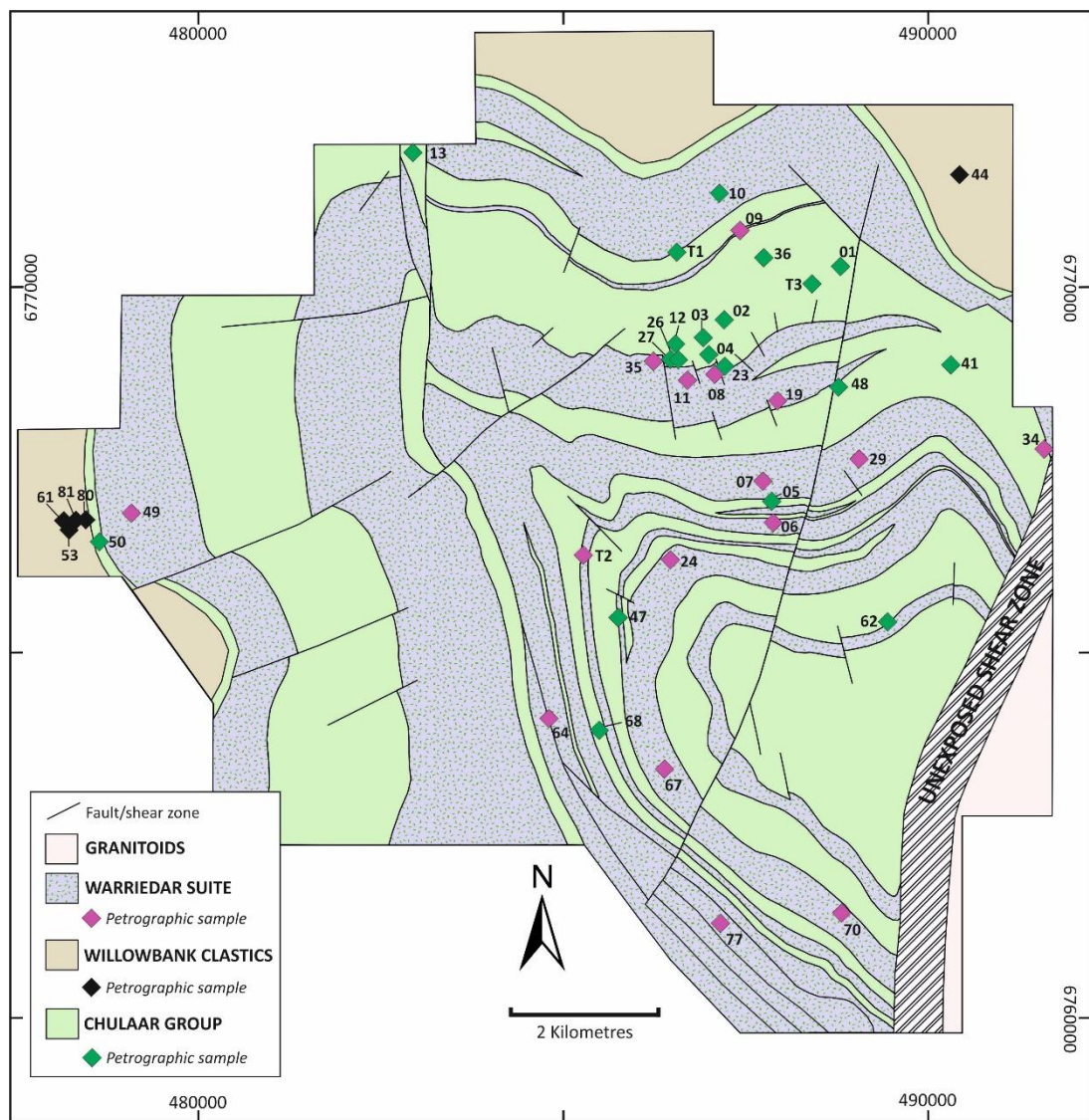


Figure 27: Simplified geological map of the Rothsay area, showing the locations of petrographic samples analysed in this study. Samples are symbolised according the stratigraphic unit to which they are assigned and labelled by sample number (prefix ROTH omitted for all samples apart from T1, T2 and T3). Grid provided in the GDA94/MGA Zone 50 co-ordinate system.

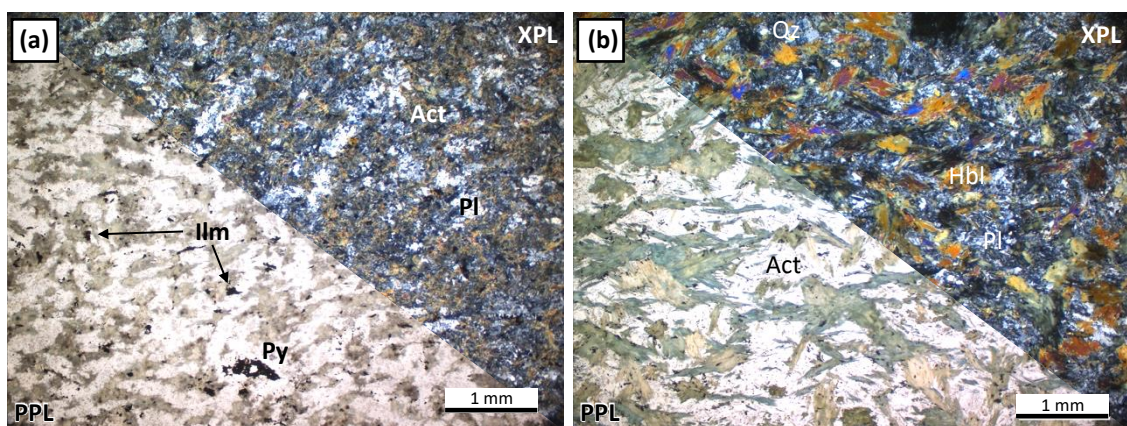


Figure 28: Photomicrographs of Chulaar Group aphyric volcanic rocks. (a) PPL/XPL view of the typical texture and mineralogy of fine-grained basalt from the Mulga Volcanics, comprising mottled plagioclase, actinolite laths, minor quartz and disseminated ilmenite (sample ROTH013); (b) PPL/XPL view of a slightly coarser-grained basalt from the Mulga Volcanics with mottled plagioclase, hornblende laths, acicular actinolite crystals and minor anhedral quartz, preserving a moderate planar fabric defined by amphibole laths (sample ROTH002).

6.3 Chulaar Group

The Chulaar Group encompasses rocks of the Macs Well Clastics, Two Peaks Volcanics, Beryl West Volcanics and Mulga Volcanics, distinguished in Section 5.1. As the petrographic characteristics of volcanic rocks in each of these constituent units are similar, petrographic descriptions are given for the main rock types observed throughout Chulaar Group rocks, with reference to specific units where necessary.

6.3.1 Aphyric volcanic rocks

Volcanic rocks of the Chulaar Group include basalts and basaltic andesites that are typically fine-grained, dark grey, massive, and aphyric in hand specimen. The petrographic samples studied come from the Two Peaks Volcanics and Mulga Volcanics. They are commonly weakly to moderately altered and are characterised by a fine-grained alteration assemblage of plagioclase, actinolite, quartz and ilmenite \pm epidote \pm chlorite \pm tremolite \pm anthophyllite \pm biotite \pm titanite. The rocks are predominantly aphanitic and comprise an equicrystalline groundmass dominated by interlocking crystals of lath-shaped amphibole (<0.3 mm) and tabular, often mottled, plagioclase (<0.5 mm) (Fig. 28a). The coarsest volcanic flows are marginally phaneritic and contain crystals up to 1 mm in length (Fig. 28b). In most basaltic and andesitic rocks, the dominant amphibole pseudomorphing primary pyroxene is actinolite, however, high-Mg volcanic rocks also contain variable amounts of tremolite and anthophyllite. The ratios of amphibole relative to plagioclase range between 67:33 and 48:52 and very fine-grained interstitial material often includes single acicular needles of metamorphic actinolite (Fig. 28b).

Quartz is regularly present as 0.1-0.2 mm anhedral crystals in aphyric volcanics and varies in abundance between 1-6%, typically occurring in close association with chlorite, epidote, biotite and variably saussuritized Ca-rich plagioclase crystals in more highly altered samples. In several instances, elevated quartz content (up to 15%) corresponds to units crosscut by abundant mm-scale quartz veinlets, signifying increased hydrothermal alteration. Disseminated oxides are ubiquitous within the groundmass (up to 1%), occurring predominantly as 0.1-0.2 mm needles of ilmenite, with lesser anhedral magnetite grains (Fig. 28a). A disseminated sulphide assemblage of pyrite \pm chalcopyrite \pm pyrrhotite is observed in a minority of units. Aphyric rocks proximal to faults and shear zones often exhibit nematoblastic textures, in which both linear and planar fabrics are preserved by actinolite laths (Fig. 28b).

6.3.2 Porphyritic volcanic rocks

Porphyritic volcanic rocks of the Chulaar Group consist of basalts, andesites and dacites characterised by the occurrence of tabular plagioclase phenocrysts in a finer-grained holocrystalline groundmass of actinolite and plagioclase. These rocks are volumetrically less abundant than aphyric and spinifex-textured rocks and are most commonly found near the base of the Two Peaks Volcanics (Section 5.1.2) and within the upper Macs Well Clastics (Section 5.1.1) in the Rothsay area. Phenocryst abundances vary from 1% to ~20% of the units and crystal sizes range between 0.5-3.5 mm, but most frequently are ~1 mm. In most units, plagioclase exhibits euhedral-subhedral shapes and preserves well-developed polysynthetic twinning, however, volcanic units containing anhedral plagioclase phenocrysts with mottled appearances and only weak traces of twinning are also present (Fig. 29a). The groundmass of porphyritic Chulaar Group rocks is essentially equivalent to that of aphyric volcanic rocks described above.

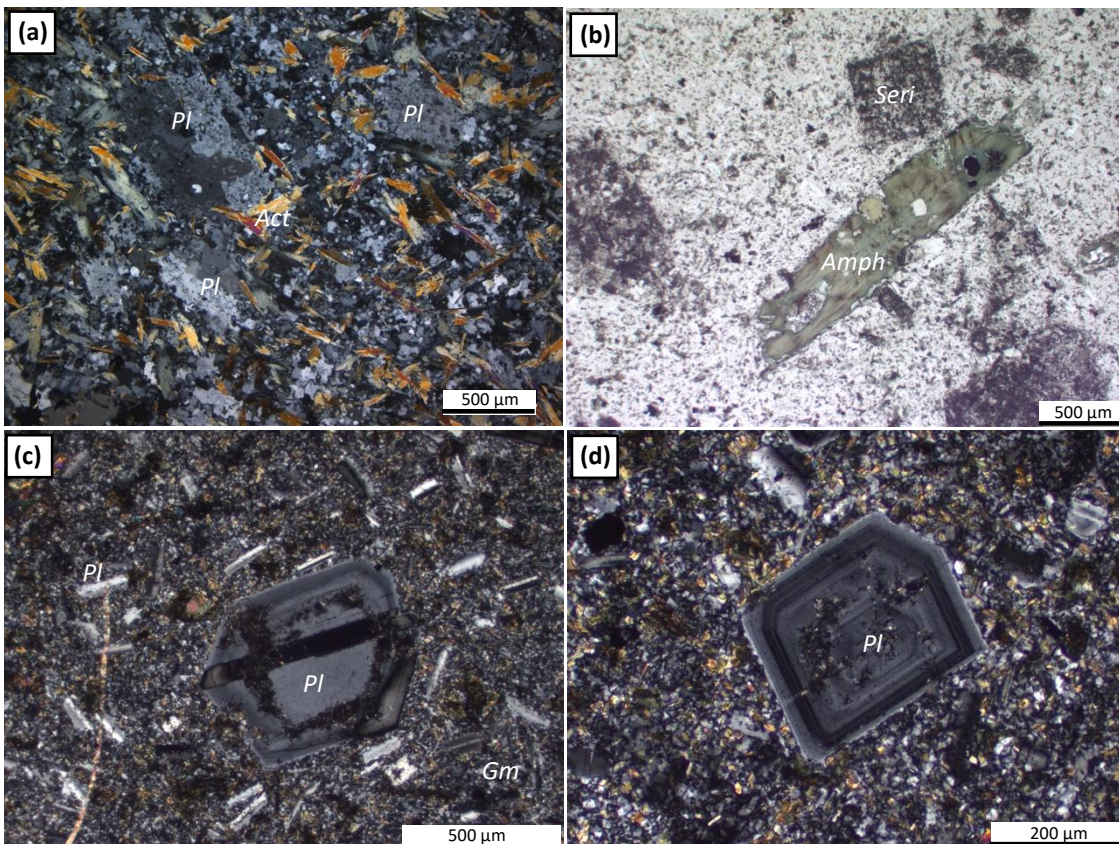


Figure 29: Photomicrographs of Chulaar Group porphyritic volcanic rocks. **(a)** XPL view of a dacite from upper part of the Macs Well Clastics, displaying mottled plagioclase phenocrysts and remnant twinning in a plagioclase, actinolite and quartz-bearing groundmass (sample ROTH062); **(b)** PPL view of sericitized plagioclase phenocrysts and elongate amphibole phenocryst with embayed margins in a Two Peaks Volcanics porphyritic dacite (sample ROTH047); **(c)** XPL view of the same Two Peaks Volcanics porphyritic dacite comprising a euhedral twinned and zoned plagioclase phenocryst with partial sericite alteration, surrounded by tabular aligned microphenocrysts deflecting around the phenocryst (sample ROTH047); **(d)** XPL view of a phenocryst with well-developed compositional zoning surrounding a rounded core (sample ROTH047).

One particular porphyritic dacite sampled from the lower Two Peaks Volcanics (sample ROTH047) contains two phenocryst phases occupying ~20% of the rock. Plagioclase phenocrysts are most abundant (~75%) and occur as subhedral-euhedral 0.6-2 mm crystals, exhibiting moderately to well-developed compositional zoning and polysynthetic twinning. Approximately half of plagioclase phenocrysts have been completely sericite-altered, such that only crystal outlines and faint relic twinning remains (Fig. 29b). In other crystals, either the core or a specific compositional zone within a phenocryst is sericite-altered (Fig. 29c), suggesting that Ca-rich zones or crystals are preferentially altered relative to Ca-poor areas. Several plagioclase phenocrysts comprise rounded homogenous cores surrounded by euhedral, compositionally zoned margins, indicative of magmatic resorption (Fig. 29d). The remaining (~25%) phenocrysts consist of elongate, subhedral amphibole crystals up to 3.5 mm in length and showing green-brown pleochroism (Fig. 29b). Basal sections are hexagonal with characteristic 120° cleavage intersections and phenocrysts frequently have irregular, embayed margins consistent with resorption (Fig. 29b). Multiple glomerocrysts composed of three to five crystals of plagioclase and amphibole occur in some parts of the unit.

The <0.1 mm holocrystalline groundmass surrounding phenocrysts also contains 0.1-0.15 mm tabular plagioclase microphenocrysts that display a trachytic texture; crystals are typically oriented and deflect around the larger phenocrysts, preserving the flow direction of the lava (Fig. 29c). This suggests that phenocrysts and microphenocrysts crystallised prior to eruption of the lava, likely in two stages due to the bimodal size distribution of crystals. Biotite, quartz and accessory zircon are also present within the holocrystalline groundmass. Porphyritic volcanic units that exhibit various types of spinifex-texture are described separately below.

6.3.3 *Variolitic volcanic rocks*

Basalts and rare andesites towards the top of the Chulaar Group include some units with abundant spherulitic structures, particularly prevalent in the lower portion of the Mulga Volcanics (Section 5.1.4). The rocks are dominated by 0.1-0.3 mm actinolite laths and 0.1-0.2 mm mottled plagioclase crystals, with lesser amounts of quartz and disseminated ilmenite and accessory apatite and pyrite. Spherules are spherical to oblate in shape and range in diameter between 0.5 mm and 12 mm but are of consistent size within a given sample (Fig. 30a). These spherules consist of increased concentrations of plagioclase ± quartz (typically 60-75%) relative to the surrounding groundmass (~10-25%), which is dominated by actinolite (Fig. 30b). Spherules are frequently zoned, with plagioclase-rich (albite) cores grading outwards into the actinolite-dominated groundmass (Fig. 30c). Many of the larger spherules also exhibit a quartz-rich halo around their margins in which plagioclase is almost entirely absent (Fig. 30a), also illustrated by element mapping (Fig. 30d). Further, ilmenite grains are often present near the centre of the spherules. The contacts between overlapping spherules are sharp and

concavo-convex (Fig. 30b, Fig. 30c). In some samples, aligned, elongate phenocrysts of amphibole up to 2 mm in length are present in the spherules and the groundmass, but do not show a consistent orientation and appear to be influenced by the spherules (Fig. 30e). The geometries and features of these spherulitic structures are consistent with a variolitic classification for these Chulaar Group volcanic rocks.

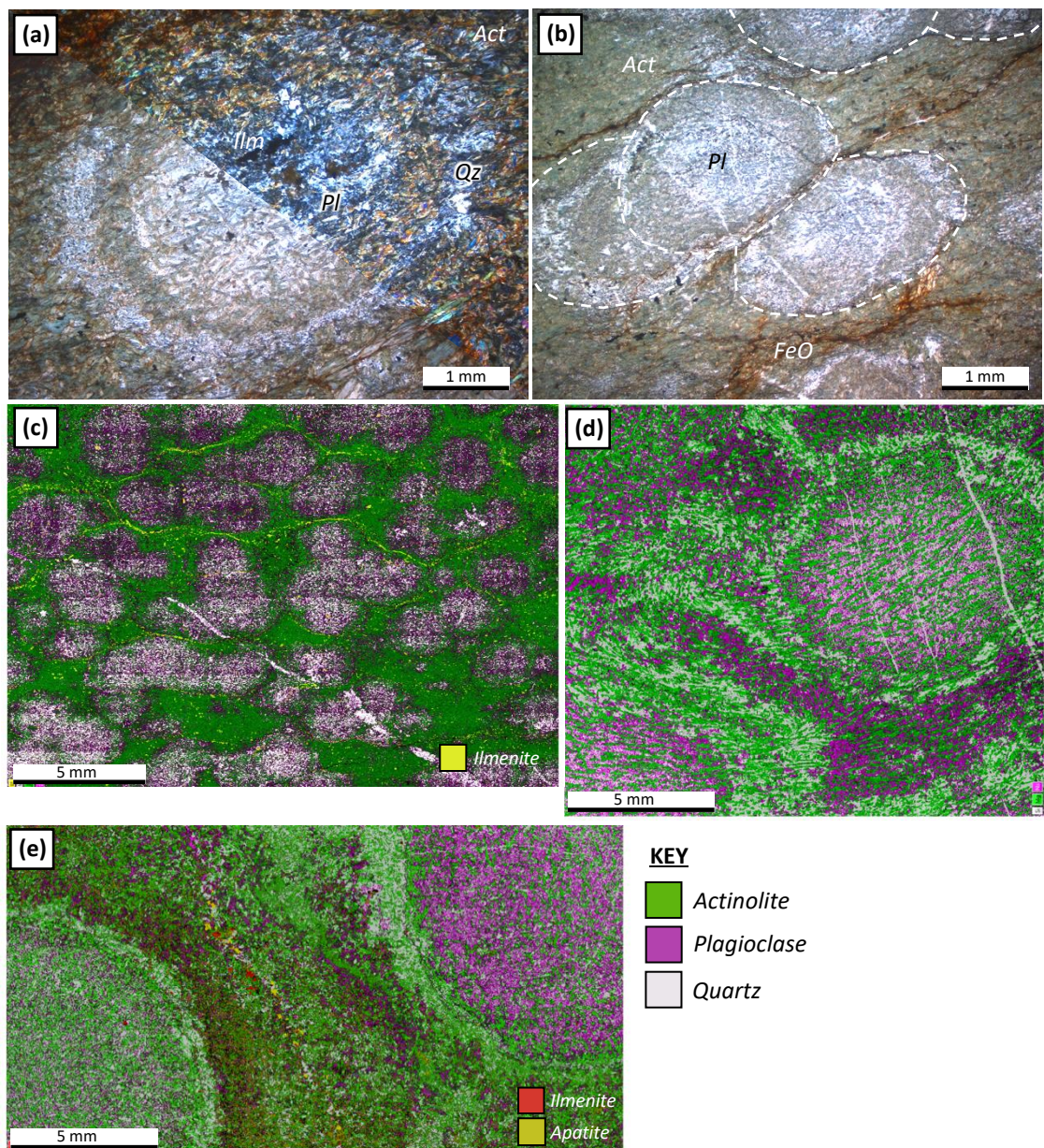


Figure 30: Photomicrographs and element maps of variolitic rocks comprising the Mulga Volcanics, Chulaar Group. (a) PPL/XPL view of a spherule comprising a plagioclase rich core and quartz-rich rim, with an intervening amphibole-rich band (sample ROTH012); (b) Smaller spherules with sharp concavo-convex contacts and higher plagioclase content than the surrounding groundmass (sample ROTH012-2); (c) Element map of ~2 mm spherules (sample ROTH012-2); (d) Element map of ~8mm spherules with plagioclase-rich cores and quartz-rich/plagioclase-poor rims (sample ROTH012); (e) ~12 mm spherules comprising plagioclase-rich cores and quartz-rich rims (sample ROTH012-1). The colour scales are broadly the same on each element map – green corresponds to actinolite, pink/purple corresponds to plagioclase and grey corresponds to quartz. In (c), yellow corresponds to ilmenite, whereas in (e), yellow corresponds to apatite and red corresponds to ilmenite.

6.3.4 Pyroxene spinifex-textured rocks

Pyroxene spinifex-textured rocks are prevalent in the upper parts of the Chulaar Group (e.g., Mulga Volcanics). Petrographic descriptions of these rocks have been separated into the following geometries of pyroxene spinifex-texture observed in hand specimen and thin section; random-acicular, oriented-acicular and random-platy (Arndt et al., 2008; Lowrey et al., 2017), in addition to cumulate basal units associated with thicker spinifex-textured volcanic units.

Cumulate basal unit

The basal portion of a spinifex-textured flow sampled at the base of the Mulga Volcanics in the Rothsay area (Section 5.1.4; Sample ROTH026) is characterised by the presence of ~28% partially serpentinised olivine in a groundmass comprised of serpentine (~30%), tremolite (~35%) and magnetite (~7%). Olivine phenocrysts are typically 1-4 mm in size, highly fragmented and anhedral and in several instances, crystals have been serpentinised to the extent that only a single 0.3 mm olivine fragment remains (Fig. 31a). Several olivine glomerocrysts comprising 3-4 crystals are representative of a primary igneous texture. Fibrous tremolite occurs as randomly oriented 0.1-0.7 mm crystals, whereas serpentine forms the fine-grained mesh-textured groundmass between tremolite and remnant olivine crystals (Fig. 31a). An apparent sub-poikilitic texture consisting of tremolite enclosed within olivine crystals is probably a metamorphic effect. Subhedral grains of magnetite 0.1-0.25 mm are associated with olivine, either enclosed within or at the margin of crystals (Fig. 31b).

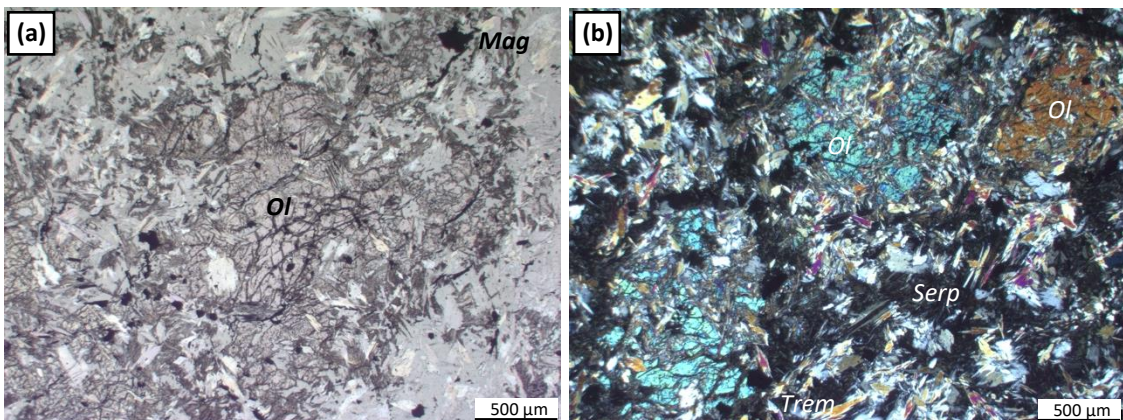


Figure 31: Photomicrographs of cumulate basal portions of spinifex-bearing volcanic units of the Mulga Volcanics. **(a)** PPL view of a fragmented olivine crystal surrounded by tremolite and serpentine with magnetite along fractures and at crystal margins (sample ROTH026); **(b)** XPL view of three fragmented olivine crystals in a groundmass of serpentine, tremolite and magnetite (sample ROTH026).

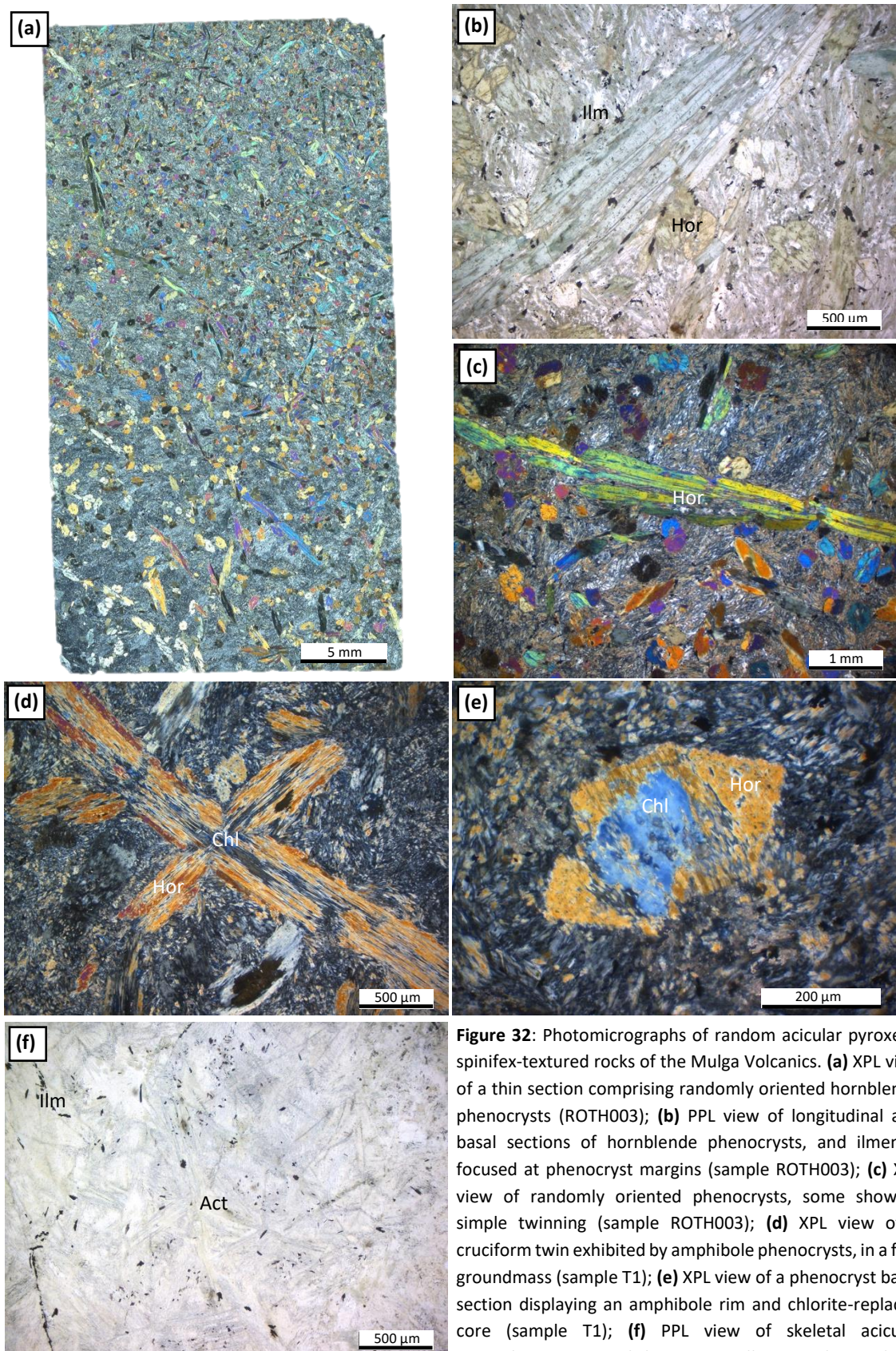


Figure 32: Photomicrographs of random acicular pyroxene spinifex-textured rocks of the Mulga Volcanics. (a) XPL view of a thin section comprising randomly oriented hornblende phenocrysts (ROTH003); (b) PPL view of longitudinal and basal sections of hornblende phenocrysts, and ilmenite focused at phenocryst margins (sample ROTH003); (c) XPL view of randomly oriented phenocrysts, some showing simple twinning (sample ROTH003); (d) XPL view of a cruciform twin exhibited by amphibole phenocrysts, in a fine groundmass (sample T1); (e) XPL view of a phenocryst basal section displaying an amphibole rim and chlorite-replaced core (sample T1); (f) PPL view of skeletal acicular microphenocrysts and ilmenite needles in a dusty, glassy groundmass (sample ROTH010).

Random acicular pyroxene spinifex

Random acicular pyroxene spinifex-textured rocks are observed in the Two Peaks Volcanics, Beryl West Volcanics and Mulga Volcanics and exhibit porphyritic to vitrophyric textures that are characterised by randomly oriented acicular phenocrysts of amphibole (Fig. 32a). The abundance of phenocrysts varies between 15-50 %, most commonly ~35%, and the predominant amphibole across much of the study area is actinolite, although hornblende increases in abundance towards the southwest (Fig. 32b). The size of phenocrysts varies considerably between units; lengths typically range between 1-14 mm but seldom reach up to 25 mm and widths range between 0.2-1.2 mm (Fig. 32c). Phenocryst size also varies within units, albeit to a lesser degree. For example, average phenocryst length doubles from ~1 mm to ~2.5 mm over the length of 4 cm in sample ROTH003 (Fig. 32a). Many of the phenocrysts display simple twinning and intermittent cruciform-shaped phenocrysts also occur (Fig. 32d). The basal sections of phenocrysts are frequently subhedral-euhedral and are typically zoned with amphibole rims and altered cores replaced by chlorite and/or plagioclase (Fig. 32e). In some instances, randomly oriented acicular crystals are thin (<0.1 mm) and consequently difficult to discern in hand specimen (Fig. 32f).

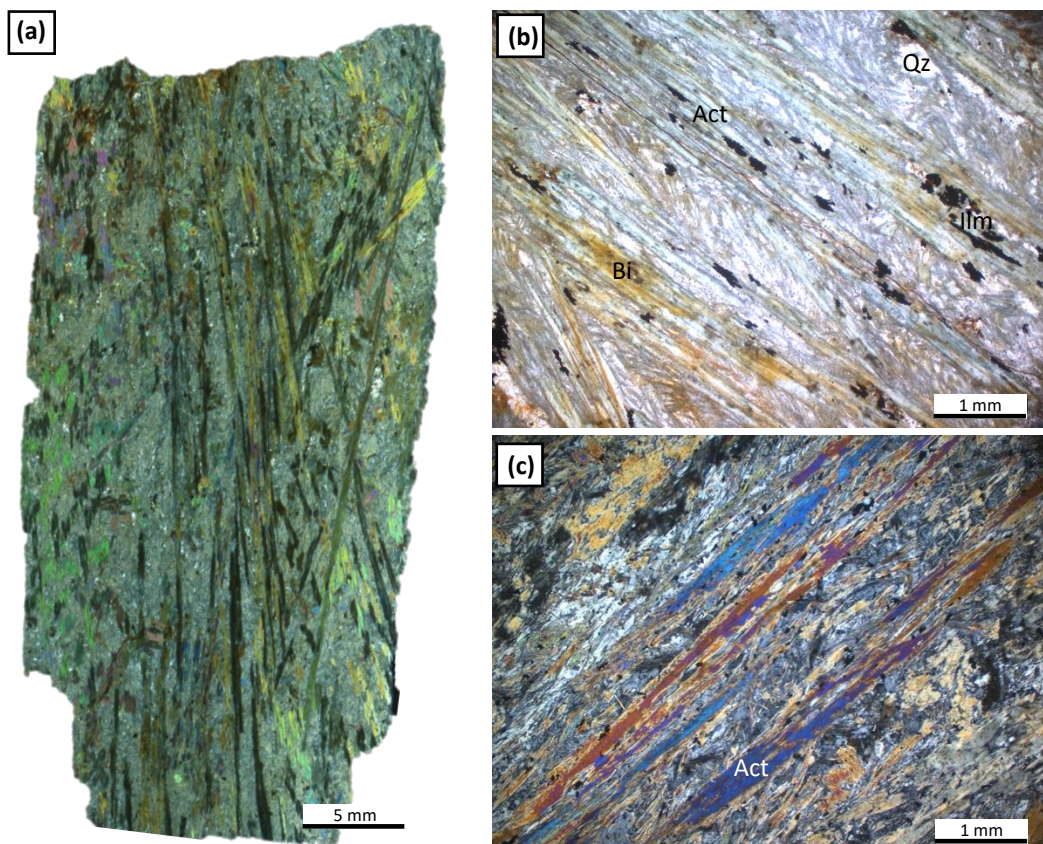


Figure 33: Photomicrographs of oriented acicular pyroxene spinifex-textured rocks of the Mulga Volcanics, Chulaar Group. **(a)** XPL view of a thin section comprising oriented elongate phenocrysts of amphibole up to 35 mm in length (sample T3); **(b)** PPL view of oriented acicular amphibole phenocrysts with oxides, primarily ilmenite, located at crystal margins and minor biotite and quartz derived from hydrothermal alteration (sample T3); **(c)** XPL view of oriented acicular amphibole phenocrysts surrounded by a very fine, plumose-textured groundmass (sample ROTH027).

The groundmass surrounding phenocrysts is most commonly very fine grained and exhibits a plumose texture, consisting of fine (<0.1 mm) acicular crystals of actinolite intergrown with plagioclase (Fig. 32d). In high-Mg basalt units, typically in the Mulga Volcanics, the groundmass is instead composed of fine (<0.1 mm) tremolite, chlorite and minor plagioclase. In slightly coarser-grained basalts, such as those in the lower Two Peaks Volcanics (Section 5.1.2), the groundmass is holocrystalline and composed of 0.1-0.6 mm mottled plagioclase, quartz crystals and single acicular crystals of actinolite up to 0.5 mm in length. Ilmenite is disseminated as <0.1-0.3 mm anhedral-subhedral grains with characteristic needle-like shapes and are often concentrated around the margins of amphibole phenocrysts (Fig. 32f). Many of the larger ilmenite grains possess a fine-grained, non-reflective halo of leucoxene derived from alteration.

Oriented acicular pyroxene spinifex

Oriented acicular spinifex-textured rocks display a variation of spinifex texture typified by aligned elongate, acicular phenocrysts of amphibole (commonly actinolite, pseudomorphing pyroxene) that range in length between 1-35 mm and width between 0.5-1 mm (Fig. 33a). This form of spinifex is less common than randomly oriented acicular spinifex and is best exemplified by several units close to the base of the Mulga Volcanics (Section 5.1.4). Actinolite phenocrysts constitute 40-65% of the rocks and are typically subhedral with ragged, irregular crystal margins. Basal sections are frequently zoned and comprise actinolite rims and irregular cores replaced by quartz or chlorite and long axes occasionally display simple twinning (Fig. 33b). The oriented acicular phenocrysts branch outwards in one direction and intersect each other at angles of <25°. A minority of phenocrysts are present as composite sets of up to 4 crystals in crystallographic continuity, both in long section and in basal section (Fig. 33c). The surrounding plumose-textured groundmass consists of intergrown plagioclase (< 0.3 mm) and acicular actinolite crystals (< 0.2mm) (Fig. 33b). Up to 7% anhedral quartz is present in the groundmass, typically <0.3 mm in size, and as minor discontinuous 4 mm veinlets, signifying hydrothermal alteration. Biotite occasionally occurs in association with quartz, including in the altered cores of actinolite phenocrysts. Oxides are abundant in interstices (~5%), particularly at the margins of actinolite crystals, and needle-like geometries suggest they are predominantly ilmenite.

These characteristics are consistent with the ‘oriented acicular pyroxene spinifex’ classification described elsewhere in Archaean terranes (e.g., Wilson & Versfeld, 1994; Lowrey et al., 2017), also referred to as ‘*String Beef*’ spinifex texture (Arndt et al., 1977).

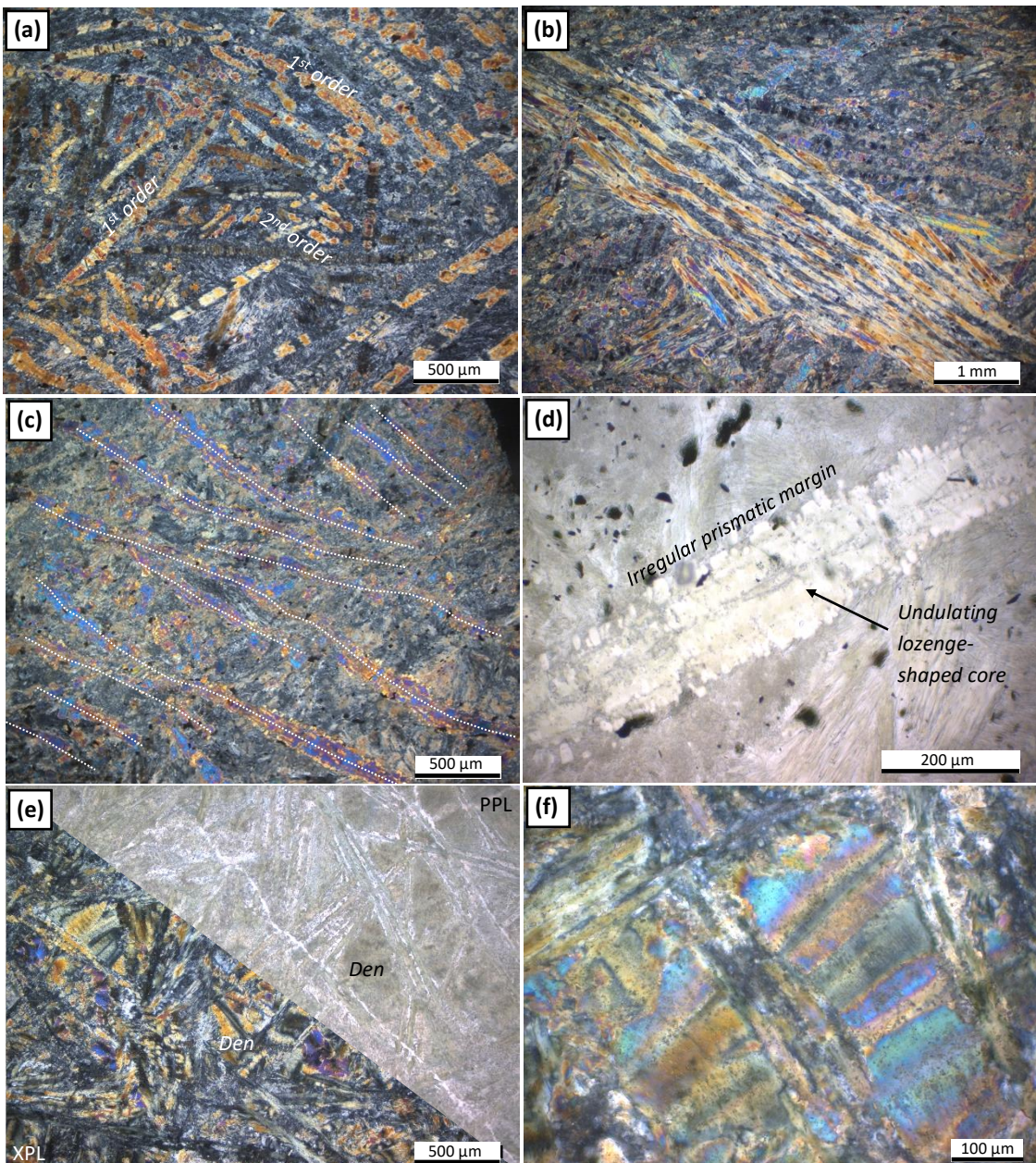


Figure 34: Photomicrographs of random platy pyroxene spinifex-textured rocks of the Chulaar Group. **(a)** XPL view of multiple randomly-oriented sets of parallel actinolite crystals, representing platy pyroxene precursors, in a spinifex-textured sample from the Beryl West Volcanics (sample ROTH041); **(b)** XPL view of a set of 9 parallel plates of actinolite (after pyroxene) reaching >10 mm in length, Beryl West Volcanics (sample ROTH041); **(c)** XPL view of a set of at least 12 sub-parallel plates in optical continuity, spaced up to 0.5 mm apart. Note the elevated alteration present in this part of the sample (sample ROTH041); **(d)** PPL view of a plate with undulating lozenge-shaped skeletal core and irregular, prismatic crystal margins, surrounded by a plumose-textured groundmass (sample ROTH041); **(e)** XPL and PPL view of a Mulga Volcanics sample displaying randomly oriented sets of actinolite plates, intermittent acicular actinolite crystals and dendritic patterns in a fine, glassy groundmass (sample ROTH036); **(f)** XPL magnified view of dendritic crystal patterns in the fine-grained groundmass interstitial to plate sets (sample ROTH036).

Random platy pyroxene spinifex

Random platy pyroxene spinifex is identified in both the Beryl West Volcanics and the upper portion of the Mulga Volcanics. These spinifex-textured rocks contain randomly oriented sets of pseudomorphed pyroxene phenocrysts with a plate-like crystal habit, akin to ‘random platy pyroxene’ (A2 zone) described for spinifex-

textured rocks in the NE Murchison Domain by Lowrey et al. (2017). In general, these rocks exhibit vitrophyric textures comprising 30-65% actinolite phenocrysts (pseudomorphing pyroxene) in a very fine glassy groundmass. The apparent elongate actinolite crystals occur on several scales. The largest ‘first order’ phenocrysts typically occur as sets of 2-6 parallel, closely spaced plates in crystallographic continuity, with lengths ranging between 0.5-13 mm and widths from 50-200 µm (Fig. 34a). These plate sets are randomly oriented and usually terminate against other first-order sets at angles of up to 90°, although some large plates crosscut one another in places. Up to 16 parallel plates occur in a single set of crystals in crystallographic continuity (Fig. 34b) and rarely, individual plates in a set are more widely spaced at up to 0.5 mm apart (Fig. 34c). At high magnification, the largest plates contain undulating, ‘lozenge-shaped’ skeletal core features along their long axes, as previously described for similar rocks by Lowrey et al. (2017) (Fig. 34d). Acicular actinolite phenocrysts are also present and of variable abundance relative to plates, suggesting a transition between platy-dominated units and acicular dominated-units. These acicular phenocrysts have euhedral-subhedral basal sections and do not cross first order plates, but occasionally are either aligned with them, or between them, and in crystallographic continuity (Fig. 34e).

In interstitial areas between first-order plates, smaller second-order sets of 2-7 plates are often present and ubiquitously terminate against the larger plates (Fig. 34a). In other interstices that do not contain platy crystals, dendritic, branching patterns are sometimes found, surrounded by a very fine groundmass (Fig. 34e). These dendritic patterns appear to be best preserved in the least altered units (Fig. 34f) and are not found in others subject to high degrees of alteration. The very fine groundmass is typically plumose-textured, comprising single acicular needles of actinolite up to 0.2 mm in length intergrown with glassy material (Fig. 34d). Infrequent patches of recrystallised quartz up to 0.8 mm are dispersed throughout the groundmass. Irregular <0.2 mm aggregates and needles of ilmenite are disseminated through the groundmass and often focussed at the margin of actinolite phenocrysts, in addition to the minor occurrence of Cr-spinel.

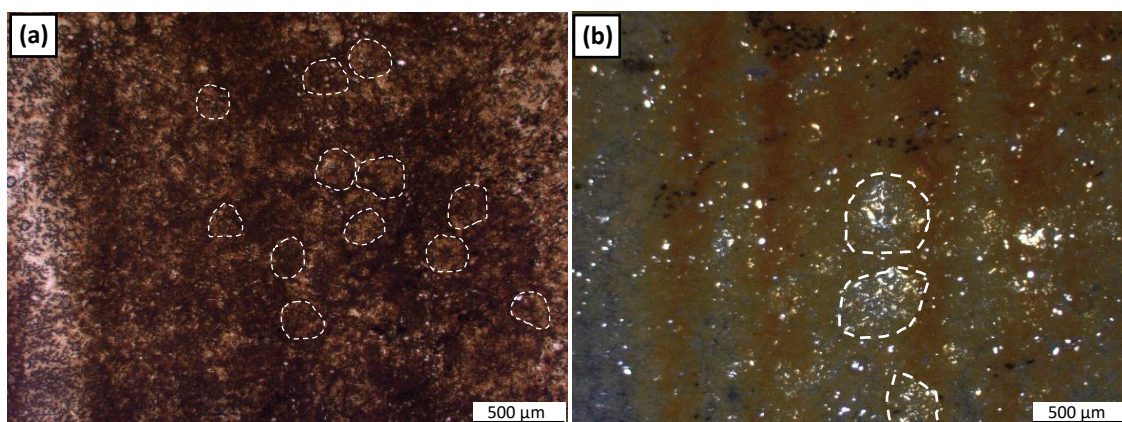


Figure 35: Photomicrographs of a banded felsic volcaniclastic unit from the Macs Well Clastics, Chulaar Group. **(a)** PPL view of rounded ?volcanic lithic clasts composed of felsic minerals in a dusty iron-rich matrix. Notice the faint vertical banding corresponding to bedding and lighter, quartz-rich intervals; **(b)** XPL view of ~0.5 mm sub-rounded clasts of quartz and feldspar, in a banded matrix comprising alternations between iron rich minerals (goethite, limonite) and quartz-rich intervals.

6.3.5 Banded felsic volcaniclastic rocks

Felsic volcaniclastic rocks of the Macs Well Clastics are characterised by a fine grained, iron-bearing, moderately to highly altered and oxidised groundmass that displays distinct orange-white banding. The rocks contain sub-angular to sub-rounded grains of quartz 0.05-0.1 mm in diameter, in addition to relict sub-rounded to rounded particles that are considered to represent felsic volcanic clasts (Fig. 35a). Banding is marked by alternations between yellow-orange, cloudy, fine-grained iron oxides and hydroxides, likely limonite and goethite, and quartz-rich intervals (Fig. 35b). The relict rounded clasts vary in diameter between 0.25-0.4 mm and comprise quartz and prismatic, tabular crystals, indicative of a quartzofeldspathic composition (Fig. 35b). These clasts are concentrated along some horizons parallel to banding, suggesting that the banding corresponds to original bedding. An opaque, highly reflective mineral is dispersed throughout the unit, likely an Fe(Ti) oxide mineral such as ilmenite, in addition to a dendritic black mineral that likely resembles an alteration feature.

6.3.6 Lapilli tuff

Lapilli-bearing tuffs of the Mulga Volcanics occur as fine-grained, friable, light grey, finely bedded to massive, ash-dominated units in hand specimen that are characterised by abundant rounded 1-3 mm volcanic clasts, interpreted as lapilli. A 5 m-thick unit that represents the base of the Mulga Volcanics in the north of the study area consists of 5-15 mm thick beds of grey ash, comprising alternating layers of fine- to medium grained quartz-bearing units, and very fine-grained lapilli-bearing units (Fig. 36a; Section 5.1.4).

The grey groundmass consists of a fine grained (<0.1 mm) Fe, Mg-bearing aluminosilicate matrix containing abundant laths of feldspar in addition to quartz. Coarser beds are poorly sorted, contain angular to sub-angular <0.05 to 0.3 mm quartz clasts (30%), fine grained ash groundmass (60%), granular iron oxide (8%), and rare 0.2 mm sub-rounded cherty lithic clasts (2%). These quartz-rich layers typically have erosive bases, including the erosion of originally rounded lithic clasts (Fig. 36a), suggesting a degree of sedimentary reworking of volcanic material. Fine grained intervals are moderately to well sorted, consist of ash (70%) and rare <0.05 mm angular quartz clasts (2%), opaque iron oxide (8%) in addition to rounded volcanic lithic clasts (20%) (Fig. 36b). These lithic clasts are typically 1-3 mm in size and comprise quartz crystals, sericitized feldspar crystals, fine ash and minor magnetite, rutile and ilmenite (Fig. 36c), though smaller 0.2-1 mm equivalents are observed in one layer. These clasts are concentrated along specific bedding horizons, are slightly elongate in the direction of bedding, often exhibit a relict crystal/cavity at their core and display fining upwards graded

bedding. These features are interpreted as lapilli, and likely represent eruptive episodes between periods of reworking. Accessory minerals present in the matrix include 0.2 mm rutile crystals, 0.1 mm ilmenite grains and <0.1 mm zircons crystals and fragments. Several rod-shaped shards of quartz about 0.2 mm in length are found, that may represent relic shards of volcanic glass. The unit is crosscut by secondary quartz veinlets up to 0.3 mm in width, and minor iron oxide, probably hematite.

Thicker units of lapilli-bearing tuff locally present at the top of the Mulga Volcanics, exposed in the west of the study area, are massive and display very similar characteristics to the fine-grained intervals described for the thin, basal tuff above; these units are dominated by fine-grained Fe, Mg aluminosilicate ash and contain identical 1-3 mm lapilli structures (Fig. 36d). Consequently, there is no evidence of sedimentary reworking and significantly less quartz clasts (< 5%) compared to the thin tuff at the base of the Mulga Volcanics (Section 5.1.4).

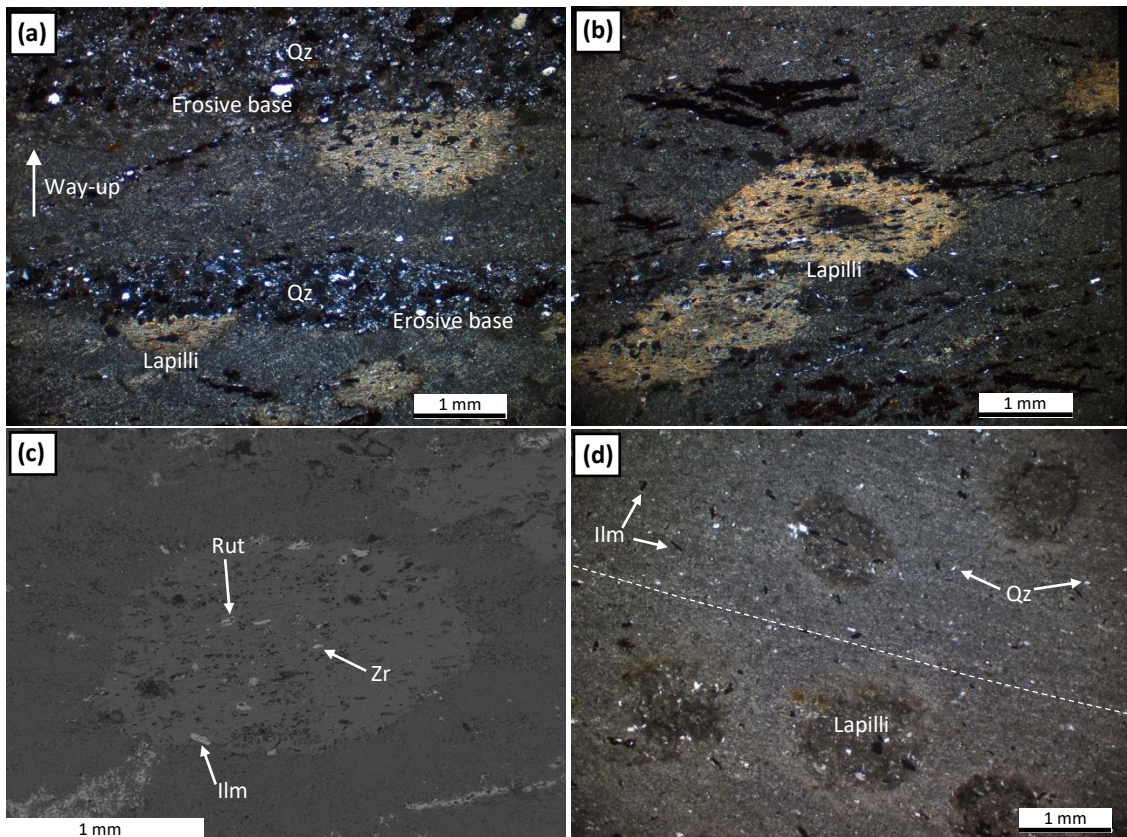


Figure 36: Photomicrographs of lapilli-bearing tuff of the Mulga Volcanics, Chulaar Group. **(a)** XPL view of ash-bearing units containing mm-scale quartz-rich beds with erosive bases that dissect lapilli and show way-up, from the base of the Mulga Volcanics (sample ROTH023); **(b)** XPL view of oblate lapilli with a central, altered core, in a fine grained matrix containing minor quartz (sample ROTH023); **(c)** Back scattered electron (BSE) image of a lapilli clast containing crystals of ilmenite, zircon and a groundmass of different composition to the surrounding matrix (shown by difference in contrast) (sample ROTH023); **(d)** PPL view of massive ash-bearing unit from the uppermost Mulga Volcanics with very weak bedding (parallel to dashed line) and rounded lapilli (sample ROTH050).

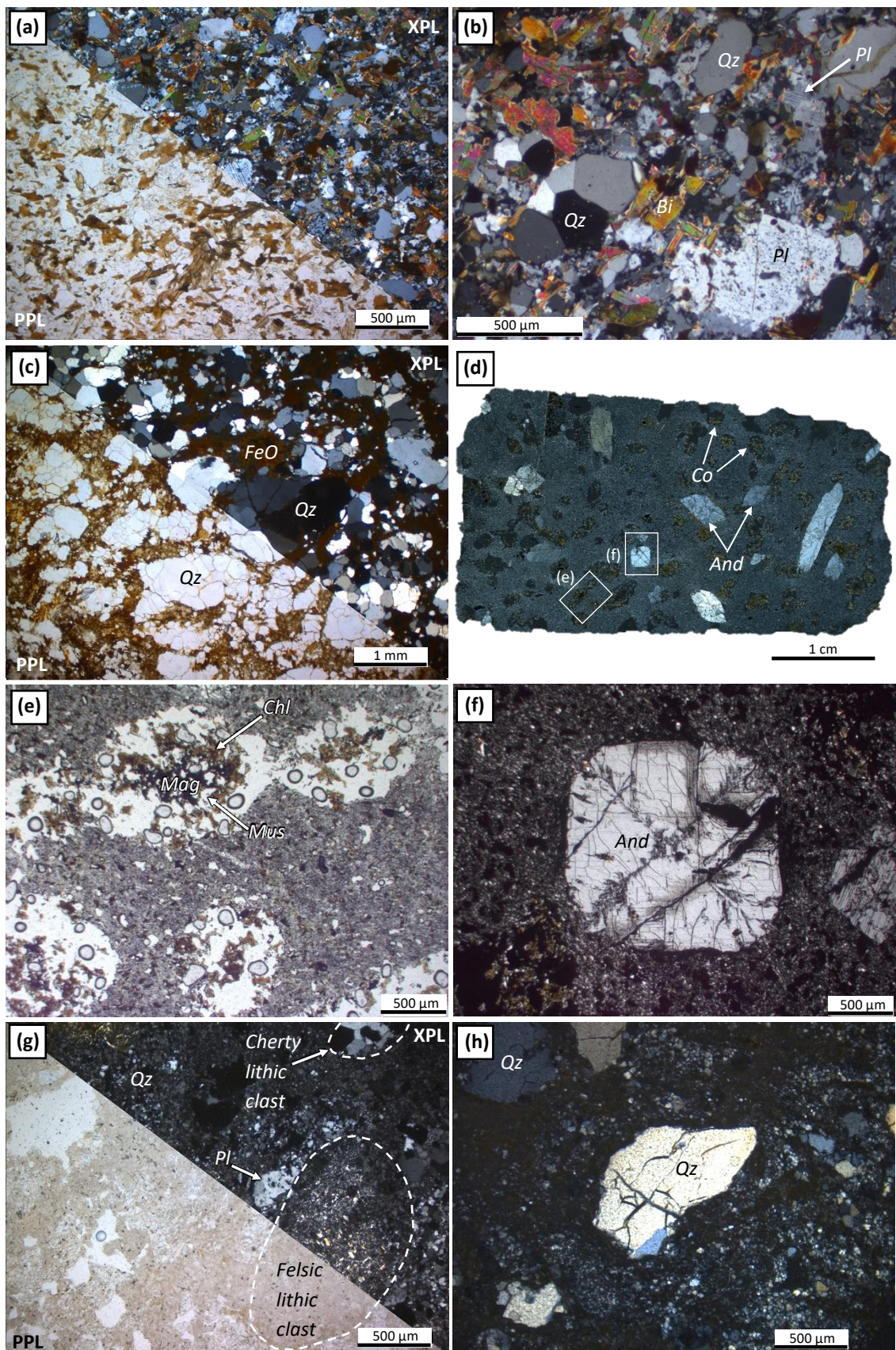


Figure 37 (previous page): Photomicrographs of Willowbank Clastics metasedimentary and metavolcaniclastic rocks sampled in the Rothsay area. **(a)** PPL/XPL view of the typical texture and mineralogy for greywacke (sample ROTH080); **(b)** XPL magnified view of a greywacke groundmass comprising clasts of plagioclase, biotite, quartz and cherty lithics (sample ROTH080); **(c)** PPL/XPL view of volcanogenic pebbly sandstone consisting of subrounded-subangular quartz clasts amongst a fine volcanogenic groundmass containing iron oxide and smaller quartz clasts (sample ROTH081); **(d)** XPL view of a thin section of a porphyroblastic mudstone comprising porphyroblasts of rounded cordierite (pinitized) and randomly oriented prismatic andalusite crystals, in a finer quartz-rich matrix (sample ROTH053); **(e)** PPL view of pinitised cordierite porphyroblasts now comprising iron oxide, yellow-brown chlorite and minor muscovite – note that much of the clear areas represent holes in the section, likely due to loss of clays during preparation (sample ROTH053); **(f)** XPL view of the euhedral basal section of an andalusite porphyroblast, surrounded by fine-grained quartz-rich matrix. **(g)** PPL/XPL view of felsic volcaniclastic rock comprising rounded cherty and felsic lithic clasts, subhedral plagioclase and anhedral quartz crystals in a quartzofeldspathic groundmass (sample ROTH060); **(h)** XPL view of a felsic volcaniclastic rock comprising angular, fractured quartz clasts within a fine-grained quartzofeldspathic groundmass (sample ROTH044).

6.4 Willowbank Clastics

The base of the Willowbank Clastics in the Rothsay area is marked by a sequence of coarsening upwards metasedimentary rocks, including siltstone, greywacke and pebbly sandstone, conformably overlain by felsic volcaniclastic rocks (Section 5.1.5).

6.4.1 Greywacke

The greywacke unit near the base of the Willowbank Clastics is a fine-grained, immature, poorly-sorted clastic metasedimentary unit composed of clasts of quartz (30%), biotite mica (25%), plagioclase feldspar (15%) and lithic clasts (4%), surrounded by a finer grained matrix (Fig. 37a). Quartz clasts are typically angular to sub-angular and vary in size between 0.1-0.5 mm., whereas plagioclase feldspar occurs as 0.2 mm anhedral grains that exhibit clear polysynthetic twinning. Biotite is present as 0.1-0.2 mm randomly oriented laths evenly distributed throughout the unit. Less common lithic clasts up to 0.6 mm in diameter are composed of granoblastic quartz (Fig. 37b). The fine-grained (< 0.1 mm) matrix accounts for ~25% of the sample and consists of quartz, lesser feldspar and minor biotite. Minor amounts of an opaque iron oxide phase are present as anhedral aggregates. The unit is both compositionally and texturally immature, suggesting it was deposited relatively close to the source region of the sediment.

6.4.2 Pebby sandstone

The pebbly sandstone directly overlying greywacke represents a medium-grained, moderately well sorted quartz-rich clastic metasedimentary rock. Quartz clasts dominate the unit (~75%) and are subrounded with a bimodal distribution; larger clasts are typically 1 mm in diameter (but up to 3 mm) and exhibit a granoblastic texture which may have been induced by metamorphic recrystallisation, in contrast to finer (0.1-0.2 mm) sub-angular quartz clasts (Fig. 37c). The unit is broadly clast-supported, with interstices between clasts accommodated by a very fine-grained, light coloured volcanogenic matrix, which includes orange-brown iron oxide discolouration (possible limonite/goethite; Fig. 37c). This unit records upwards increases in average grain size, maturity and volcanogenic content relative to the underlying greywacke unit.

6.4.3 Porphyroblastic mudstone

A porphyroblastic mudstone unit near the base of the Willowbank Clastics in the Rothsay area contains two porphyroblast phases accounting for approximately 25% of the unit (Fig. 37d; Section 5.1.5). The most abundant phase comprises rounded, anhedral 1-2 mm aggregates of muscovite, yellow-brown chlorite and iron oxide, representing pinitization of cordierite crystals (Fig. 37e). Further euhedral and prismatic porphyroblasts of andalusite are randomly orientated and up to 1 cm in length (Fig. 37f). The surrounding matrix comprises subrounded to rounded clasts of quartz, minor plagioclase and muscovite, and randomly oriented needle-shaped crystals of ilmenite, in addition to predominant silt-sized material.

6.4.4 Felsic volcaniclastic rock

Willowbank Clastics felsic volcaniclastic rocks are typically fine-grained, cream-white, weakly bedded to massive and friable in hand specimen. They are characterised by variable abundances of quartz clasts and lithic clasts in a fine grained quartzofeldspathic groundmass. The microcrystalline groundmass accounts for 45-50% of these units and comprises fine grained (<0.1 mm) angular to sub-angular quartz crystals and relict feldspar crystals with elongate crystal shapes and traces of complex twinning, likely plagioclase (Fig. 37g). The groundmass also contains sericite, in addition to localised fibrous crystals of actinolite (0.1-0.2 mm). In some more highly altered samples, the matrix has been subject to kaolinitic alteration. Quartz clasts account for 20-25% of these units and consist of angular to sub-angular grains up to 1.2 mm in size dispersed throughout the matrix (Fig. 37h). In contrast, lithic clasts (25-30%) are sub-rounded, 0.5-2 mm in size and predominantly comprise microcrystalline quartz, reflecting clasts of chert. Less common (up to 5%) are sub-rounded lithic clasts up to 1.4 mm in size that consist of an aluminosilicate groundmass, randomly oriented plagioclase crystals and secondary actinolite crystals, interpreted as felsic volcanic lithic clasts (Fig. 37g). Quartz, chert and lithic clasts are frequently elongated and aligned in the local fabric direction. The microcrystalline groundmass contains sparse 0.2 mm opaque iron oxide crystals, probably secondary limonite, in addition to accessory rutile and barite. Abundant euhedral zircon crystals and fragments are present in the matrix and in felsic volcanic lithic clasts, and are up to 0.2 mm in size with oscillatory zoning evident.

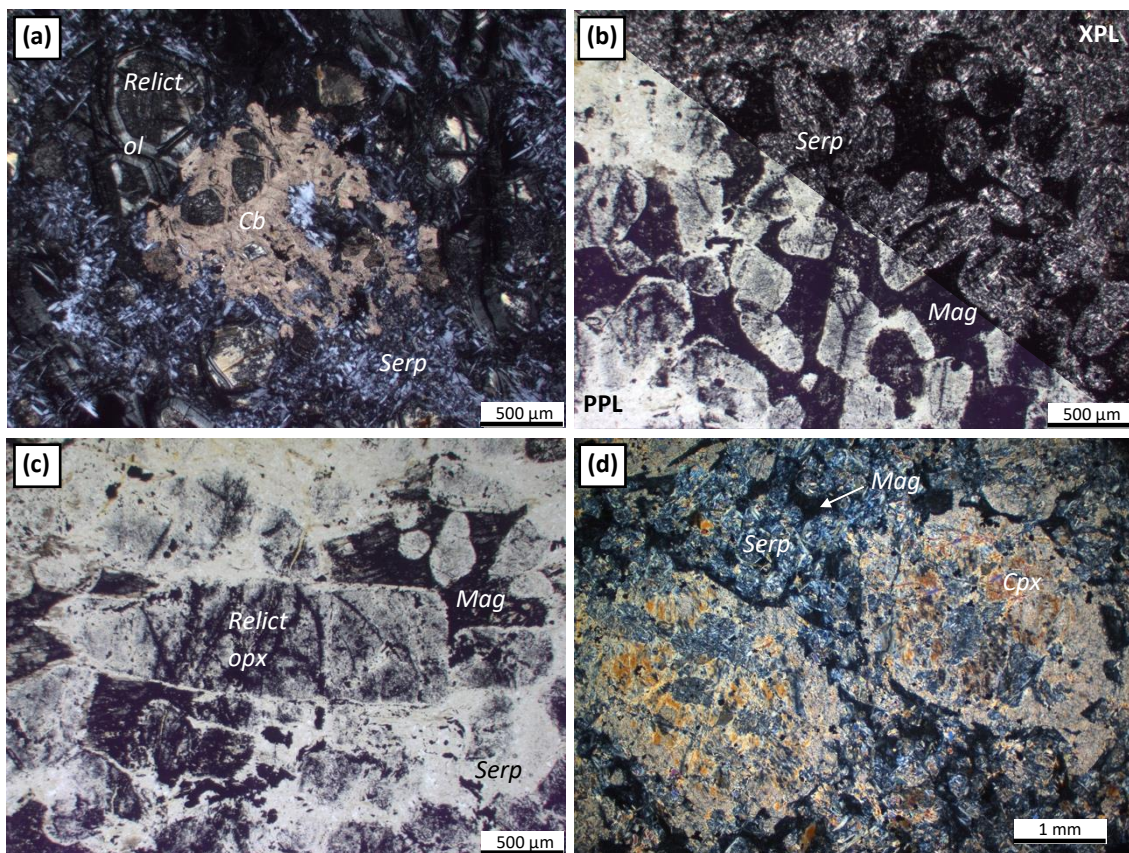


Figure 38: Photomicrographs of Warriedar Suite ultramafic cumulate rocks, from comparable Warriedar Suite sills to the northeast of the Rothsay area. **(a)** XPL view of a carbonate altered serpentinite comprising poikiloblastic carbonate patches enclosing and surrounded by serpentine and relict olivine crystals (sample CHU003); **(b)** PPL/XPL view of a serpentinite containing serpentinised olivine crystals surrounded by magnetite-bearing interstices preserving an primary igneous orthocumulate texture (sample CHU009); **(c)** PPL view of serpentine pseudomorphs of cumulate olivine surrounded by magnetite, and uncommon larger, tabular crystals interpreted as pseudomorphs of pyroxene, possibly orthopyroxene (sample CHU009); **(d)** XPL view of an olivine-pyroxene cumulate rock containing subhedral, prismatic phenocrysts of clinopyroxene enclosing and surrounded by smaller, serpentinised relict olivine crystals and interstitial magnetite (sample BAD002).

6.5 Warriedar Suite

Stratigraphic subdivision of Warriedar Suite intrusions is based primarily on mineralogical and textural variations corresponding to well-developed magmatic layering. For example, many of the thickest sills can be subdivided into a basal cumulate ultramafic unit, overlying pyroxenitic rocks, massive gabbroic/doleritic rocks and an uppermost quartz dioritic unit. As the petrographic characteristics of the individual Warriedar Suite intrusions are generally similar and in order to avoid unnecessary repetition, petrographic descriptions will be given for the main rock types observed throughout the suite.

6.5.1 Cumulate ultramafic rocks

Unfortunately, no thin sections were prepared from Warriedar Suite cumulate ultramafic rocks mapped in the Rothsay area and described in this study. However, samples taken from ultramafic cumulate portions of

analogous Warriedar Suite intrusions located to the northeast of the study area are mineralogically and texturally similar to those in the Rothsay area. Thin sections have been prepared from three such comparable samples from three separate Warriedar Suite intrusions (BAD002, CHU003, CHU009), the locations of which are provided in Table 2. The petrography of these samples is described below.

Ultramafic rocks present at the bases of many Warriedar Suite intrusions are typically dominated by serpentine (65-70%) with up to 10% tremolite and 5-10 % iddingsite, in addition to magnetite and Cr-spinel, which together constitute ~10% of the samples. Spots of poikiloblastic magnesite 1-3 mm in size enclose serpentine and account for up to 15% of some samples (Fig. 38a), demonstrating partial carbonation of the ultramafic protolith. Complete serpentinization of olivine is typical, with the extensive development of mesh-textured serpentine that preserves ortho- to meso-cumulate primary igneous textures (Fig. 38b). Abundant rounded crystal shapes between 0.25-2 mm in diameter are pseudomorphed and highlighted by alteration phases, and display the characteristic anhedral, fractured appearance of olivine. Less common subhedral, tabular crystals, often exhibiting a bastite texture, indicate the presence of orthopyroxene in the cumulate assemblage (Fig. 38c). Based on relict crystal morphology, cumulate olivine and orthopyroxene account for approximately 70-75% and 5-10% of the ultramafic protoliths, respectively. Relict olivine is seldom preserved and only occurs as isolated fragments within a matrix of serpentine and magnetite. In the upper portions of basal ultramafic cumulates, the proportion of pyroxene relative to olivine increases and clinopyroxene joins the fractionating cumulate assemblage. In one such unit, euhedral-subhedral prismatic clinopyroxene crystals (partially pseudomorphed by actinolite) between 1.5-3.5 mm in size enclose abundant 0.2-0.3 mm olivine crystals pseudomorphed by serpentine and magnetite (Fig. 38d). The surrounding groundmass is dominated by fine grained acicular actinolite and serpentine.

6.5.2 Pyroxenitic rocks

Originally pyroxenitic rocks, often overlying ultramafic cumulate units in Warriedar Suite intrusions, are typically equicrystalline and dominated by ~80-90% of interlocking lath-shaped amphibole crystals ranging between 0.4-0.8 mm in size. In some instances, this amphibole is actinolite (pale green-dark green pleochroism), but in other units, the dominant amphibole is tremolite (colourless-light green pleochroism). In both cases, the amphiboles are pseudomorphs after pyroxene. The interlocking amphibole crystals often exhibit a relic cumulate texture (Fig. 39a), with interstitial phases consisting of acicular needles of actinolite and variably altered plagioclase crystals, commonly present as mottled/cloudy crystals or even sericite in more altered samples.

Pyroxenitic rocks are often porphyritic, with phenocrysts of plagioclase or amphibole occupying up to 20% of the units and giving outcrops a distinctive mottled appearance, particularly evident in the Rothsay Sill in the southwest of the study area. Amphibole phenocrysts generally occur as subhedral laths 1-8 mm in length (Fig. 39b). Plagioclase phenocrysts 1-3 mm occur as anhedral crystals that have invariably been subject to saussuritization, and now comprise a fine-grained assemblage of zoisite, sericite, actinolite ± carbonate ± epidote ± quartz (Fig. 39c, d). In some units, relict fragments of twinned plagioclase crystals form part of the saussurite assemblage. Intergrowths of ilmenite and magnetite are frequently present as 0.1-0.2 mm anhedral grains in the groundmass, surrounded by a leucoxene halo, derived from breakdown of ilmenite (Fig. 39b). Accessory apatite and sphene are common and pyroxenitic rocks in some intrusions contain sulphide mineralisation; for example, several pyroxenite samples from the Rothsay Sill contain disseminated pyrite, chalcopyrite and bornite.

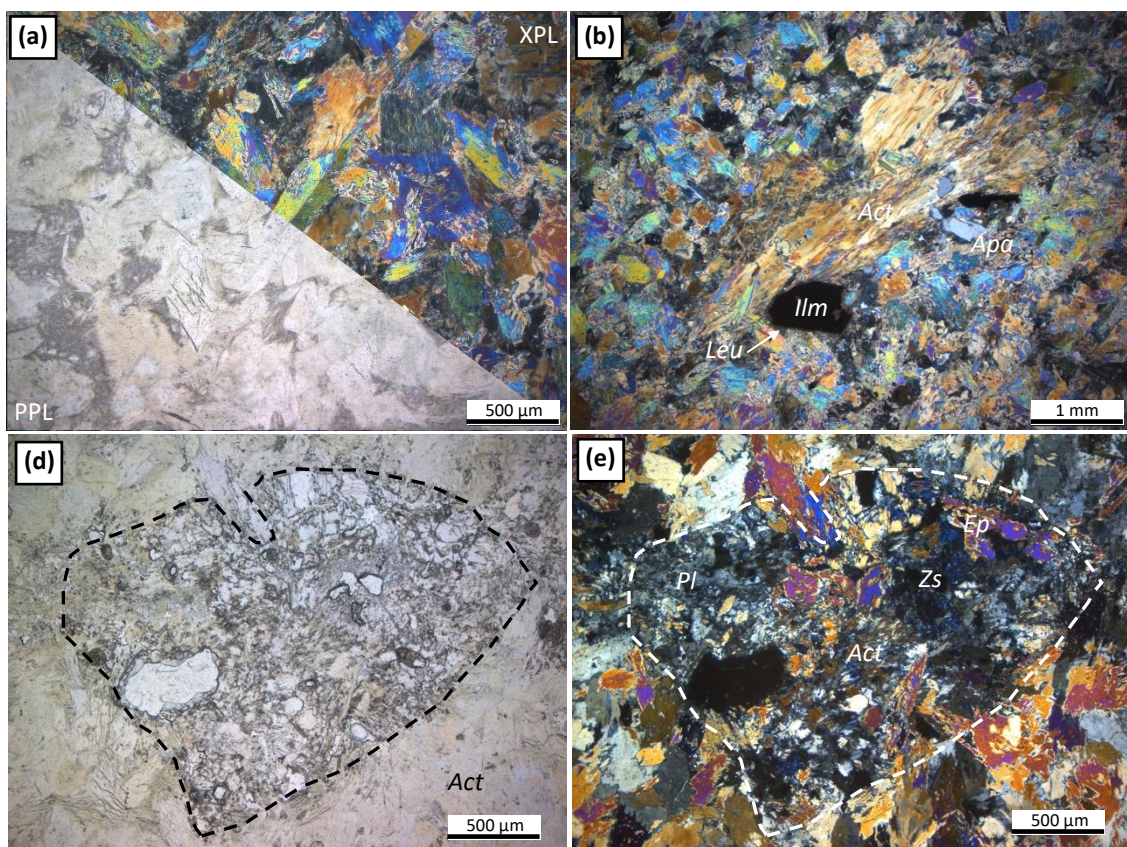


Figure 39: Photomicrographs of Warriedar Suite pyroxenitic rocks. (a) PPL/XPL view of the typical texture of a pyroxenite from the Rothsay Sill, now composed of anhedral, equicrystalline tremolite and actinolite laths and minor dusty areas likely representing saussuritised plagioclase (sample ROTH007); (b) XPL view of pyroxenite displaying an original porphyritic texture comprising elongate actinolite phenocrysts (after pyroxene), surrounded by minor apatite, ilmenite with leucoxene halo and interlocking amphibole laths (sample ROTH007); (c) PPL view of a saussuritised plagioclase phenocryst with relic tabular crystal shape in an actinolite groundmass, in a porphyritic pyroxenite from the Rothsay Sill (sample ROTH077); (d) XPL view of (c) displaying the products of saussuritisation of plagioclase; epidote, zoisite, actinolite and minor remnant plagioclase (sample ROTH077).

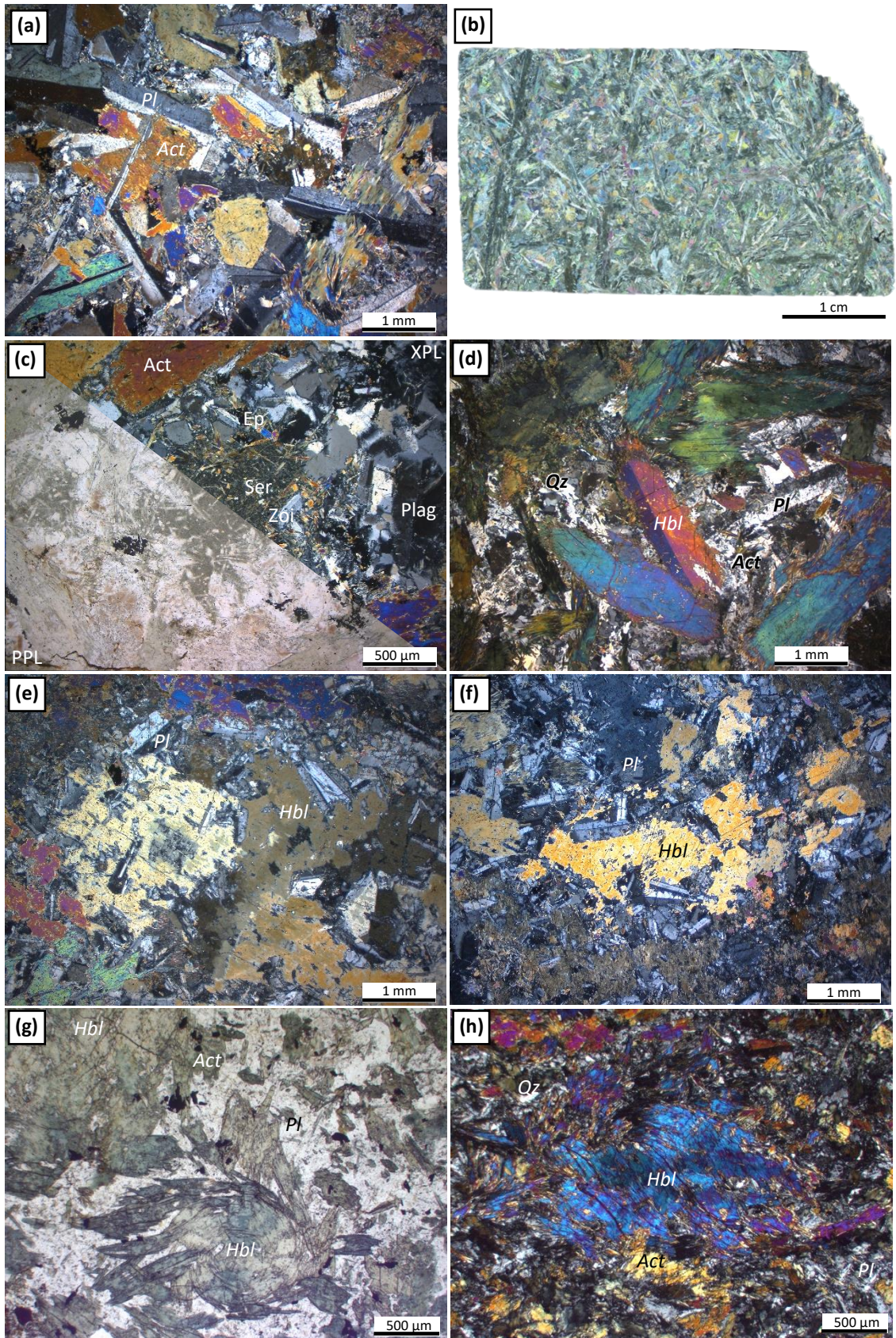


Figure 40 (previous page): Photomicrographs of Warriedar Suite gabbroic rocks. **(a)** XPL view of typical texture and mineralogy of equicrystalline dolerite from the Gardner Sill – crystals are cross-cutting one another due to metamorphism (sample ROTH008); **(b)** XPL thin section view of a harrisitic-textured gabbro from the Gardner Sill, comprising feathery, interlocking crystals of plagioclase and amphibole that mimic spinifex texture (sample ROTH019); **(c)** PPL/XPL view of a gabbro comprising moderately altered and saussuritised plagioclase, replaced by fine grained sericite, zoisite, epidote, and actinolite (sample ROTH008); **(d)** XPL view of a Rothsay Sill porphyritic gabbro comprising simple twinned hornblende phenocrysts in a plagioclase and quartz-bearing groundmass (sample ROTH029); **(e)** XPL view of poikiloblastic gabbro from the Mountain View Sill comprising large amphibole oikocrysts (after clinopyroxene) that contain tabular plagioclase chadacrysts (sample ROTH024); **(f)** XPL view of an ophitic texture in a Mountain View Sill gabbro comprising ~1 cm amphibole crystals invaded by tabular plagioclase crystals (sample ROTH024); **(g)** PPL view of the typical texture of Honeycomb Gabbro, typified by rounded, deformed amphibole porphyroblasts in a plagioclase-quartz-actinolite groundmass (sample T2); **(h)** XPL view of Honeycomb Gabbro containing a large, deformed porphyroblast of hornblende (sample ROTH006).

6.5.3 Gabbro/doleritic rocks

Warriedar Suite gabbroic rocks (and finer grained equivalents – described as dolerite) display varied modal mineralogy and a variety of textures, due to them forming the most voluminous component of all Warriedar Suite intrusions. The predominant metamorphic amphibole in Warriedar Suite gabbroic rocks is actinolite, however intrusions in the southwest of the Rothsay area also contain hornblende. Disseminated needles of ilmenite (\pm magnetite) are invariably present, principally focussed at the margins of amphibole crystals and often possess secondary haloes of leucoxene, which in some instances, replace the oxides entirely. Gabbroic rocks can be broadly separated into three groups based on textural features: equicrystalline gabbro, porphyritic gabbro and cumulate gabbro.

- Equicrystalline gabbroic rocks typically consist of medium to coarse (0.5-8 mm), randomly oriented and interlocking euhedral crystals of amphibole and plagioclase feldspar (Fig. 40a), with proportions of amphibole:plagioclase varying between 72:28 and 49:51 (including plagioclase alteration products). Locally in some intrusions, most notably the Gardner Sill, elongate, feathery interlocking crystals of plagioclase and amphibole up to 30 mm in length mimic a spinifex-textured volcanic rock (Fig. 40b). In some units, plagioclase has been variably altered and this takes the form of either sericitisation or more commonly, saussuritization, resulting in partial to complete replacement of plagioclase by a fine-grained assemblage of zoisite, actinolite, chlorite, quartz, epidote and carbonate (Fig. 40c). Such alteration is frequently localised along cleavage planes and at crystal margins, but also forms randomly oriented assemblages within crystals. Minor amounts of scattered secondary quartz are locally disseminated and associated with fractures or veinlets, occasionally accompanied by secondary biotite.
- Porphyritic gabbro exhibits very similar characteristics to the previously described porphyritic pyroxenites in that they are typified by 1-2.5 mm anhedral, altered plagioclase phenocrysts, but with increased groundmass plagioclase content (up to 34%) interspersed with actinolite crystals. In some units, particularly in the Rothsay Sill, subhedral phenocrysts now composed of amphibole (after pyroxene) are also present and up to 4 mm in length (Fig. 40d).

- Cumulate-textured gabbroic rocks are characterised by poikiloblastic textures, consisting of randomly oriented, euhedral, tabular plagioclase crystals 0.5-1 mm in length enclosed within 3-8 mm oikocrysts of actinolite or hornblende (after pyroxene) (Fig. 40e). Sub-ophitic textures are commonly preserved, with plagioclase crystals penetrating the margins of actinolite oikocrysts (Fig. 40f). Less commonly, 1-10 mm subhedral and elongate crystals of actinolite are also present, representing the addition of a cumulate pyroxene phase. In these instances, plagioclase crystals are aligned around the margins of cumulate pyroxene (now amphibole) crystals, indicating that the order of crystallisation is cumulate plagioclase → cumulate pyroxene → interstitial pyroxene. Minor amounts of a fine-grained (<0.5 mm) groundmass occurs interstitial to cumulate phases and oikocrysts, comprising acicular actinolite needles and plagioclase laths, the latter frequently saussuritised. Cumulate-textured gabbros are best exemplified in the lower portions of the Mountain View Sill (Section 5.2.1).

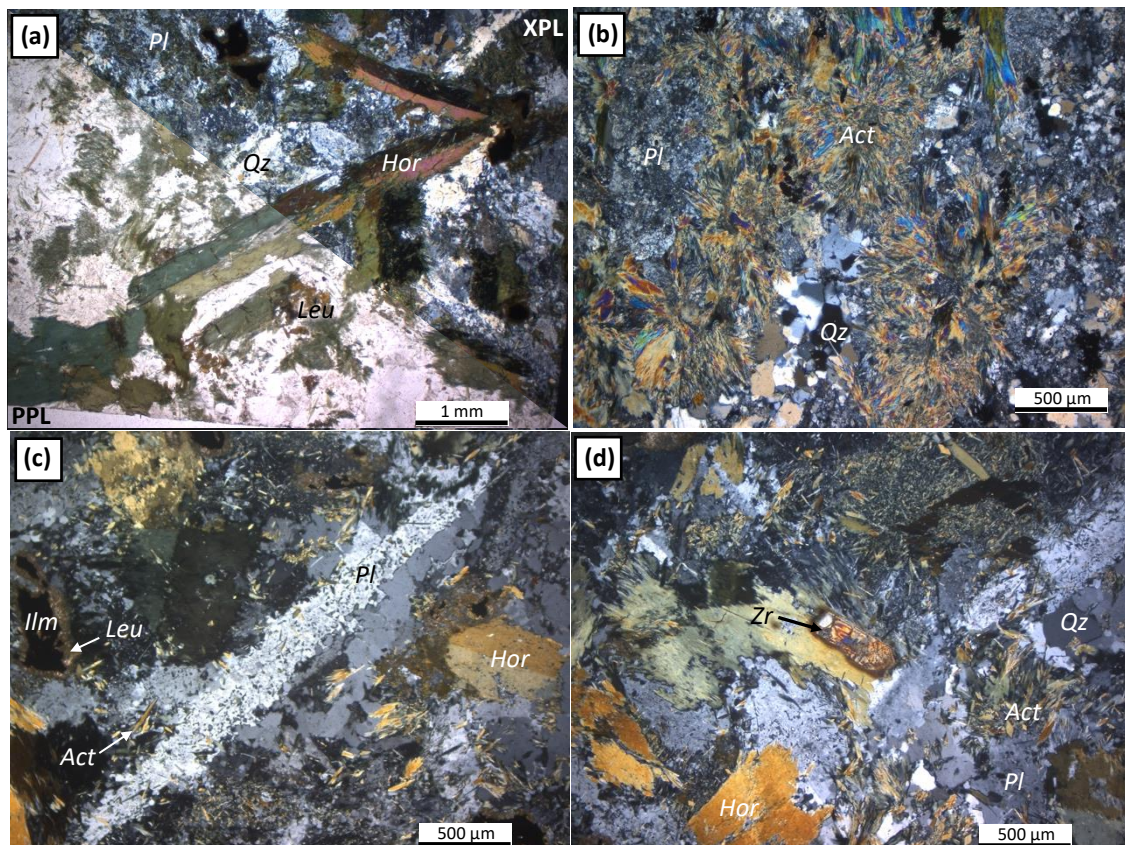


Figure 41: Photomicrographs of Warriedar Suite leucogabbroic and quartz dioritic rocks. (a) PPL/XPL view of porphyritic quartz diorite from the Damperwah Sill comprising elongate phenocrysts of hornblende (after pyroxene) exhibiting simple twinning in a groundmass of quartz and mottled plagioclase (sample ROTH034); (b) XPL view of radiating acicular crystals of actinolite with mottled plagioclase and patches of recrystallized quartz in a leucogabbro of the Gardner Sill (sample ROTH035); (c) XPL view of elongate granophyric-textured feldspar containing inclusions of quartz in crystallographic continuity (sample ROTH034); (d) XPL view of a large ~500 μm euhedral zircon crystal interstitial to hornblende, acicular actinolite, plagioclase and quartz (sample ROTH034).

The Honeycomb Gabbro (Section 5.2.2), situated at the top of the Mountain View Sill, exhibits a distinctive texture and mineralogy not commonly observed in other Warriedar Suite intrusions. Blocky amphibole crystals 0.8-2.5 mm in size occupy ~65% of the unit and define a porphyritic texture. Interstices between these amphibole crystals consist of fine grained (<0.5 mm) plagioclase (labradorite), quartz, acicular actinolite and ilmenite crystals. The combination of blocky amphibole phenocrysts and interstitial felsic minerals give this unit its characteristic honeycomb texture (Fig. 40g). Amphibole crystals invariably consist of two phases; cores consist of anhedral, fragmented grains of hornblende in crystallographic continuity, whereas the rims and intervening areas comprise actinolite (Fig. 40g). These relations imply the partial conversion of hornblende to actinolite during metamorphic retrogression. Further, these phenocrysts are strongly deformed, displaying undulose extinction with some crystals shaped as σ -clasts (Fig. 40g, h).

6.5.4 Quartz dioritic rocks

Quartz dioritic rocks are present at the tops of many Warriedar Suite sills and are typified by approximately equal proportions of plagioclase and amphibole (either hornblende or actinolite, 35-40%) and ubiquitous quartz content (~15%). In general, these horizons comprise increased feldspar content relative to the underlying intrusive units, consistent with them being the uppermost, most evolved portion of the intrusions. In several instances, these units exhibit porphyritic and harrisitic textures that consist of elongate, subhedral hornblende crystals 0.5-20 mm in length with green-brown pleochroism and simple twinning along their long axes (Fig. 41a). In contrast, quartz dioritic rocks of the Gardner Sill contain amphibole in the form of fibrous, acicular actinolite crystals 0.2-1 mm in length, which radiate outwards radially to define star-shaped patterns (Fig. 41b; Section 5.2.4). The surrounding groundmass is generally comprised of 0.5-4 mm plagioclase laths of andesine composition, a minority of which display granophytic textures (Fig. 41c) and in some intrusions, is subject to moderate sericite alteration. Quartz generally occurs as 0.2-2 mm, frequently granoblastic, anhedral aggregates of crystals in the groundmass interstitial to plagioclase, occasionally displaying a slight undulose extinction. Oxides generally constitute 4-5 % of quartz dioritic units. The most abundant oxide, ilmenite, occurs as subhedral 0.1-1 mm grains that are typically located at the margins of amphibole crystals. Most ilmenite grains are surrounded by a halo of fine grained, granular leucoxene, an alteration product of ilmenite, and several are entirely converted to leucoxene (Fig. 41c). This is best exemplified in the Rothsay area by the quartz diorite from the uppermost portion of the Damperwah Sill (Section 5.2.5). Less frequently, magnetite also forms part of the oxide assemblage, and occurs as 0.5-3 mm fragmented grains with <0.1 mm exsolution lamellae of ilmenite. Furthermore, numerous large (up to 450 μm), euhedral zircon crystals are commonly found in these quartz dioritic rocks (Fig. 41d).

6.6 Summary of Petrographic Analysis

This section has presented the petrography of supracrustal and mafic-ultramafic intrusive rocks comprising the greenstone stratigraphy in the Rothsay area. A total of 46 thin sections have been examined from lithologies throughout the area to characterise mineral assemblages and textures.

Petrographic analysis has confirmed that all supracrustal rocks have been affected by metamorphism. In mafic extrusive and intrusive igneous rocks, metamorphic assemblages are typically hornblende-actinolite-albite, demonstrating upper greenschist to lower amphibolite facies metamorphism. This is consistent with previous regional geological studies that identified an increase in metamorphic grade towards the southwest of the Yalgoo-Singleton greenstone belt (Watkins & Hickman, 1990). Sedimentary and volcaniclastic rocks contain quartz clasts that often exhibit granoblastic textures, consistent with metamorphic crystallisation, and contain minor amounts of actinolite. Several units display textures and assemblages consistent with retrograde metamorphism. This is best displayed by the Honeycomb Gabbro, which contains fragmented hornblende breaking down into actinolite and chlorite. The cordierite-andalusite porphyroblast assemblage, preserved in a metasedimentary unit of the Willowbank Clastics near Rothsay, shows clear evidence of contact metamorphism, in contrast to the more pervasive regional metamorphism observed elsewhere.

Variable amounts of alteration are displayed by rocks in the belt. In igneous rocks, plagioclase often displays a mottled appearance or is visibly subject to sericite alteration or saussuritization. In the most extreme cases, plagioclase is completely replaced by a finer-grained saussurite alteration assemblage. In mafic intrusive rocks, ilmenite commonly possesses a leucoxene halo that in some instances entirely replaces ilmenite grains and composites. Furthermore, quartz present in many mafic-ultramafic igneous units is clearly secondary, due to its close association with quartz veinlets that crosscut units. Felsic volcaniclastic units are occasionally altered to clay. Serpentinitisation of olivine bearing ultramafic rocks is ubiquitous and is occasionally accompanied by carbonate alteration.

Despite metamorphism and alteration, many primary textures are preserved in supracrustal rocks. Volcaniclastic and sedimentary rocks commonly preserve primary features including bedding, erosive bases and graded bedding. In mafic and ultramafic intrusive rocks, a variety of primary igneous textures are preserved including cumulate, porphyritic, poikilitic and ophitic textures, and extrusive igneous rocks conserve porphyritic, amygdaloidal, variolitic and spinifex textures. Additionally, primary olivine, orthopyroxene and clinopyroxene can be found in rare instances within rocks of the Warriedar Suite, however, these are much more commonly pseudomorphed by serpentine, tremolite and magnetite (olivine) and actinolite-hornblende (pyroxene). In samples displaying increased metamorphic grade (particularly in the far southwest), textures in metaigneous rocks gradually become more porphyroblastic or granoblastic, metasedimentary rocks develop a lepidoblastic texture and primary minerals and textures are rare.

7. Structure

7.1 Introduction

Rocks in the Rothsay area are deformed into a broad, 12 km-wavelength, refolded, northwest-plunging antiformal fold structure, and are host to three discernible foliations, a lineation, folding on a cm- to km-scale, multiple generations of faults and two major shear zones. Collectively, these structures demonstrate that the study area has been subject to a complex and protracted deformational history. In this study, deformational events are numbered according to their relative order of occurrence and given the notation D (D_1 , D_2 etc.). Folds, fabrics and lineations assigned to a deformational event are given the notation F, S and L respectively, followed by the corresponding deformational event number (e.g., F_3 and S_3 resulting from D_3). The structural geology of the Rothsay area can be summarised by six episodes of deformation (D_1 - D_6) following emplacement of supracrustal rocks and intrusive sills (D_0). These events comprise an early inconspicuous deformational episode (D_1), followed by two shortening events (D_2 , D_3), an episode of shearing (D_4) and two subsequent events dominated by faulting (D_5 , D_6). D_4 shearing resulted in the development of two major shear zones in the Rothsay area; the Rothsay Shear Zone (RSZ), host to the historically-exploited Rothsay gold deposit, and the Enchanted Shear Zone (ESZ). The structures associated with each deformational event are summarised in Table 3 and will be described sequentially in the sections below.

7.2 Bedding (S_0) and Way-Up Criteria

Bedding in the Rothsay area is preserved by numerous metasedimentary lithologies. Most commonly, bedding orientations are recorded by the many laterally-extensive BIF units that occur throughout the supracrustal succession, including as rafts and screens within sill complexes. In these units, banding occurs on a <1 mm to ~2 cm scale and consists of highly variable proportions of chert, magnetite and hematite. In the Macs Well Clastics, bedding is well preserved by ferruginous siltstone in the form of mm-scale laminations, however, interbedded quartzite units are typically too massive to display bedding. Lapilli-bearing tuffs of the Mulga Volcanics are locally well-bedded on a mm- to cm-scale, particularly the lowermost basal unit, and contain several sedimentary features that can be used as way-up criteria. Felsic volcaniclastic units of the Willowbank Clastics are typically poorly bedded, however, bedding orientations can occasionally be determined through the identification of minor changes in average grain size or the concentration of quartz clasts.

Bedding surfaces in metasedimentary and volcaniclastic rocks typically dip at angles between 40-80° and consistently dip in a radial direction away from the core of the Rothsay Fold, i.e. to the north on the northeast limb and to the (south)west on the southwest limb (Fig. 42, Fig. 43a). As such, bedding measurements partially define a domal pattern, although supracrustal units in the southeast are dissected and deformed by the ESZ (Section 7.6.1). Several way-up criteria are present in both supracrustal units and mafic-ultramafic intrusive rocks.

Deformation Event	Setting	Features
D₆	E-W shortening	NNE-striking dextral D₆ fault, minor N-S faulting
D₅	NE-SW shortening?	ENE-striking sinistral D₅ faults, associated fault drag, granite and pegmatite dyke intrusion, ?oblique fabrics
D₄	Continued E-W shortening	D₄ shear zones, duplex development, S₄ shear fabric, oblique down-dip L₄ lineation, F₄ folding parallel to ESZ
D₃	E-W shortening	S₃ N-S fabric, F₃ N-S fold axes refolding F ₂ folds,
D₂	NE-SW shortening	F₂ NW-SE trending fold axes
D₁	?	Domal geometry, S₁ layer-parallel fabric
D₀	Extension/rifting	Intrusion of mafic-ultramafic layered sills, screens/rafts of supracrustal units
D₀	Extension/rifting	Deposition of volcanosedimentary supracrustal succession, S₀ bedding

Table 3: Table outlining the deformational framework for the Rothsay Fold area, comprising the interpreted structural setting and features observed for each event.

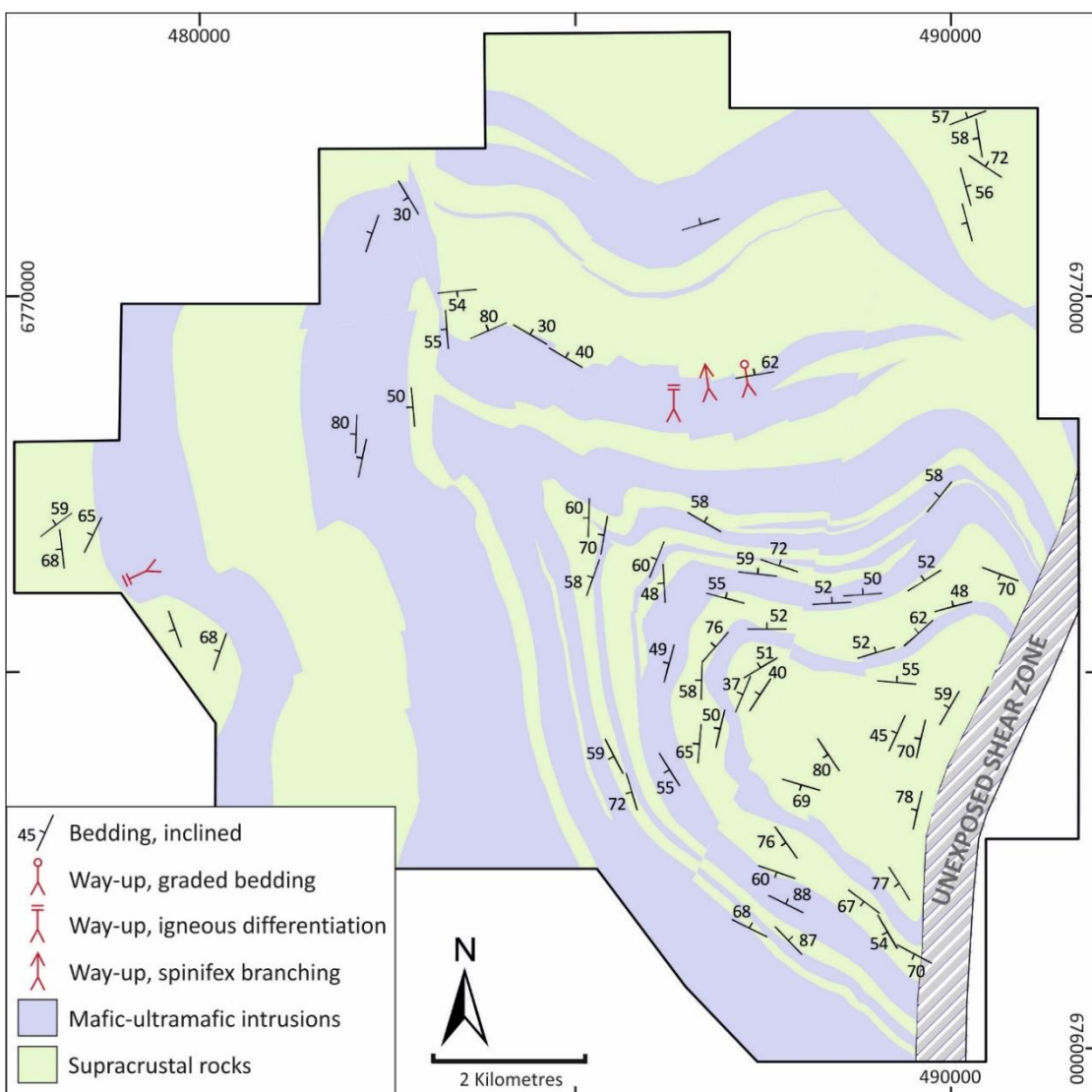


Figure 42: Simplified geological map of the study area showing representative bedding measurements and the locations and types of way-up indicators.

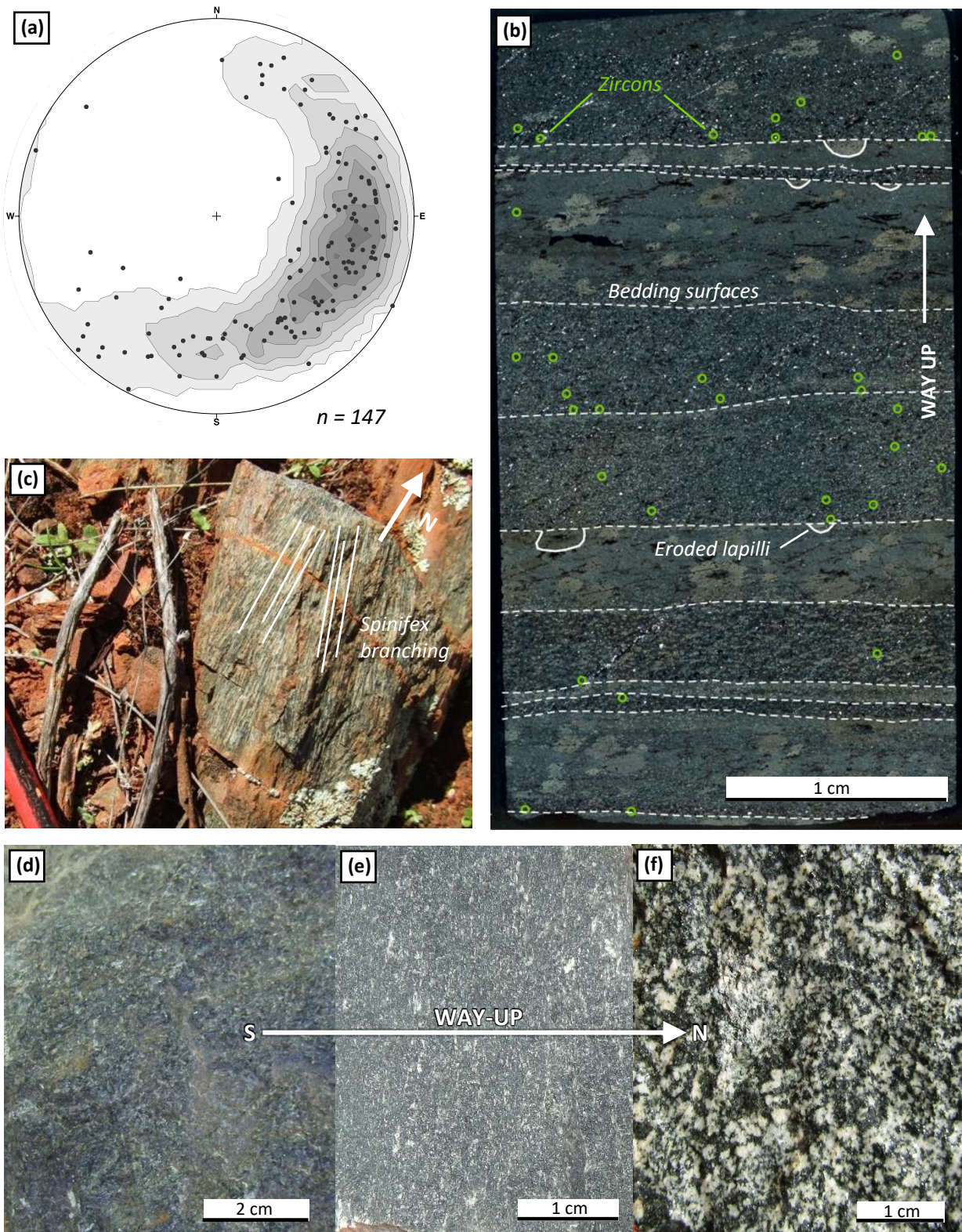


Figure 43: Bedding orientations and way-up criteria in the Rothsay area. **(a)** Lower hemisphere equal area stereonet of bedding orientations from the study area ($n=147$), with kamb contours drawn at 2σ intervals shaded in grey; **(b)** Thin section photomicrograph of lapilli-bearing tuff from locality 8.184, showing bedding surfaces and multiple way-up criteria; the distribution of zircon crystals in the section (green; largely concentrated at the base of coarser grained beds) and originally rounded lapilli (outlined in white) cut by erosive surfaces. Cross-polarised light; **(c)** Outcrop of spinifex-textured basalt at locality 8.188 showing branching of spinifex towards the south and thus demonstrating way-up to the north; **(d)(e)(f)** Photographs of intrusive rocks from the Gardner Sill displaying increasing feldspar content towards the north over a ~ 150 m stratigraphic interval from the southernmost feldspar-poor dolerite at locality 8.104a **(d)**, to dolerite at locality 8.118 **(e)**, to northernmost leucogabbro at locality 8.178 **(f)**, demonstrating way-up to the north. Note that coarser crystal size in **(f)** corresponds to the evolved uppermost ~ 10 metres of the Gardner sill, which in some instances displays harrisite-like textures.

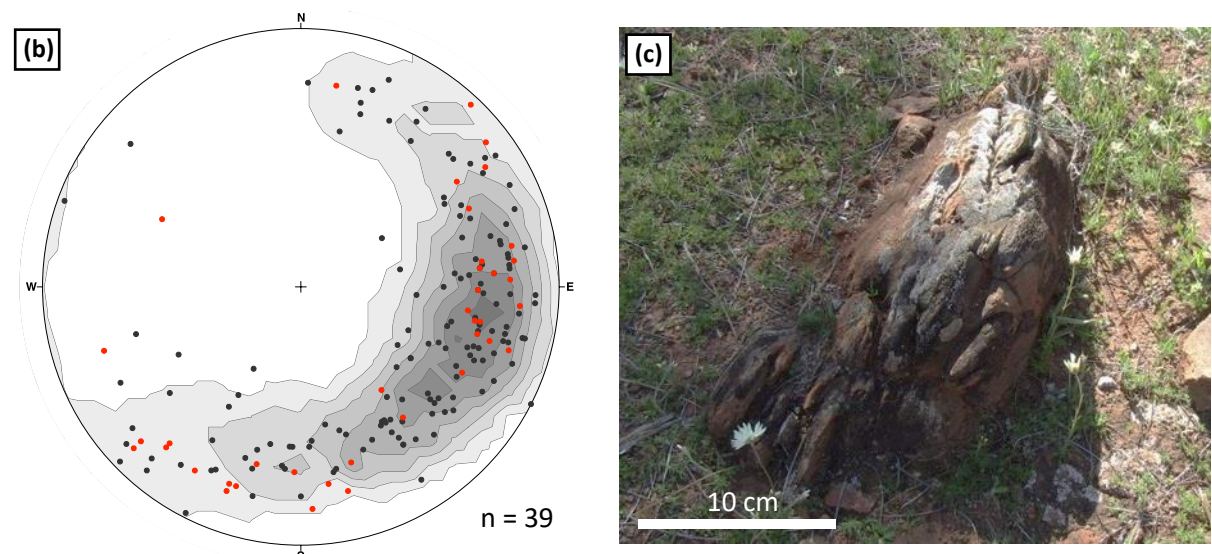
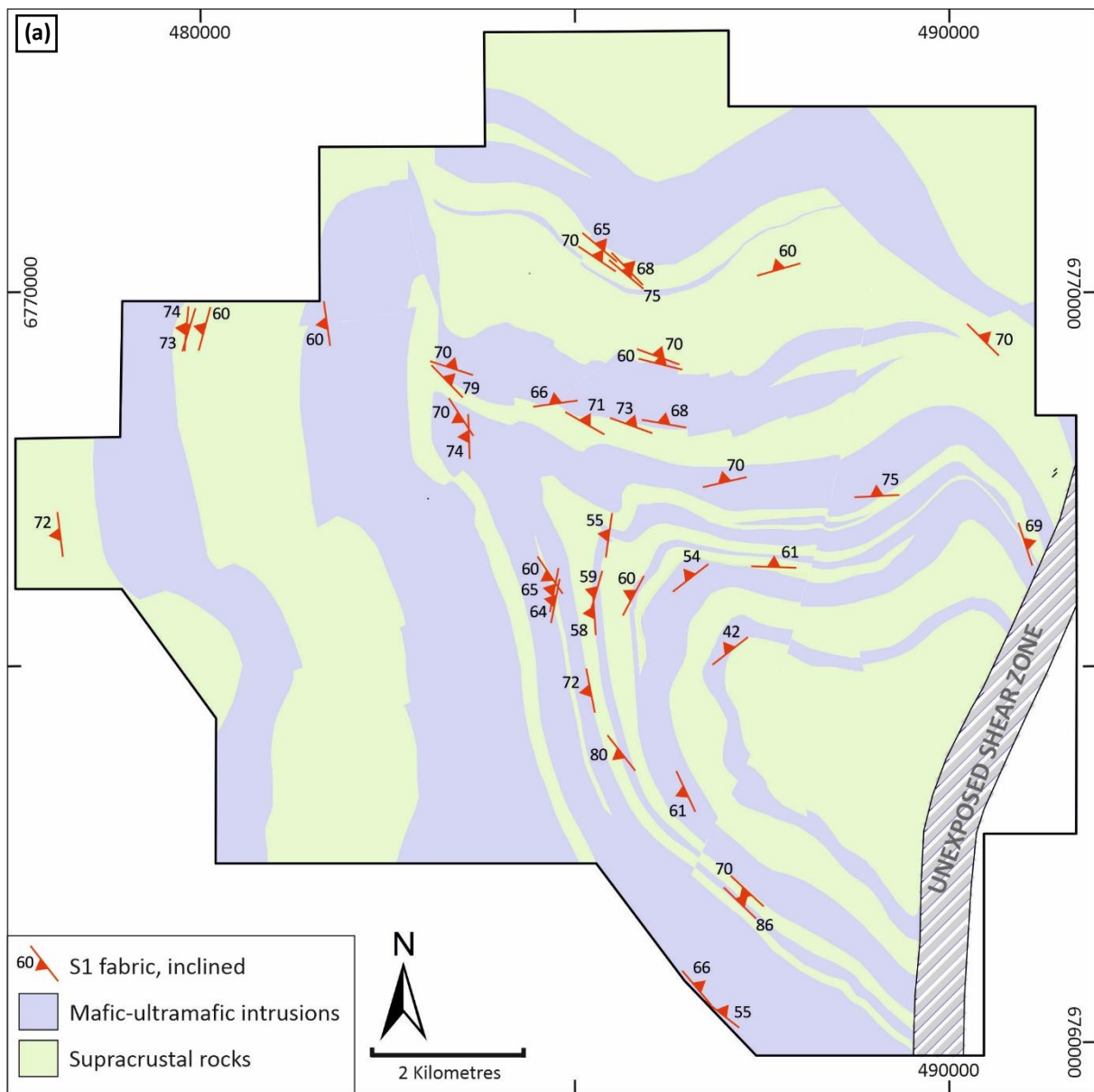


Figure 44: Map, stereonet and field photograph of S1 layer-parallel fabric. **(a)** Simplified geological map showing the orientation of S1 fabrics measured in the study area; **(b)** Lower hemisphere equal area stereonet showing orientations of S1 bedding parallel-fabric (red) relative to bedding (grey). Kamb contours for bedding measurements are drawn at 2σ intervals; **(c)** Outcrop of fine grained metabasalt showing S1 bedding parallel foliation (loc. 1.029).

At the base of the Mulga Volcanics in the north of the study area (Fig. 42), a lapilli-bearing bedded tuff is characterised by 5-15 mm beds of a grey-ashy groundmass and rounded lapilli up to 3 mm in size. Petrographic analysis of an orientated sample of this bedded tuff (loc. 8.184) has identified several way-up criteria. Following detailed sample mapping undertaken for geochronological work (see Chapter 7), zircon crystals are consistently found at the base of individual beds within the Mulga Volcanics bedded tuff, demonstrating pseudo-graded bedding (Fig. 43b). Coarser quartz crystals (0.3 mm) are also concentrated at the bases of beds compared to finer-grained upper portions (< 0.05 mm). Furthermore, erosive bases are identified in several instances, distinguished by originally rounded lapilli cut by subsequent bedding surfaces (Fig. 43b). All three of these criteria support the succession being the right way-up and younging away from the core of the fold. Immediately overlying the lapilli-bearing tuff, an oriented acicular spinifex-textured unit exhibits elongate crystals of amphibole (after pyroxene) up to 7 cm in length and 1-2 mm in width. At a good exposure in the north of the area (loc. 8.188; Fig. 42), acicular spinifex crystals consistently branch towards the south (i.e. down-sequence), consistent with the succession being the right way up (Fig. 43c).

The fractionation of mafic-ultramafic intrusive sills also serves as way-up criteria, best exemplified by the Gardner Sill in the north of the study area (Fig. 42). The base of the sill is marked by two ultramafic units containing relic cumulate textures and invariably serpentinised olivine crystals. The central part of the Gardner Sill consists of coarse-grained gabbro and feldspar content consistently increases with stratigraphic height (Fig. 43d, Fig. 43e), with the most evolved, quartz-bearing leucogabbro occurring in the uppermost 20 m of the intrusion (Fig. 43f). Similar highly evolved tops are shown in the west by the Damperwah Sill (Fig. 42). These features demonstrate differentiation of the intrusive sills and support the succession being the right-way up.

7.3 D₁ Deformation

D₁ deformation comprises several features that predate all other structures in the Rothsay area. The oldest discernible fabric is a layer-parallel S₁ fabric, which is characteristically oriented parallel to the bedding of layered metasedimentary rocks (Fig. 44a). The orientation of this fabric consistently imitates bedding around the Rothsay Fold and correlates well with bedding orientations (Fig. 44b). The S₁ layer-parallel fabric is most frequently observed in fine-grained metaigneous rocks such as basalt and serpentinite, of which outcrops are typically strongly foliated and commonly aligned parallel to the strike of the S₁ fabric (Fig. 44c). The fabric is also found as a weak foliation or spaced cleavage in coarser grained mafic intrusive rocks, such as gabbro and dolerite, and in volcaniclastic rocks. The intensity of S₁ increases towards major rheological contacts, most notably the base of the Gardner Sill (within ultramafic cumulate rocks) and the lowermost contact of the Rothsay Sill (within basaltic rocks), but occurs throughout all exposed units. There is no lineation associated with S₁ and no conclusive shear sense indicators have been identified. S₁ is crosscut by all other fabrics in the Rothsay area.

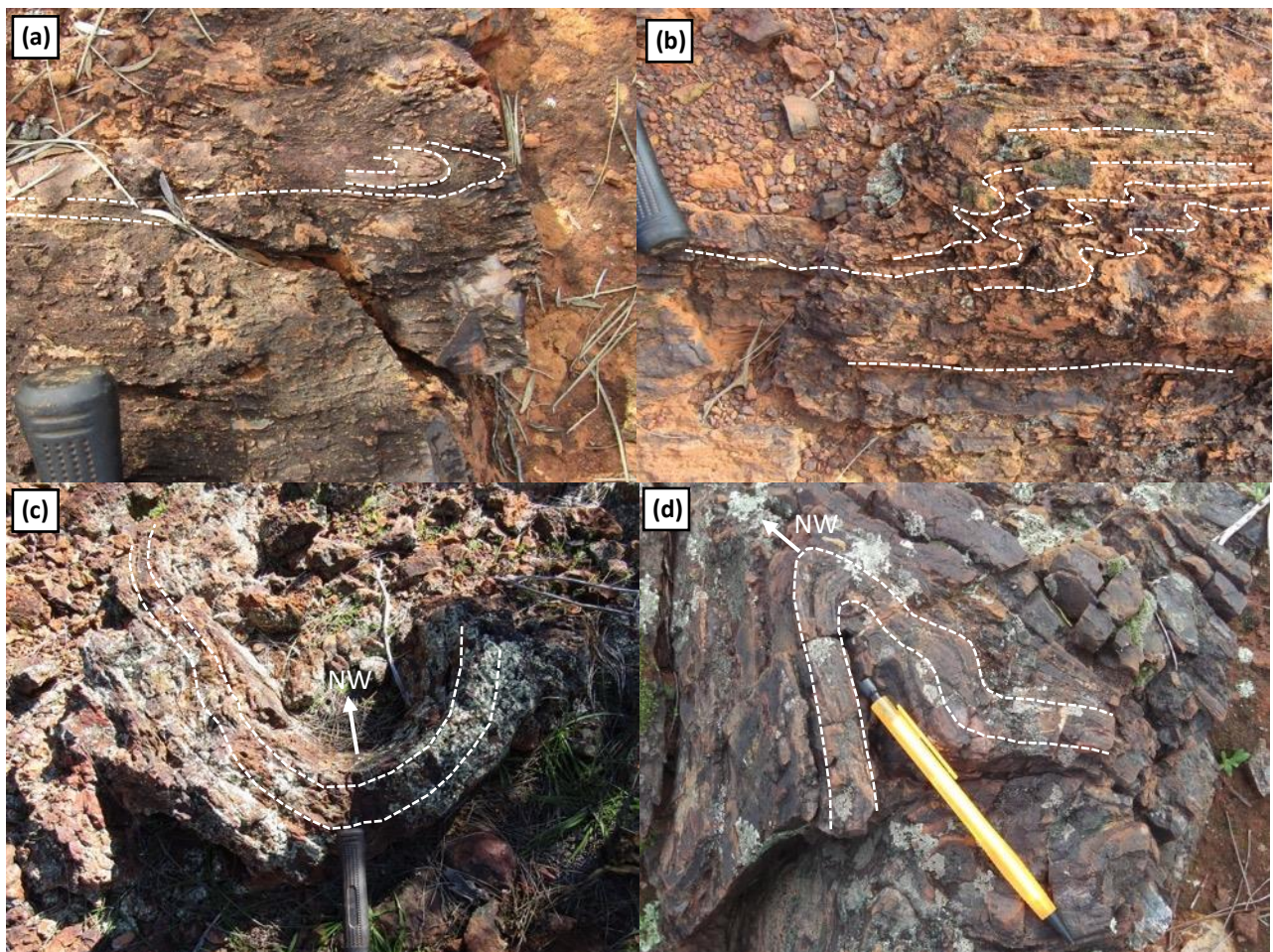


Figure 45: Photographs of outcrop-scale folding in the Rothsay area. **(a)** Layer-parallel F₁ isoclinal folding in banded iron formation of the Macs Well Clastics, with axial planes parallel to bedding (loc. 13.043); **(b)** Tight to isoclinal F₁ folding in fine-grained metapelitic rocks (loc. 13.044); **(c)** Open, cylindrical folding of interbedded quartzite and siltstone – fold axes plunging to northwest parallel to surrounding bedding, hammer handle for scale (loc. 13.023b); **(d)** Decimetre-scale asymmetric folding of banded iron formation close to a major F₂ antiformal fold hinge, plunging parallel to the major fold axes (loc. 6.098).

Other structures associated with D₁ include centimetre- to decimetre-scale, isoclinal, layer-parallel F₁ folding preserved in several BIF units, possessing fold hinge surfaces that are parallel to both bedding surfaces and the layer-parallel S₁ fabric (Fig. 45a, Fig. 45b). These are the earliest folds preserved in the area and have been deformed by all subsequent deformational events.

The radial, outward-dipping pattern of bedding measurements in the Rothsay area define the geometry of a dome (Section 7.2; Fig. 42). Furthermore, the slight, gradual curvature of units on the southwest limb of the Rothsay Fold, most clearly demonstrated by the upper Two Peaks Volcanics, may represent an expression of the original dome prior to multiple episodes of refolding (Fig. 42). This early dome precedes all other large-scale folds and is deformed and refolded by subsequent events in the same manner as the layer-parallel S₁ fabric and F₁ folding. It is possible that the domal geometry and layer-parallel fabric could be attributed to separate deformation events. However, as there is no way to distinguish these features and the dome, layer-

parallel fabric and layer-parallel folding predate all other structures apart from bedding, they are collectively ascribed to D₁.

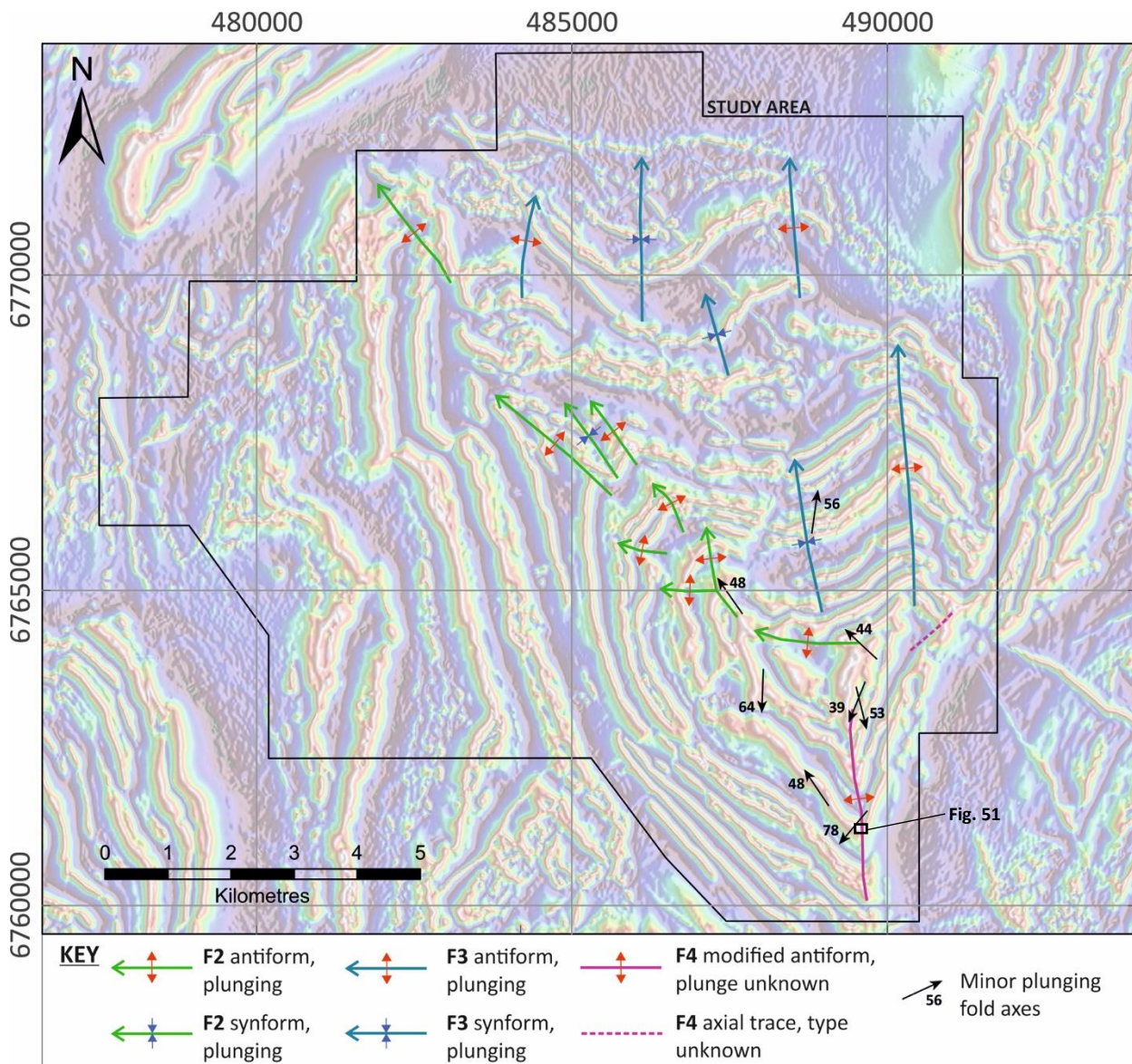


Figure 46: Reduced to pole (RTP) aeromagnetic map of the study area with different generations of folding symbolised, in addition to the trend of minor, outcrop scale fold axes and their plunge angles. The location of major fold axes is based on geological mapping and various aeromagnetic imagery, including that shown above (courtesy of Minjar Gold Pty.). The approximate location of Figure 51 is indicated in the southeast.

7.4 D₂ Deformation

D₂ deformation is characterised by a group of NW-SE trending metre- to kilometre-scale F₂ folds that are focussed in the central portion of the study area, including the major ~12km-wavelength fold axis that defines the Rothsay Fold (Fig. 46). F₂ consists of open to tight, upright and symmetrical folds that plunge towards the northwest at angles of 35-55°. Two pairs of box folds occur within the axis of the major F₂ structure, hosted by rocks of the upper Macs Well Clastics and Mountain View Sill (Fig. 46). At and near the hinges of major F₂ folds, outcrops of layered units such as BIF and ferruginous siltstone are usually highly deformed and contain abundant tight to isoclinal metre-scale F₂ folding, also northwest-plunging at similar angles to the

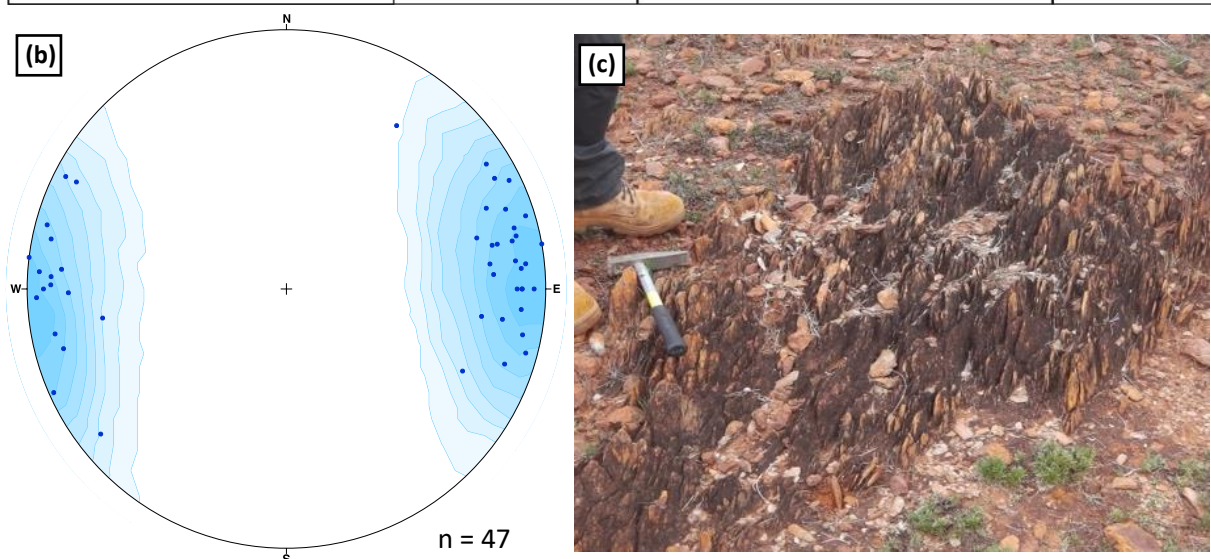
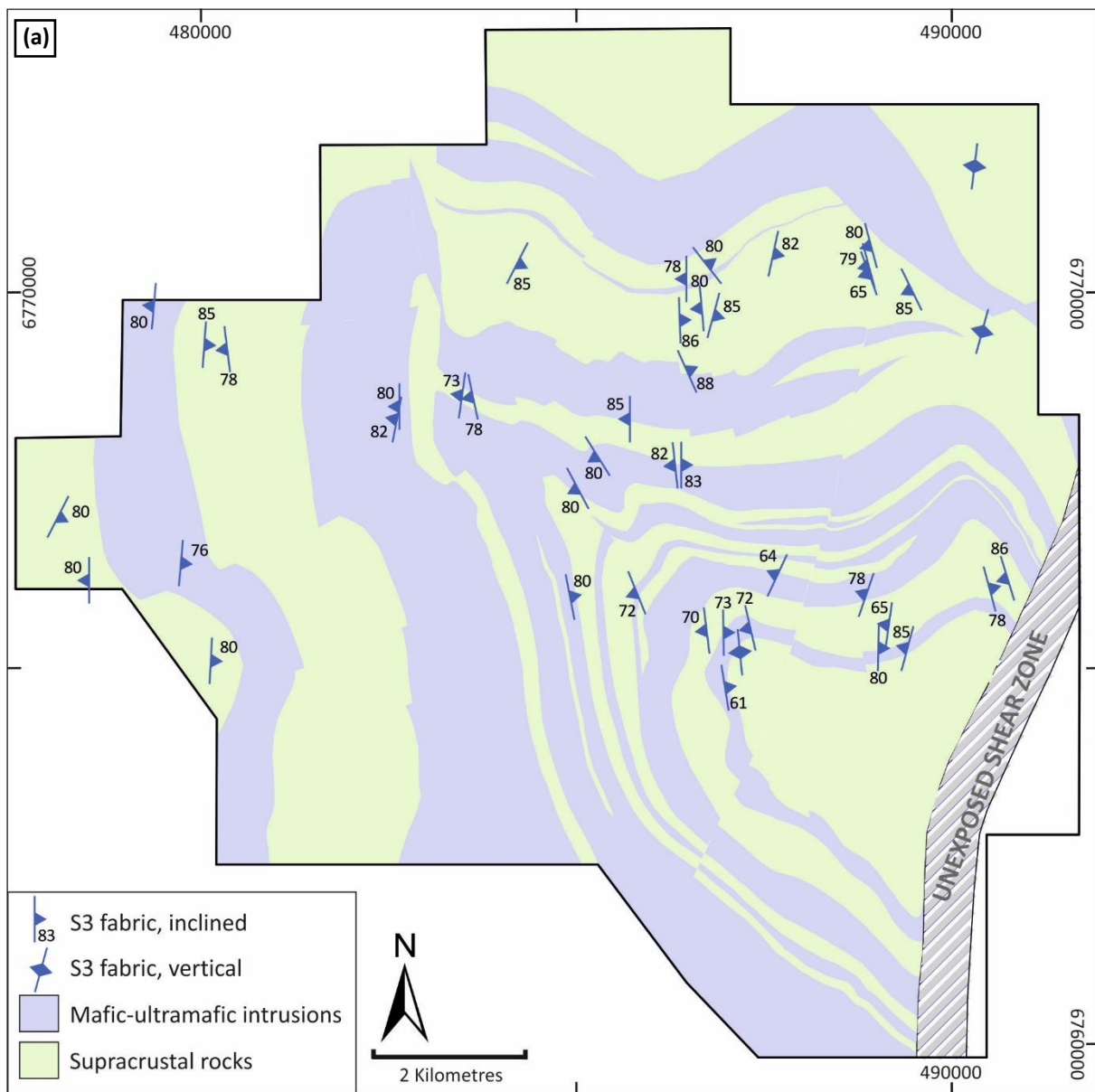


Figure 47: Map, stereonet and field photograph of S3 fabric. **(a)** Simplified geological map showing the orientation of S3 fabrics measured in the study area; **(b)** Lower hemisphere equal area stereonet of S3 N-S trending fabric, with kamb contours shaded in blue at contour intervals of 2σ ; **(c)** Outcrop of metabasalt with well-developed S3 N-S trending fabric (loc. 8.092).

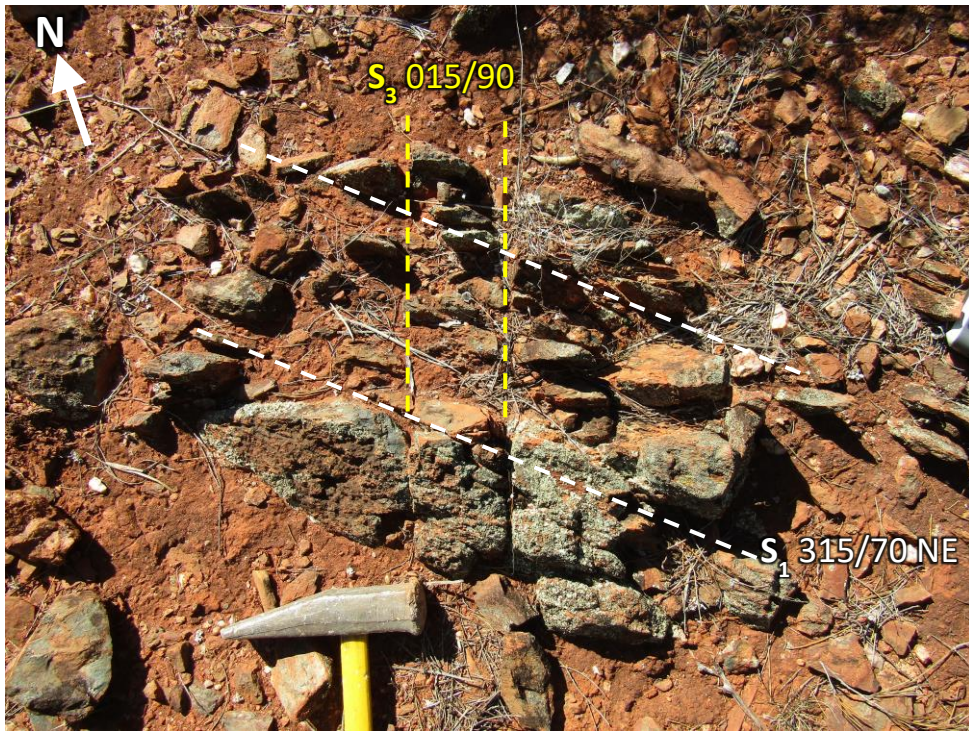


Figure 48: Foliated basalt outcrop comprising an S_1 fabric (315/70 NE) overprinted by an S_3 spaced cleavage (015/90). Note that this outcrop contains a less penetrative S_3 fabric than typically present (loc. 10.059).

major folds (Fig. 45c). Several F_2 folds close to major fold hinges are asymmetric, consistent with parasitic folding (Fig. 45d). The F_2 group of folds are not associated with an axial planar fabric. F_2 folds deform bedding and the S_1 layer-parallel fabric and refold the D_1 dome structure, but predate shearing and faulting according to cross-cutting relations.

7.5 D_3 Deformation

D_3 deformation is characterised by refolding of F_2 folds into a series of N-S trending F_3 folds and the widespread development of an axial planar S_3 fabric. F_3 folds comprise several km-scale upright, symmetrical antiform-synform pairs on the northeast limb of the Rothsay Fold, with north-plunging fold axes (Fig. 46). These folds refold the northeast limb of the major F_2 fold and the S_1 layer-parallel fabric, and therefore postdate D_1 and D_2 deformation. Outcrop-scale F_3 folds preserved in metasedimentary units in the north of the study area replicate the larger F_3 folds with axes that plunge towards the north at ~55° (Fig. 46). Less common instances of similar metre-scale folding in the south have axes that plunge 60–65° towards the south, despite the absence of larger, km-scale F_3 folds as found in the north.

The most extensively-developed fabric in the Rothsay area is a pervasive S_3 foliation that varies in orientation from NNE to NNW and is axial planar to F_3 folds (Fig. 47a). S_3 typically dips steeply to the west or the east at

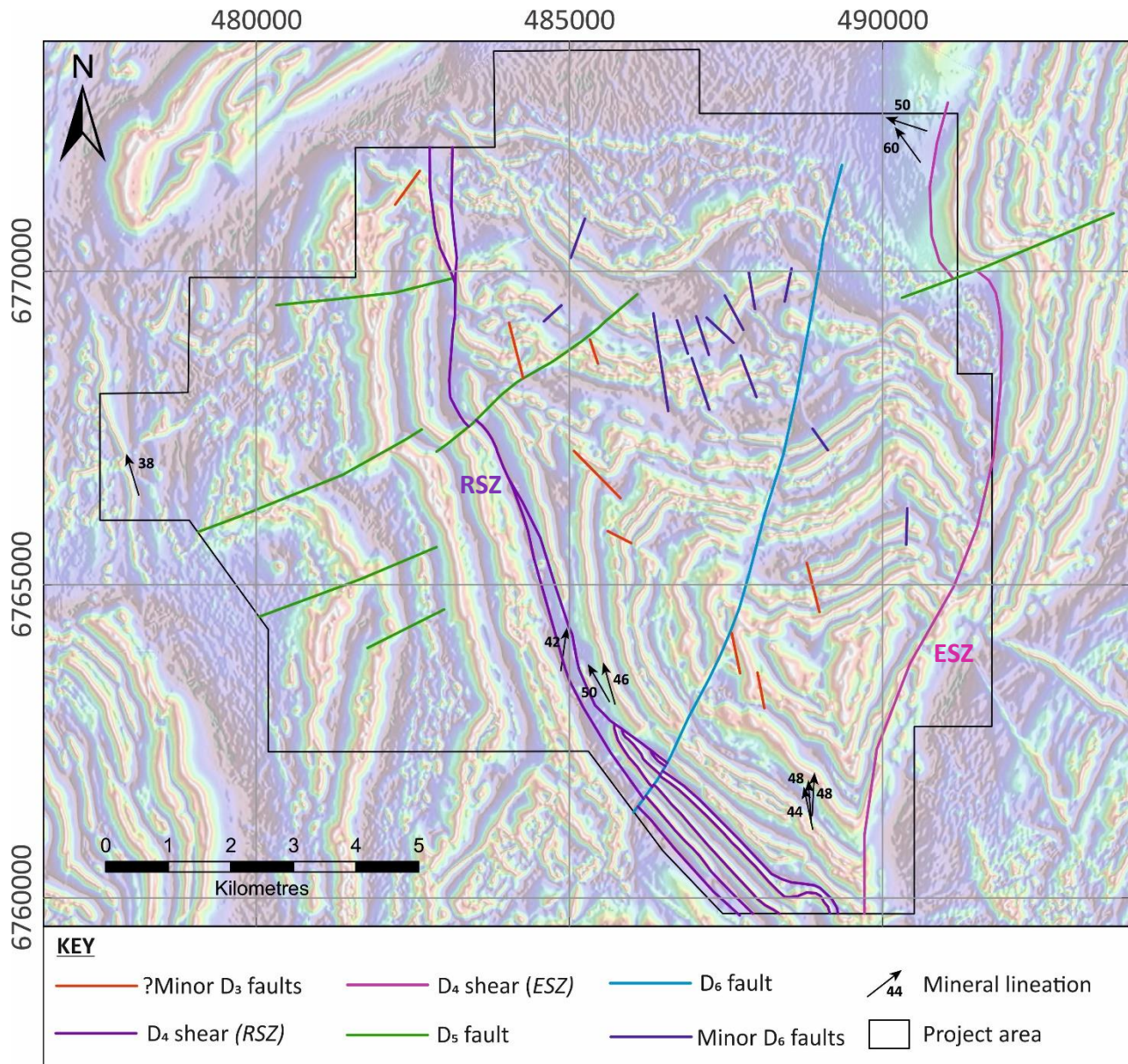


Figure 49: Reduced to pole (RTP) aeromagnetic map of the study area, with all major faults and shears symbolised by type and mineral lineations symbolised with plunge angles labelled. ESZ = Enchanted Shear Zone; RSZ = Rothsay Shear Zone. Aeromagnetic imagery courtesy of Minjar Gold Pty.



Figure 50: Outcrops with linear fabrics; (a) conglomerate close to the Enchanted Shear Zone with elongated clasts defining the lineation (shown by pencil; hammer handle points north; loc. 10.101); (b) Linear fabric shown by a fine-grained basalt outcrop – hammer handle points north (loc. 15.045).

angles of 65–85° and is occasionally vertical (Fig. 47b). This fabric is typically preserved in aphyric and spinifex-textured basalts, particularly well developed in rocks of the Two Peaks Volcanics (Fig. 47c), as well as serpentinite in mafic-ultramafic intrusive complexes. Less commonly, S_3 is found in coarse grained mafic intrusive rocks as a spaced cleavage. No lineations have been identified in association with S_3 . In outcrops where multiple fabrics are preserved, the S_3 fabric crosscuts the layer-parallel S_1 fabric (Fig. 48) and also transects F_2 folds. S_3 can be most easily distinguished from the layer-parallel S_1 fabric in areas where bedding is at an oblique angle to S_3 , such as the northeast limb of the Rothsay Fold, however, in areas where the strike of S_1 and S_3 is close to parallel, they are more difficult to differentiate. In contrast to the layer-parallel S_1 fabric, S_3 does not increase in intensity towards lithological contacts, but is pervasive throughout the succession. Several minor NW to NNW-trending sinistral faults with <40 m offset in the hinge zones of D_3 folds may be attributed to the late stages of D_3 shortening (Fig. 49).

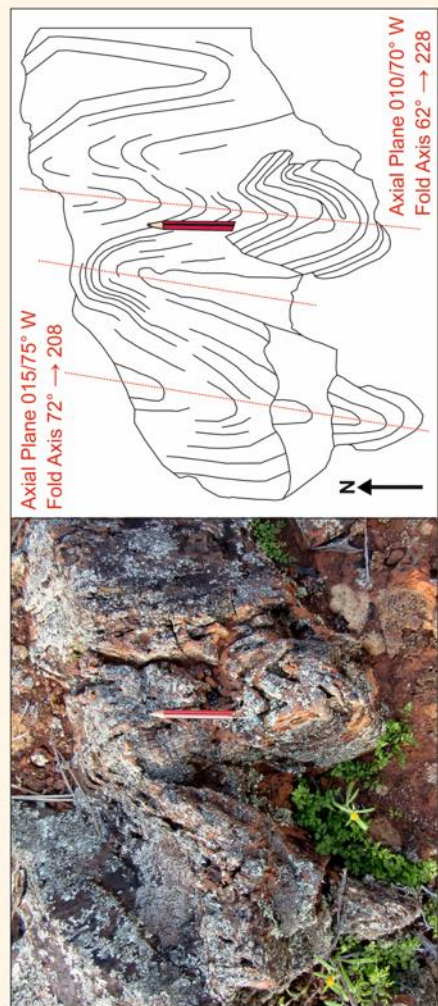
7.6 D_4 Deformation

D_4 deformation is represented by two major NNE- to NNW-trending D_4 shear zones in the Rothsay area, namely the Enchanted Shear Zone (ESZ; Section 7.6.1) and the Rothsay Shear Zone (RSZ; Section 7.6.2), each described in detail below. These D_4 shear zones are continuous for at least ~15 km along strike and are characterised by strongly foliated and lineated rocks (Fig. 49). Foliation intensity increases proximal to and within these two shear zones, defining an S_4 fabric that overprints S_1 and S_3 foliations. The orientation of S_4 foliations are parallel to the regional trend of the respective shear zone (north-northwest to north-northeast), which is broadly similar to that of S_3 foliations. However, S_4 fabrics are typically more intense than S_3 and S_4 is commonly accompanied by a mineral lineation (L_4).

L_4 lineations within D_4 shear zones consist of mineral stretching lineations in rocks where individual crystals can be distinguished, such as coarse-grained mafic intrusions. Conglomerate outcrops proximal to the Enchanted Shear Zone possess an L_4 lineation, defined by the elongation of quartz clasts (Fig. 50a). In fine-grained volcanic rocks, foliated outcrops themselves can possess a linear fabric despite the grain size being too small to distinguish minerals (Fig. 50b). L_4 lineations for both D_4 shear zones in the Rothsay area consistently trend towards the north-northwest to north-northeast, and plunge at angles between 38–60°, most frequently ~50°.

D_4 shear zones dissect F_2 fold axes and S_1 layer-parallel fabrics and the intense S_4 foliation associated with these shear zones consistently overprints the regionally pervasive S_3 fabric.

Sketch map of folding present at locality 13.043, facing north



Tight to isoclinal folding located ~20 metres west

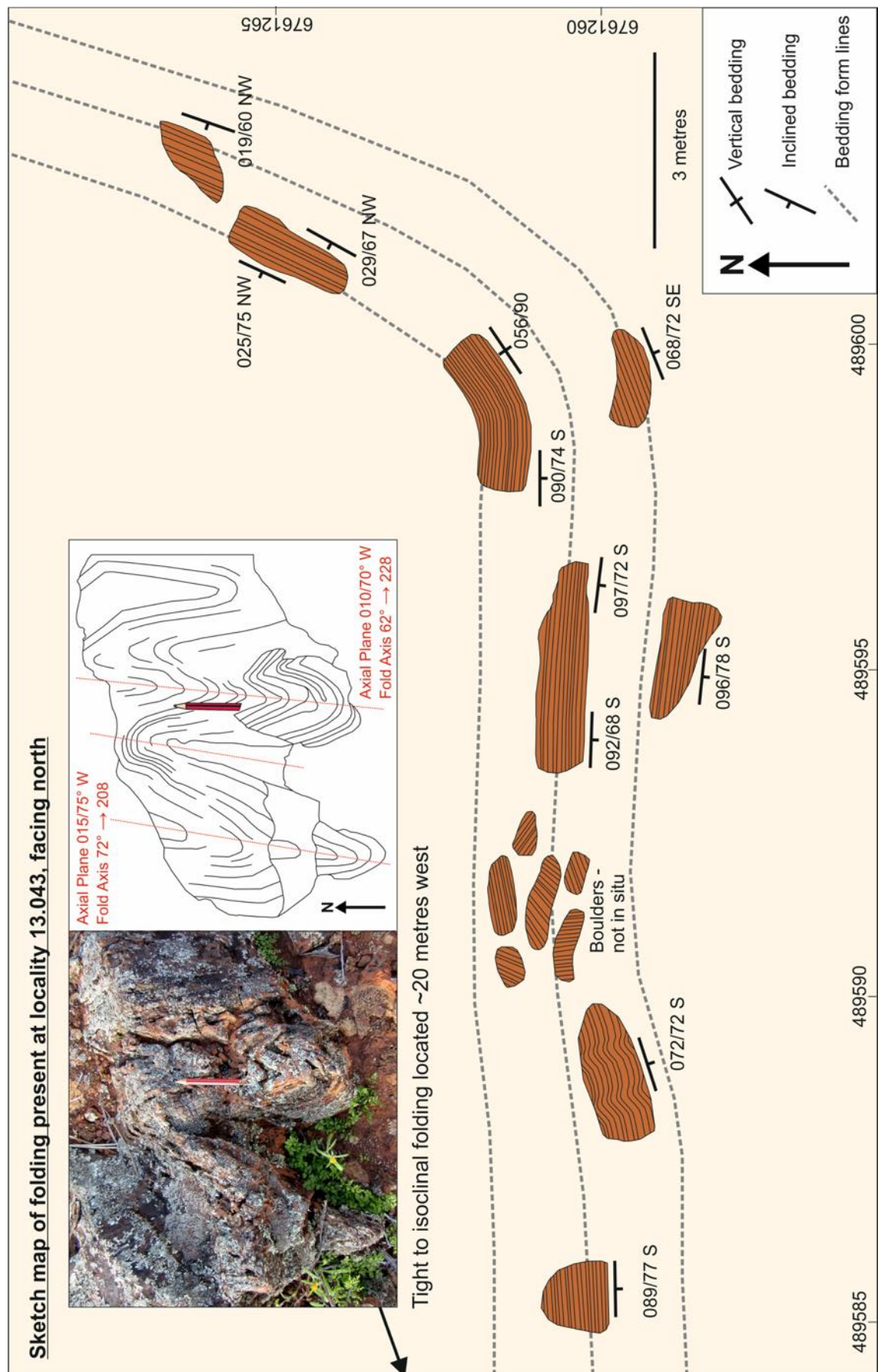


Figure 51: Sketch map of outcropping ferruginous siltstone and BIF at locality 13.049, showing the change in orientation of bedding on approach to the Enchanted Shear Zone. The inset photograph and accompanying sketch show folding present in this unit 20 metres west – axial planes are marked in red and are parallel to the orientation of the transposed bedding.

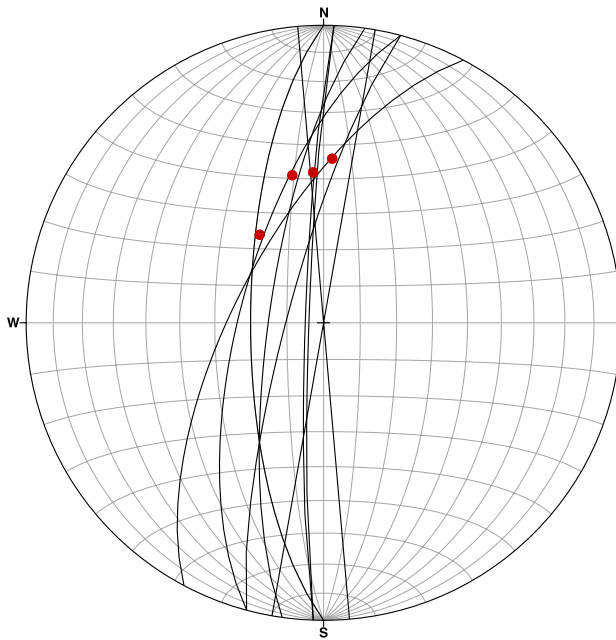


Figure 52: Lower hemisphere equal area stereonet showing foliation planes proximal to the Enchanted Shear Zone (black), and mineral lineation measurements taken on some of these planes (red).

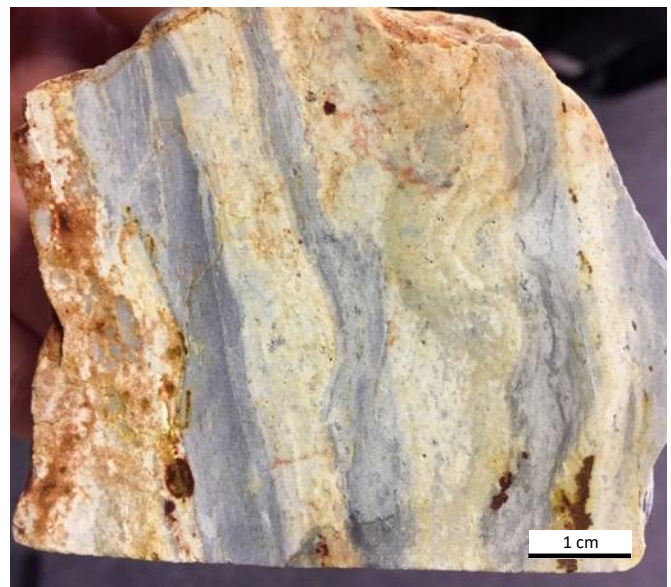


Figure 53: Strongly foliated banded quartzite sampled close to the Enchanted Shear Zone (loc. 12.008).

7.6.1 Enchanted Shear Zone (ESZ)

The ESZ is a NNE-trending D₄ shear zone situated at the eastern margin of the study area that is largely unexposed, covered along its length by superficial cover (Fig. 49). S₄ foliation measurements in rocks exposed along the shear zone are steeply west-dipping at 65-80° to vertically-dipping in some outcrops. L₄ mineral lineations are prevalent in strongly foliated outcrops close to the shear, and consistently plunge towards the north-northwest at angles of 44-60° (Fig. 52). The orientation of this lineation suggests an oblique sense of movement along the shear, and the presence of a vertical component of movement. Unfortunately, no shear sense indicators have been observed within the ESZ; a consequence of the generally poor exposure.

Multiple 100 m-scale fold structures present at the western margin of the ESZ are visible on aeromagnetic imagery, and represent folding associated with deformation along the ESZ. Furthermore, these folds also give an indication of the original geometry of the D₁ dome in this part of the area, which has since been subject to multiple refolding events and shearing. In the far south of the study area, several southeast striking magnetic anomalies deflect towards the northeast on approach to the ESZ, ostensibly defining an additional southeast limb (Fig. 46). Unfortunately, outcrop is generally poor in this part of the area, however, a small exposure is present at locality 13.043, located on the hinge of one of these folds (Fig. 46). At this locality, a 5 m-thick unit of bedded ferruginous siltstone can be traced across one such fold, from the southwest limb to the apparent southeast limb (Fig. 51). The orientation of bedding changes significantly across the outcrop: to the west, bedding is southeast-striking and dips 60-70° southwest, consistent with the outward-dipping pattern of

bedding elsewhere in the area. Bedding in the western part of the outcrop is rotated such that it is E-W striking and dipping 70-80° south. Over the course of 20 metres towards the east, the orientation of bedding progresses to ENE-striking and vertical to NNE-striking and dipping 60-75° northeast (Fig. 51), matching the trend of magnetic anomalies (Fig. 49). This supports the presence of a southeast limb and indicates that the units comprising this limb are overturned, dipping steeply to the northwest. (Fig. 9; Cross Section 2).

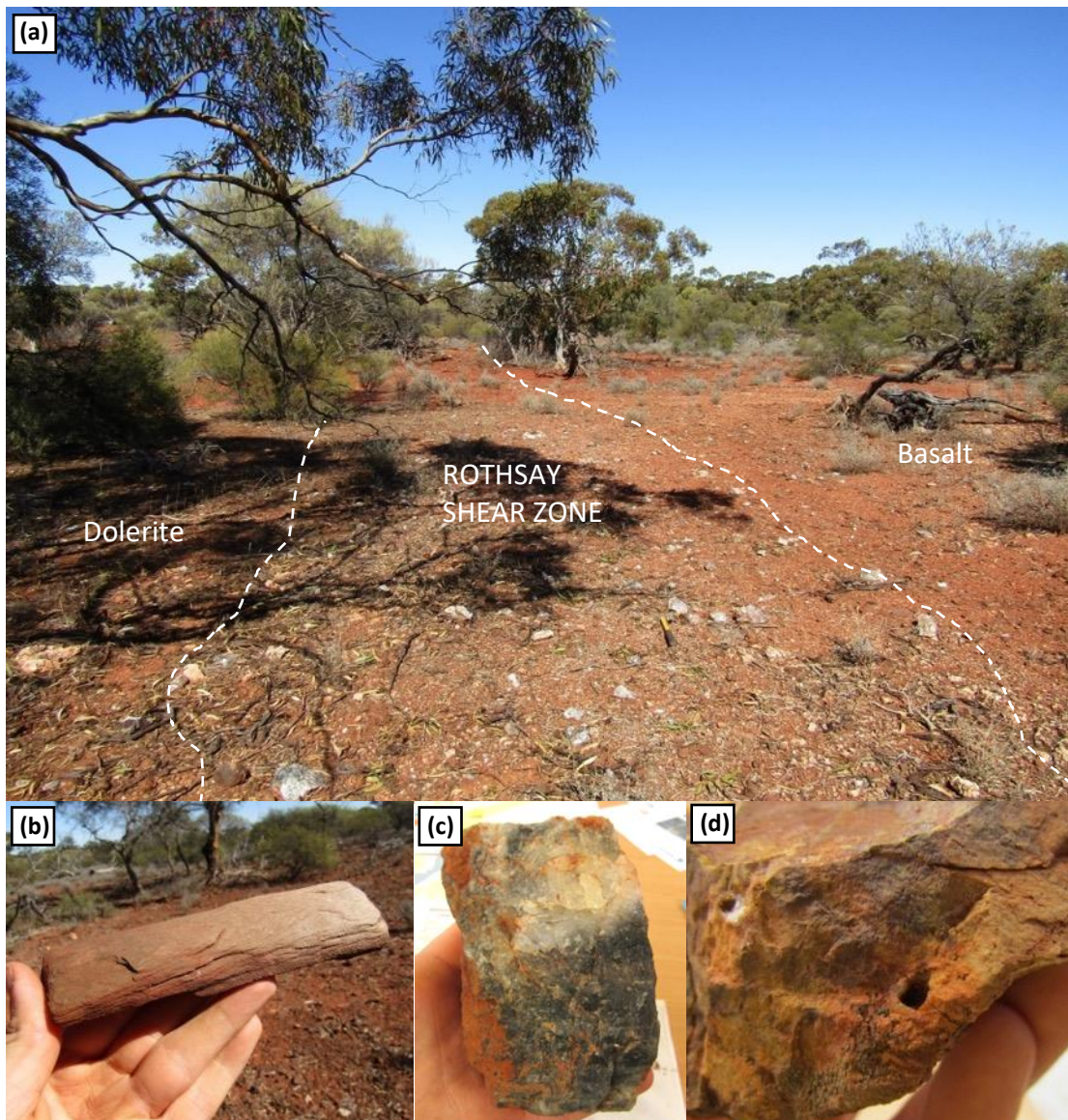


Figure 54: Features observed along the Rothsay Shear Zone at locality 6.124. **(a)** View facing south showing the change in subcrop from dolerite (E) to basalt (W) across the shear zone and quartz and highly foliated material along the contact trending at 350°; **(b)** Sheared material; **(c)** Grey/white quartz from the contact; **(d)** Leached material and mouldic cast, possibly after pyrite.

Elsewhere along this southeast limb (e.g., loc. 12.008), an outcrop of bedded quartzite is also NNE-striking and dips towards the northwest at 77°. This quartzite outcrop comprises yellow and grey banding, which in places is intensely folded (Fig. 53). Foliation measurements along the margins of the shear zone also dip steeply to the northwest, suggesting that bedding has been deformed into the shear. Occurrences of 50 cm-scale folding

are present at locality 13.043, near the Enchanted Shear Zone (Fig. 51). The axial planes of these folds are parallel to the bedding on the southeast limb and parallel to foliation measurements close to the shear zone. Therefore, these folds are interpreted as minor F_4 folds formed during D_4 shearing. The coincidence of overturned bedding and axial planes of outcrop-scale folding, both of which are parallel to the northwest-dipping S_4 fabric along the ESZ, is indicative of shortening and supports a reverse component of shearing along the ESZ.

7.6.2 Rothsay Shear Zone (RSZ)

The RSZ is a north to NNW-striking D_4 shear zone located in the western part of the study area (Fig. 49). The shear is parallel to the supracrustal stratigraphy along much of its length, focused along the contact between the Rothsay Sill and overlying Beryl West Volcanics. The exposure and geometry of the RSZ is different in the northern and southern portion of the Rothsay area. In the north, the shear zone is generally poorly exposed, rarely outcropping as strongly foliated talc-chlorite schist, but usually concealed by superficial cover. In areas of cover, the position of the RSZ can be distinguished from changes in float lithology (Fig. 54a), usually accompanied by strongly foliated and occasionally lineated float (Fig. 54b), dense quartz float (Fig. 54c) and leached, oxidised rocks (locally containing sulphide mouldic casts; Fig. 54d). The shear zone appears to be relatively narrow (<50 m) based on float mapping. The few foliation measurements taken from sporadic outcrops are inconsistent, dipping to the west or east at 65–85°. An L_4 mineral lineation close to the RSZ plunges to the north at 42°.

The southern extent of the Rothsay Shear Zone is markedly different to that in the north (Fig. 49). A striking feature in the south is the repetition of a distinctive 200–250 m-thick sequence of rocks three times, as opposed to once elsewhere along strike. These rocks comprise serpentinite, porphyritic pyroxenite and gabbro of the intrusive Rothsay Sill, and host at least six discrete shears located along lithological contacts, primarily at the margins of serpentinite units. The rock units within the RSZ and between individual shears are overturned and dip towards the northeast at 68–78° (Fig. 10; Cross Section 3). An S_4 foliation that dips ~65° northeast is consistent with the orientation of the shears. On aeromagnetic imagery, there is a lack of horizontal displacement along shears, suggesting a significant vertical component to movement. Further to the northeast of the shear zone, rocks in the underlying succession that dip to the southwest gradually become more steeply dipping, to vertical, to overturned and dipping ~65° northeast on approach to the RSZ (Fig. 10; Cross Section 3). This geometry is consistent with the development of a duplex structure along the southern extent of the RSZ and supports a significant reverse component to D_4 shearing.

7.7 D₅ Deformation

D₅ deformation is represented by a series of ENE-striking, sinistral, brittle D₅ faults. As is the case with shear zones, faults are very poorly exposed in the Rothsay area, largely as a consequence of prolonged weathering. These structures are most easily identified on aeromagnetic imagery as offset magnetic anomalies. Field evidence also confirms the presence of faults and shear zones. In the field, these structures are typically characterised by several distinctive features: linear valleys in areas of outcrop, thick transported cover dispersed with large eucalyptus trees, waterways following the trend of the structure, and an increase in quartz float on the surface, signifying hydrothermal activity. Due to the lack of sufficient outcrop, little is known about the sub-surface orientation of most of these structures.

D₅ sinistral faults have apparent offsets on the order of 120-250 m, and step towards the northwest (Fig. 49). One such D₅ fault outcrops at locality 8.164, where it comprises a narrow (<10 m) outcrop of green talc-chlorite schist and exhibits ~200 m sinistral offset of a BIF unit. Gentle folding of supracrustal units adjacent to D₅ faults is consistent with fault drag associated with synchronous D₅ faulting and demonstrates both brittle and ductile deformation during this episode of deformation. The occurrence of several oblique fabrics with similar orientations on outcrops proximal to D₅ faults may be attributed to D₅ deformation, however these fabrics have not been fully characterised due to a limited dataset.

D₅ faults and their associated fault drag transect F₂ and F₃ fold axes and deform both D₄ shear zones, thus D₅ faults post-date D₄ shearing. Notably, pegmatite dykes mapped in the area are also ENE-trending and broadly parallel to D₅ structures (Section 5.4).

7.8 D₆ Deformation

D₆ deformation, signifying the most recent deformation observed in the Rothsay area, is represented by a major NNE-striking dextral D₆ fault that is continuous for over 10 km and cross cuts all other structures, including the RSZ and D₅ faults (Fig. 49). The apparent offset along this D₆ fault varies from 75 m in the north, to 150 m in the south, based on offset aeromagnetic anomalies (Fig. 49). In contrast to D₅ faults, no fault drag is associated with this D₆ structure. There is very little exposure along its length, and it is instead typified by thick transported cover and increased density of vegetation. Minor N-S striking dextral faults located in the north of the study area are not laterally continuous and commonly correspond to minor valleys in the field (Fig. 49). As these faults have similar orientations and similar apparent offsets (typically 50-80 m, but up to 140 m) to the major D₆ fault, these may represent minor D₆ faults developed during this late deformational event.

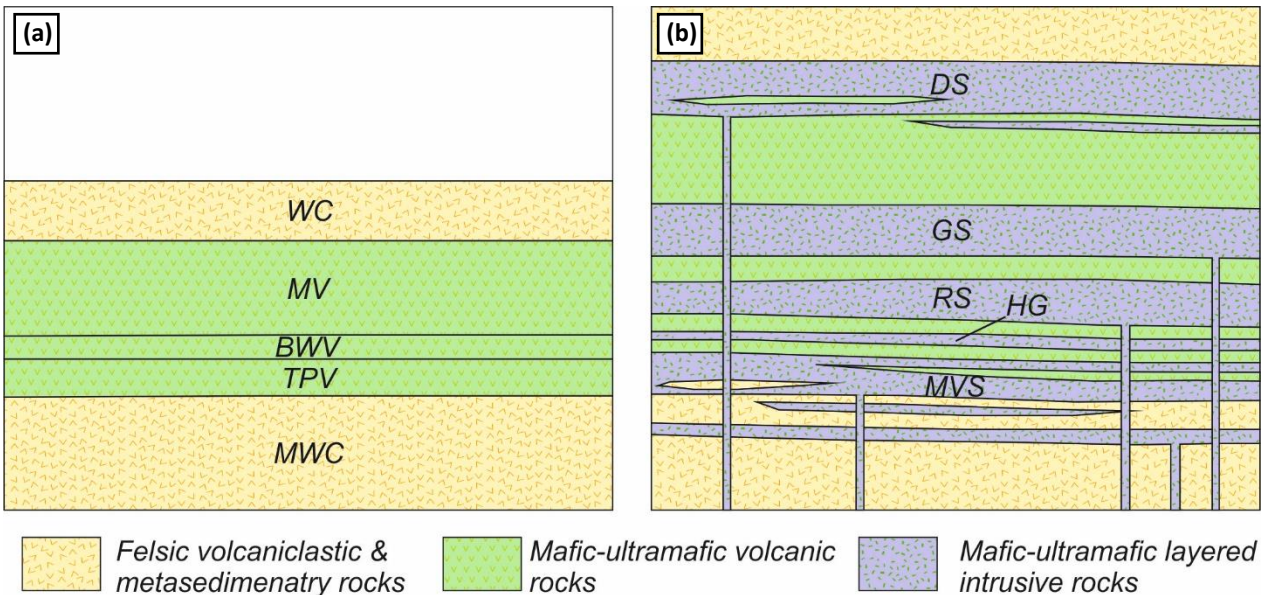


Figure 55: Schematic diagrams for the stratigraphic development of rocks in the Rothsay area. **(a)** Emplacement of the supracrustal succession comprising a lower sequence of felsic volcaniclastics and metasedimentary rocks (MWC; Macs Well Clastics), an overlying mafic succession (TPV; Two Peaks Volcanics, BWV; Beryl West Volcanics, MV; Mulga Volcanics), and an upper felsic/metasedimentary sequence (WC; Willowbank Clastics); **(b)** Subsequent intrusion of a network of mafic-ultramafic layered sills (MVS; Mountain View Sill, HG; Honeycomb Gabbro, RS; Rothsay Sill, GS; Gardner Sill, DS; Damperwah Sill).

8. Discussion

8.1 Supracrustal History

The ~4.2 km-thick volcano-sedimentary stratigraphy in the Rothsay area comprises a broadly bimodal succession, akin to other supracrustal greenstone successions in the Murchison Domain and elsewhere in the Yilgarn Craton (e.g., Watkins and Hickman, 1990; Van Kranendonk et al., 2013). A lower ~1.4 km-thick package of felsic volcaniclastic and metasedimentary rocks (Macs Well Clastics) is overlain by a ~2 km-thick mafic volcanic-dominated succession (Two Peaks Volcanics, Beryl West Volcanics, Mulga Volcanics), representing the Chulaar Group. In turn, these rocks are succeeded by further (>750 m-thick) felsic volcaniclastic and lesser metasedimentary rocks (Willowbank Clastics; Fig. 55a). Contrasting lithologies and features of the two felsic successions, as well as a lack of structures indicative of structural repetition, demonstrate that the upper and lower felsic packages are distinct and form separate components of the bimodal succession. Together, the supracrustal units at Rothsay form part of two volcanic cycles, as has previously been described for the northeastern Murchison Domain by Van Kranendonk and Ivanic (2009). These cycles record a change from effusive mafic and ultramafic volcanism, to more explosive felsic volcanism, separated by intervals of sedimentation.

Metasedimentary rocks of the lower Macs Well Clastics are representative of a marine depositional environment and a period of broad volcanic quiescence. Fluctuations in the depositional energy in the system

resulted in alternations between deposition of quartz sandstone-dominated units and finer-grained ferruginous siltstone. The increasing occurrence of felsic volcaniclastic interbeds with stratigraphic height reflect the onset of felsic volcanism in the region, coincident with the minor eruption of porphyritic dacitic lavas in the Rothesay Area. The upper Macs Well Clastics record a coarsening of metasedimentary units, consistent with increasing depositional energy that likely reflects shallowing of the water column. Pebby sandstone units with conglomeratic horizons are succeeded by thicknesses of bedded felsic volcaniclastic rocks, which contain evidence for sedimentary reworking in the form of cross-bedding. Volcaniclastic units are significantly thicker in some areas than in others, potentially signifying closer proximity to volcanic vents.

After this episode of felsic volcanism, the minor deposition of BIF during volcanic quiescence was followed by the eruption of a significant ~750 m pile of largely aphyric basalt, represented by the Two Peaks Volcanics and Beryl West Volcanics. Occasional, thin flows of porphyritic dacite near the base of this pile represent more fractionated lavas and multiple thin (5-15 m) horizons of BIF and quartzite within the mafic succession represent sedimentation during interruptions in volcanism. A single ~30 m unit of pyroxene spinifex-bearing volcanic rocks towards the top of the Two Peaks Volcanics denotes the first such komatiitic rock of the succession, which increase in both abundance and thickness with stratigraphic height. A further cessation in mafic volcanism is represented by the deposition of a laterally-continuous magnetite-chert BIF unit across the area (>20 km). This is immediately followed by a thin 5 m horizon of lapilli-bearing bedded tuff, recording ongoing distal volcanism. The presence of erosive bases and graded bedding indicate that these tuffs were at least partly affected by sedimentary reworking. Tuff deposition was followed by the resumption of extensive mafic volcanism, resulting in the development of a 1250 m-thick lava pile comprising variolitic, pillow and spinifex-textured basalts. This period of volcanism commenced locally with the eruption of a thick (~20 m) unit that cooled to form pyroxene spinifex-textured volcanic rocks and allowed the development of an ultramafic olivine-bearing cumulate. Similar spinifex-textured units are interspersed amongst the dominantly mafic succession, signifying pulses of komatiitic volcanism during the overall mafic volcanic episode. The lateral continuity of individual spinifex-bearing flows reflects the development of extensive lava plains (e.g., Watkins and Hickman, 1990) and pillow structures exhibited by some basalt flows are indicative of extrusion in a submarine setting. The prevalence of spinifex-textured pyroxene rather than olivine is a feature of many greenstone belts in the Murchison Domain (Lowrey et al., 2017; Van Kranendonk et al., 2013). The textures observed in the Rothesay area are consistent with the acicular, platy and string-beef pyroxene spinifex-textures described by Lowrey et al. (2017) in the northeastern Murchison Domain. Mafic volcanic rocks are overlain by a further, more extensive 140 m-thickness of lapilli-bearing tuff. These rocks are almost identical in appearance to the thin tuff horizon at the base of the Mulga Volcanics and demonstrate ongoing distal volcanism following the end of local volcanism, albeit for a significantly longer period. The top of the bedded tuff signifies the cessation of mafic volcanism.

Overlying poorly-outcropping black mudstone of the Willowbank Clastics represents deposition in a low-energy, environment with little volcanic input, such as a deep marine or an anoxic lake setting. The upwards transition from mudstone to increasingly coarse, more mature and volcanogenic sedimentary rocks, including greywacke and pebbly sandstone, documents increasing energy and closer proximity to felsic volcanism. Proximal felsic volcanism is represented by overlying lapilli-bearing volcanioclastic rocks and ash beds that show a progressive compositional evolution up sequence. Ongoing felsic volcanism has resulted in several hundred metres of fine-grained felsic volcanioclastic rocks, minor felsic volcanic interbeds and welded tuffs, the latter retaining primary flow fabrics. Towards the top of this sequence, laterally-discontinuous lenses of quartz conglomerate containing large (10 cm+) clasts bound by volcanogenic sandstone represent subaerial exposure, and the movement of rivers reworking largely volcanioclastic material at the surface, marking the top of the stratigraphy exposed in the study area.

The mapping undertaken in this study is considerably more detailed than that by Baxter and Lipple (1985). As such, a multitude of new units have been identified, some of which form important components of the stratigraphy, for example the felsic volcanioclastic rocks near the base of the succession. The application of float mapping in areas of little exposure has also allowed the correlation of distinctive marker horizons across a greater extent of the area than in previous, large-scale mapping. As a consequence of more detailed mapping, the relationship between supracrustal rocks and mafic-ultramafic intrusive rocks has been much better constrained (see Section 7.2). Recent regional-scale synthesis geological mapping has suggested that a significant unconformity is present in the northern and western margins of the study area, marking the unconformable contact between the main greenstone supracrustal succession and overlying metasedimentary rocks of the Mougooderra Formation (Ivanic, 2019). Elsewhere in the YSGB, this contact is exposed as a sheared angular unconformity (Watkins & Hickman, 1990), which is proposed to represent an interval of up to 60 Ma (Zibra et al., 2018). It is not clear whether the Willowbank Clastics form part of the Mougooderra Formation based on the geological mapping presented in this study. Further, the contact between the Willowbank Clastics and the underlying Chulaar Group rocks is not exposed in the Rothsay area and so the presence of an unconformable contact cannot be fully established. In this study, no clear supporting evidence has been identified in favour of such an unconformity; bedding measurements remain consistent either side of the contact and deformation is consistent throughout the stratigraphy. However, it must be noted that the northern and western peripheries of the study area suffer from poor exposure, so it is possible that superficial cover is obscuring evidence. Very similar features are shown by the upper Macs Well Clastics and upper Willowbank Clastics, whereby fine grained metapelites are overlain by increasingly mature and coarse metasedimentary rocks (pebbly sandstone, conglomerate), prior to felsic volcanioclastic units. This likeness suggests that the units are part of a repeated volcanic cycle. Similar repeated volcanic cycles are demonstrated by Norie Group and Polelle Group rocks in the northeastern Murchison Domain (Van Kranendonk et al., 2013).

8.2 Intrusion of Mafic-Ultramafic Rocks

Mafic-ultramafic intrusive rocks comprise a significant component (2.6 km; ~39%) of the stratigraphic succession exposed in the Rothsay area. This is consistent with the northeastern Murchison Domain, where several generations of mafic-ultramafic layered intrusive rocks comprise approximately 40% by volume of the greenstones present (Van Kranendonk and Ivanic, 2009). Mafic-ultramafic intrusive complexes also form an integral component of greenstone belts in other cratons, such as the Kaapvaal Craton of South Africa (Anhaeusser, 2006).

At Rothsay, five distinct sills are present at different stratigraphic levels, all of which display compelling evidence for a concordant intrusive relationship with supracrustal rocks (Fig. 55b). This is best exemplified by the lowermost Mountain View Sill, which shows upward chemical evolution, decreasing grain size towards its top, an upper, finer-grained chilled margin, rafts of supracrustal units (BIF and basalt) within the intrusion and lenses of underlying supracrustal rocks (felsic volcaniclastics) near its base. These features are consistent with the intrusion of a network of mafic-ultramafic sills of variable thickness following emplacement of the volcano-sedimentary stratigraphy (Fig. 55b). It is not clear whether the sills were intruded progressively coeval with the emplacement of supracrustal rocks or intruded subsequently. Mafic-ultramafic intrusive complexes have been deformed and metamorphosed in the same manner as surrounding supracrustal rocks, thus were intruded horizontally prior to deformation and metamorphism of the succession. Some of the intrusions are focussed at significant rheological boundaries, such as the contact between felsic volcaniclastic and mafic volcanic successions, and their upper and lower boundaries are frequently in contact with BIF units.

Dolerite and gabbro are the dominant lithologies present in the intrusions. In-situ differentiation of thick (up to 700 m) sills has led to well-developed magmatic layering, comprising cumulate olivine-bearing peridotite bases, coarse-grained pyroxenite and gabbroic centres, which grade upwards into dolerite and variably leucogabbroic and granophyric tops. Some of the intrusive complexes display a single differentiation trend, thus represent a single, thick pulse of magma into the crust, which has subsequently differentiated (e.g. Gardner Sill, Rothsay Sill). In contrast, the Mountain View Sill shows ambiguous differentiation trends and lacks any significant cumulate ultramafic layer(s), suggestive of multiple thinner, overprinting pulses of magma. The Damperwah Sill has a highly evolved quartz dioritic upper portion, including the presence of primary quartz, however, little else can be ascertained about its structure due to extremely poor exposure. In the northeastern Murchison Domain, mafic-ultramafic complexes are interpreted as having been the emplaced as shallow-level subvolcanic sills during eruption of the overlying supracrustal units (Van Kranendonk and Ivanic, 2009). The older, lowermost intrusions show evidence of multiple magmatic pulses and complex layering, in contrast to younger sills which are typically thinner and resemble a single pulse of magma (Ivanic et al., 2010). This same

trend is observed in the Rothsay area, with the lowermost Mountain View Sill comprising multiple overprinting intrusions, and overlying Rothsay and Gardner sills more closely resembling a single pulse of magma.

A notable characteristic of the layered mafic-ultramafic sills at Rothsay is the significant lateral continuity of component lithologies. The distinctive Honeycomb Gabbro can be traced along strike for at least 15 km, and a thin (<30 m) ultramafic cumulate portion of the Rothsay Sill is present over a strike length of > 19 km. Such extensive continuity of layering is indicative of the relatively rapid intrusion of large volumes of magma into the crust. With the assumption that the other horizontal direction at least equals the observed strike length, the ~550 m-thick Rothsay Sill represents the emplacement of magma with a volume of at least 198 km³. Other intrusions, most notably the Gardner Sill, pinch out towards the east, marking the margins of the intrusive complex.

The typical characteristics described above are remarkably consistent with rocks of the ~2800-2790 Ma Warriedar Suite, mapped in the western Youanmi Terrane, including the northern part of the YSGB (Zibra et al., 2017, 2016). The Warriedar Suite consists of mafic-ultramafic intrusive rocks, present largely as sills as well as a number of large intrusive complexes, including the ~66 x 4.5 km Gnanagooragoo Igneous Complex (Ivanic, 2019). Rocks of this suite are typified by well-developed magmatic layering, ultramafic cumulate bases, evolved often granophyric tops, and geometries that are laterally extensive for thicker sills, and that wedge out along strike for thinner sills (Ivanic, 2019). All these features are exhibited by the sills in the Rothsay area, suggesting that they are equivalent to intrusions of the Warriedar Suite.

8.3 Intrusion of Felsic Rocks

Felsic intrusions exposed in the Rothsay area are limited to several narrow (< 5 m) felsic, post-deformational pegmatite dykes that cross-cut all stratigraphic units, major structures and lode-gold mineralisation in the area. Pegmatite dykes are ENE-oriented and increase in abundance towards an unexposed granitic intrusion present in the southeast; part of the 50 x 25 km Seeligson Monzogranite that dissects the Yalgoo-Singleton Greenstone Belt (Zibra et al., 2018; Fig. 2). The close association of felsic pegmatites with the Seeligson Granite supports a genetic relation between the two, and suggests they were emplaced as part of the same intrusive episode, following folding, shearing and emplacement of lode-gold mineralisation. These observations are consistent with the ‘post-tectonic granitoid’ classification ascribed to the Seeligson Monzogranite by (Watkins and Hickman, 1990). The Seeligson Monzogranite has since been assigned to the Walganna Suite of Low-Ca felsic intrusions, comprising biotite ± muscovite monzogranites to syenogranites (Van Kranendonk et al., 2013; Zibra et al., 2018). As is the case in the Rothsay area, Walganna Suite intrusions are known to host pegmatites enriched in LILE elements (Fetherston et al., 2017). Where pegmatites have intruded through Cr-enriched

ultramafic rocks, they have been known to crystallise green beryl (emerald), such as at Poona, near Yalgoo (Ivanic, 2019). This explains the occurrence of emerald to the south of the Rothsay mine, where pegmatites intrude ultramafic cumulate portions of the Rothsay and Gardner sills.

8.4 Deformational History

The structural geology of the Rothsay area records a complex history comprising at least six discrete deformational episodes. Several features formed early during the deformational sequence, namely the layer-parallel S_1 fabric and the D_1 domal geometry, can be explained in terms of several different deformational mechanisms. D_1 doming could be explained in terms of fold superposition or alternatively, granitic diapirism, whereas the layer-parallel S_1 fabric could signify an early episode of layer-parallel shearing, or a manifestation of diapirism. The evidence supporting each of these mechanisms is evaluated in the following sections, with comparisons drawn to deformation in other Archean terranes. A structural model for the Rothsay area is then presented in Section 8.5.

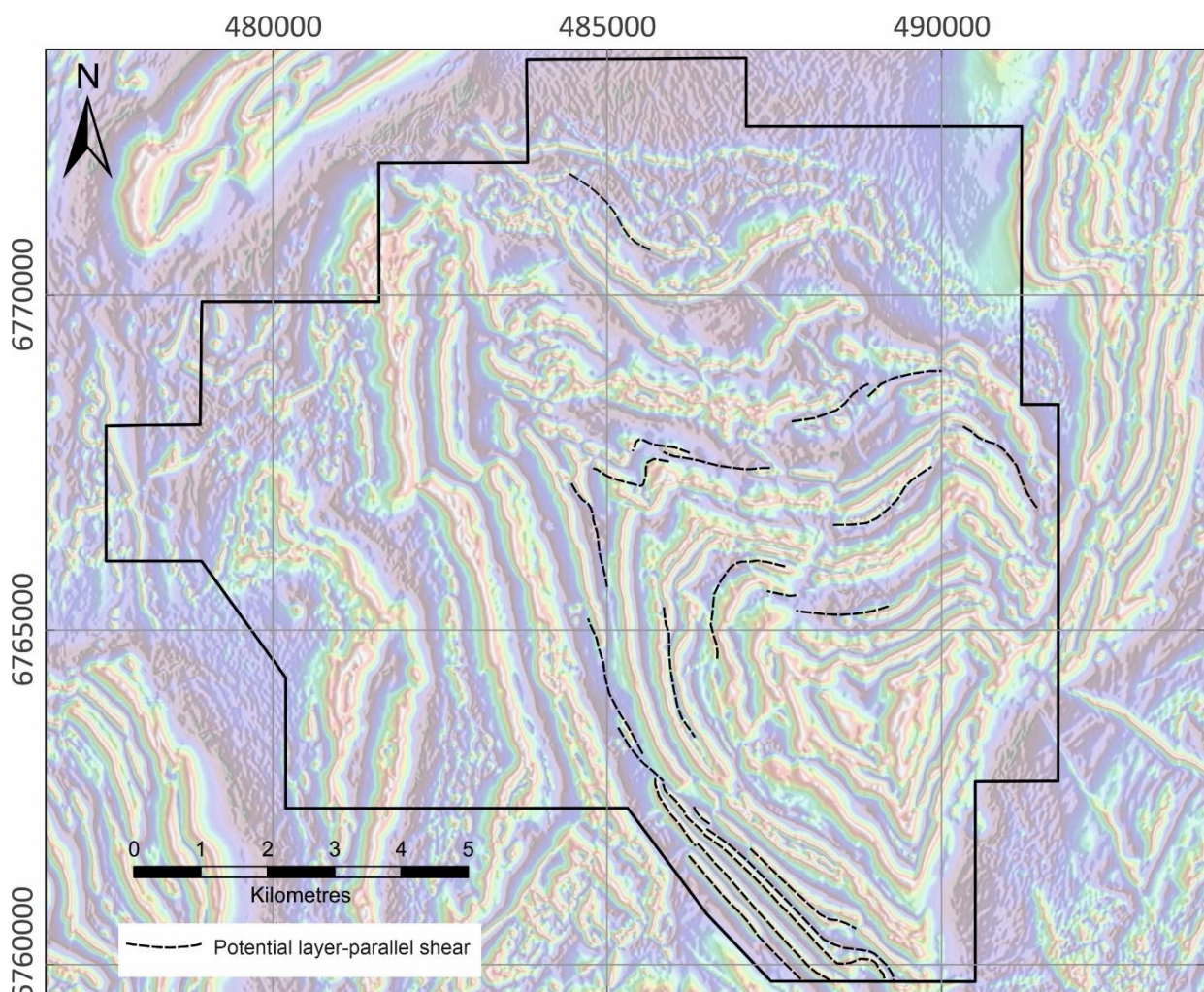


Figure 56: Reduced to pole (RTP) aeromagnetic map of the study area outlining the potential location of layer-parallel shears based on discontinuous magnetic anomalies or structural repetition of units.

8.4.1 Layer-Parallel Shearing

The layer-parallel S_1 fabric observed in the Rothsay area could be interpreted as evidence of an early episode of layer-parallel shearing. Minor metre-scale layer-parallel folding may also be attributed to this early layer-parallel deformation. Early sub-horizontal, layer-parallel fabrics are a feature frequently observed in supracrustal belts in many Archaean cratons (e.g., Swager & Griffin, 1990; Kwelwa et al., 2018). Detailed structural mapping in several greenstone belts has identified low-angle structures associated with layer-parallel fabrics within supracrustal assemblages, which are interpreted to represent early layer-parallel tectonism. In the eastern Yilgarn Craton, Swager & Griffin (1990) recognised early subhorizontal thrust faults that resulted in significant thickening of the supracrustal sequence and stratigraphic repetition in duplex structures. Imbricate stacking of supracrustal units in the Zimbabwe Craton has also been attributed to an early episode of layer-parallel shearing (Dirks & Jelsma, 1998; Hofmann et al., 2001). This deformation was preserved by a layer-parallel D_1 foliation associated with an anastomosing network of narrow shear zones (Dirks & Jelsma, 1998).

In the Rothsay area, no layer-parallel shears have been observed, although the intensity of the layer-parallel S_1 fabric does increase at particular stratigraphic levels. Unlike many areas in which layer-parallel shears have been identified (e.g., Swager & Griffin, 1990; Hofmann et al., 2001), there is no significant repetition of the supracrustal stratigraphy at Rothsay, other than that present along the Rothsay Shear Zone (Section 7.6.2). Although no layer-parallel shears have been mapped, it could be argued that the many instances of laterally-discontinuous or intermittent units are representative of attenuation of the stratigraphy against layer-parallel structures. These discontinuities are most clearly illustrated on aeromagnetic imagery, whereby magnetic units such as ferruginous siltstone, BIF and peridotite pinch out along strike, sometimes multiple times (Fig. 56). Furthermore, the structural repetition of units along the southern portion of the Rothsay Shear Zone (Fig. 56) could be interpreted as having formed during an early period of layer-parallel thrusting, then subsequently reactivated during D_4 shearing. In the Geita greenstone belt, Tanzanian Craton, early sub-horizontal shears within the succession can be very thin and inconspicuous, despite the widespread and pervasive nature of associated layer-parallel fabrics (Sanislav et al., 2017). For this reason, the generally sparse outcrop in the Rothsay area is not good enough to preclude the presence of early layer-parallel shears.

Conversely, most of the laterally-discontinuous units present in the Rothsay area can be suitably explained in terms of magmatic processes and relationships (Section 5.4), such as the prevalent screens and rafts of BIF and basalt within intrusive sill complexes. Similarly, structural repetition along the RSZ could be wholly attributed to D_4 shortening (Section 7.6) in the absence of early layer-parallel deformation. The identification of the S_1 layer-parallel fabric in parts of the study area where all units appear to be continuous for many

kilometres (even 10's of km) also disputes the occurrence of significant sub-horizontal, layer-parallel structures in the area.

8.4.2 Fold Superposition

The general outward-dipping pattern of bedding measurements in the Rothsay area (Section 7.2), together with the identification of a deformed southeastern limb at the margin of the ESZ (Section 7.6), are consistent with the former presence of a dome, which precedes D₂ and all subsequent deformation. The origin of domal geometries in granite-greenstone terranes have long been a subject of controversy (e.g., Snowden & Bickle, 1976). One of the principal dome-forming mechanisms proposed to explain such structures is fold interference, whereby superposition of folds from at least two broadly orthogonal horizontal shortening events results in the development of a domal structure, commonly in the form of a doubly plunging anticline. It has been postulated that fold interference is responsible for the archetypal granite-greenstone pattern of the Pilbara Craton, in which most domes are dominated by vast granitic batholiths (Blewett, 2002). Fold superposition has also been suggested for the development of the greenstone-dominated North Pole Dome of the Pilbara Craton, which is cored by a ~5 km-wide granitic stock at the current erosional level (Blewett et al., 2004) and closely resembles the geometry of the Mt. Mulgine Dome, to the northwest of the study area (Fig. 2). Similarly, Myers & Watkins (1985) suggested fold interference was responsible for the dominant granite-greenstone pattern in the southwestern Murchison Domain of the Yilgarn Craton, and in particular, the ovoid geometry of the Yalgoo Dome, situated immediately northwest of the study area. The Yalgoo Dome was attributed to superposition of upright folds from an earlier period of N-S shortening and subsequent E-W shortening (Myers & Watkins, 1985).

Superposition of multiple fold generations has undoubtedly played a role in the later stages of the structural development of the Rothsay area, as evidenced by multiple F₃ folds within the northeast limb of the major northwest-plunging F₂ fold. However, the role of fold interference in forming the initial domal structure is less clear. It is possible that such a dome-shaped structure could have resulted from superposition of two broadly orthogonal, upright folding events, as suggested locally by Myers & Watkins (1985). Fold interference would have to have occurred after the development of the layer-parallel S₁ fabric, as this fabric is deformed in the same manner as the dome. A similar sequence of events has been documented in the Geita greenstone belt, Tanzania, in which an early layer-parallel S₁ fabric was subsequently affected by D₂-D₃ interference folding of the succession (Kwelwa et al., 2018). However, considering that F₂ folds in the Rothsay area developed during an episode of NE-SW shortening, this would require a preceding or subsequent shortening episode to have been oriented approximately NW-SE, in order to form a dome. Crucially, no structural evidence (i.e. fabrics, folds) supporting an episode of NW-SE shortening in the early stages of deformation have been observed in the Rothsay area.

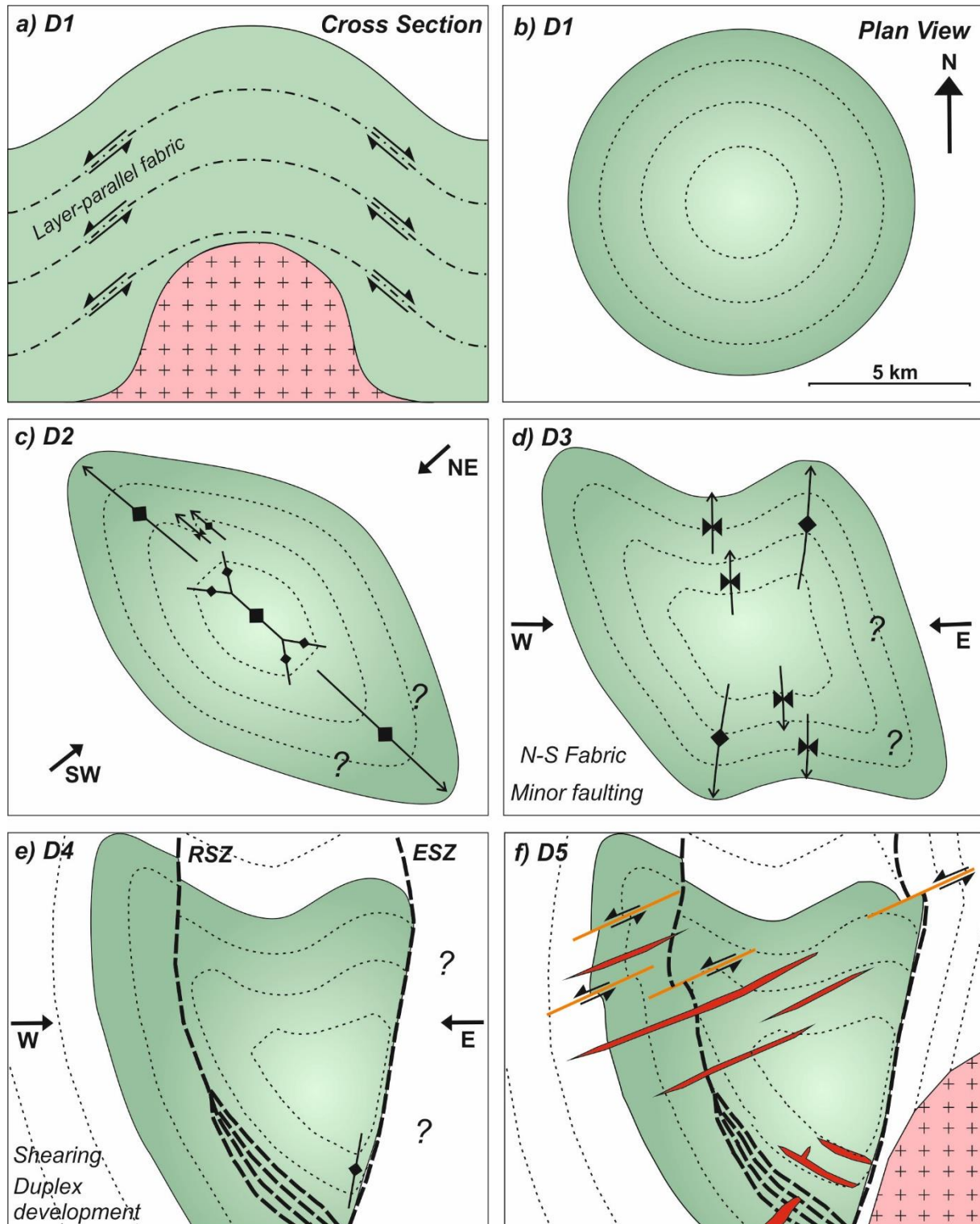
8.4.3 Diapirism

An alternative explanation for the early domal geometry observed in the Rothsay area is that it developed during a period of granitoid diapirism and/or partial convective overturn, and was subsequently refolded and deformed by multiple shortening events. Doming of supracrustal material can be achieved through the diapiric emplacement of granitic material and the outward movement of overlying rocks, resulting from gravitational instability (Collins, 1989; Collins et al., 1998; Van Kranendonk et al., 2002). These diapiric processes have been proposed for the formation of domes and the characteristic dome-and-keel regional patterns in the Pilbara Craton (Van Kranendonk et al., 2004) and in the Zimbabwe Craton (Jelsma et al., 1993). Furthermore, granite-cored domes in the eastern Yilgarn Craton have also been attributed to granitic diapirism (Davis, et al., 2010). Recently, diapirism has been proposed for the development of the Yalgoo Dome (Zibra et al., 2018; Zibra et al., 2020) (Fig. 2), in contrast to previous models invoking fold superposition (Myers & Watkins, 1985; Watkins & Hickman, 1990). Zibra et al. (2018) also suggested that the structural framework of the areas surrounding the Yalgoo Dome were affected primarily by interference between roughly coeval diaps.

If diapirism is considered responsible for the development of the initial dome in the Rothsay area, then modification of the structure through NE-SW shortening (forming plunging F₂ folds) and E-W shortening (forming F₃ folds) can suitably account for the present, refolded domal architecture. The Rothsay area would therefore comprise a diapiric dome refolded by at least two superposed groups of folds. An episode of granite diapirism could also sufficiently explain the layer-parallel S₁ fabric in the Rothsay area, which could have developed during layer-parallel shearing between units as a consequence of diapiric uplift (e.g., Zibra et al., 2018). Such shearing would likely have been focussed in weaker units (i.e., basalt, peridotite) and at contacts between units with significant competency contrasts, accounting for the apparent increase in intensity of S₁ fabrics at major lithological contacts. Furthermore, and perhaps most compelling, is the presence of an analogous domal structure 15 km to the northeast of the study area, where the Mt. Mulgine Dome is composed of outward dipping supracrustal units and is cored by a granitic intrusion (Fig. 2). This granite, known as the Mt. Mulgine granite, is genetically related to the Yalgoo Dome, for which there is extensive structural evidence in favour of diapirism (e.g., Zibra et al., 2018; Clos et al., 2019). The Mt. Mulgine Granite and granitic rocks comprising the Yalgoo Dome have been dated at ca. 2750 Ma (Champion & Cassidy, 2002; Zibra et al., 2018), consistent with regional polydiapirism at this time (Zibra et al., 2020). Supracrustal units deformed around the Mt. Mulgine Dome also preserve a layer-parallel foliation and host radially-oriented faults (Fig. 2); both attributed to doming associated with diapirism (Zibra et al., 2018).

During the geological mapping undertaken as part of this study, no granitic intrusion has been observed at or near the core of the dome at Rothsay, as would be expected for a diapiric dome (e.g., Van Kranendonk et al., 2004; Davis et al., 2010). Furthermore, no evidence of contact metamorphism or hydrothermal alteration has

been observed in supracrustal rocks comprising the core of the fold, and metasedimentary units are relatively unaltered, albeit very poorly exposed. A plausible explanation is that the granitic core is unroofed at the current level of erosion and remains at depth, in contrast to other neighbouring diapiric intrusions which are exposed at the cores of structures such as the Yalgoo and Mt. Mulgine domes (Fig. 2).



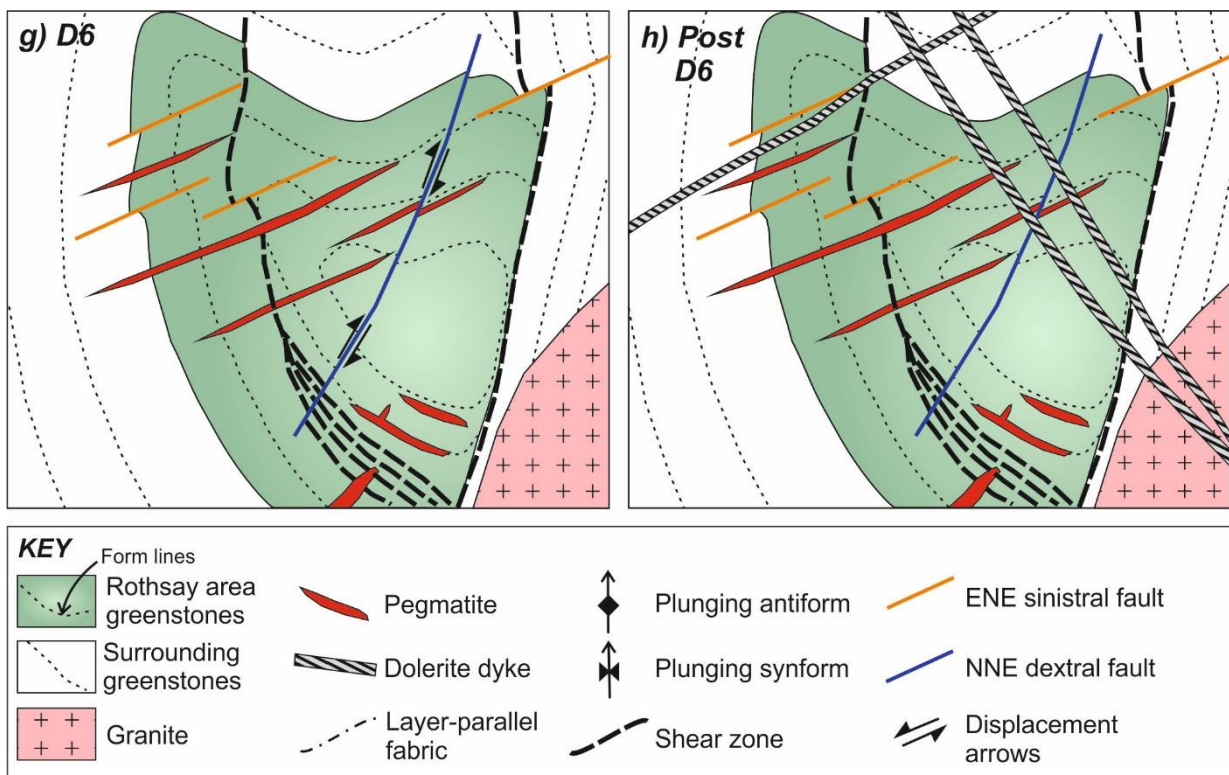


Figure 57: Schematic diagrams illustrating the structural development of the Rothsay Fold. **(a)** D1 – Cross section illustrating granite diapirism forming a domal structure in overlying supracrustal units. Layer-parallel shearing developed the layer-parallel foliation, focused in fine grained units and at contacts between units of high competency contrast; **(b)** D1 – Plan view of dome structure, consisting of a radial pattern of outward dipping units; **(c)** D2 – NE-SW shortening, leading deformation of the domal structure and the formation of a major NW-plunging antiform and associated box fold axes, in addition to minor NW-SE trending fold axes; **(d)** D3 - E-W shortening resulting in the development of overprinting N-S trending fold axes on the northeast limb of the structure (possibly replicated on the southern limb) and a pervasive N-S striking fabric; **(e)** D4 – Localisation of strain during continued E-W shortening leads to the development of two major shear zones (ESZ; Enchanted Shear Zone, RSZ; Rothsay Shear Zone), which both show evidence of a significant vertical component to movement. The RSZ displays duplex development in the south and the southeastern limb of the dome is inverted by the ESZ; **(f)** D5 - ENE-oriented sinistral faulting and associated folding (fault-drag) that deform shear zones, coeval with the intrusion of parallel ENE-striking pegmatite dykes, directly related to the intrusion of the Seeligson Monzogranite to the southeast; **(g)** D6 – Late-stage, brittle, dextral fault dissecting the area including shear zones; **(h)** Post-D6 – Intrusion of (near)-vertical doleritic dykes discordant to all units and structures in the area, marking the final stage of crustal development.

On balance, deformation associated with granite diapirism sufficiently explains both the early domal architecture and the layer-parallel fabric, and is also consistent with regional geological studies in the southwestern Murchison Domain (e.g., Zibra et al., 2018; Clos et al., 2019; Zibra et al., 2020), which provide compelling evidence in favour of a major episode of granitic diapirism in the region at c. 2750 Ma. For these reasons, granitic diapirism is considered the favoured mechanism for the early structural development of the Rothsay area according to this study. However, in the absence of further detailed structural mapping and with limited exposure, early layer-parallel shearing and formation of a dome through fold interference cannot currently be fully discounted.

8.5 Structural Model

In this section, a model for the structural deformational framework of the Rothsay area is presented, based on the structural observations and measurements described in this study. The model comprises six deformational episodes (D_1 - D_6). The earliest deformation, for which evidence is the most ambiguous, occurred subsequent to the emplacement of a thick succession of supracrustal units and laterally-extensive, voluminous mafic-ultramafic intrusions, attributed to a period of broad extension (D_0). The details and features associated with each of these deformational episodes are outlined in Table 3 and illustrated schematically in Figure 3.57.

The first deformational event (D_1) distinguished in the Rothsay area is relatively well-preserved as a layer-parallel S_1 fabric and the original domal geometry of the area (which has since been significantly modified). Doming developed during a period of granitic diapirism, in association with several other diapirs in the surrounding areas including the Yalgoo Dome and the Mt. Mulgine Dome (Zibra et al., 2020) (Fig. 57b). As a consequence, supracrustal rocks overlying a granitic diapir were uplifted, and layer-parallel shearing occurred along lithological contacts, primarily focussed in weaker rock types and resulting in a conspicuous S_1 layer-parallel fabric (Fig. 57a). The discontinuity of some units, primarily basalt and BIF, can be fully explained in terms of magmatic processes relating to the intrusion of a network of mafic-ultramafic sills prior to deformation.

The second deformational event, D_2 , consisted of a period of NE-SW shortening, resulting in the constriction of the domal structure and the formation of a northwest-plunging antiform in the northwest, associated with other minor, parasitic F_2 folding (Fig. 57c). Some box-folding also developed during this shortening episode. It is possible that an equivalent southeast-plunging antiform developed in the southeast, however evidence is obscured by subsequent deformation and granite intrusion. No discernible fabric is associated with D_2 deformation.

The third episode of deformation (D_3) comprised a period of E-W shortening, resulting in refolding of the northern part of the dome into a series of north-plunging and north-south striking open F_3 folds (Fig. 57d). The major F_2 fold axes may also have been slightly deformed towards the north during D_3 . This event is also responsible for the pervasive N-S striking, steeply-dipping fabric (S_3) frequently preserved in rocks of the area, broadly axial-planar to F_3 folding. This fabric is equivalent to the regional tectonic grain present across much of the Murchison Domain (Van Kranendonk et al., 2013; Watkins and Hickman, 1990).

Subsequent D_4 deformation is attributed to the localisation of strain during ongoing E-W shortening, resulting in the development of the two major NNE- and NNW-trending shear zones in the area, the Rothsay Shear Zone and the Enchanted Shear Zone (Fig. 57e). Both shear zones display evidence for a significant vertical

component of shear. For example, the RSZ exhibits a complex duplex structure consisting of overturned supracrustal units, an oblique down-dip stretching mineral lineation and the thickness of mafic-ultramafic sills differs considerably on either side of the shear. Furthermore, abundant sub-horizontal ladder veins observed in the Rothsay mine along the RSZ also support a vertical component of shear, considering that mineralisation was concomitant with shearing (de Vries, 2015). The ESZ also possesses an oblique down-dip mineral lineation, exhibits small scale F₄ folding with axial surfaces parallel to the shear plane and is responsible for overturning the south-eastern limb of the original domal architecture of the Rothsay Fold (Fig. 57e). The orientation of the RSZ and ESZ matches that of other major shear zones in the belt (Fig. 2), indicating they formed as part of the same sustained episode of E-W shortening. It is possible that the ESZ is the southernmost extension of the Mougoderra Shear Zone, located to the north (Fig. 2). The RSZ and ESZ also broadly match the NNE to NNW-striking shear zones present in the northeastern Murchison Domain (Van Kranendonk et al., 2013; Watkins and Hickman, 1990). Seismic reflection profiles across the Murchison Domain and neighbouring Southern Cross Domain display listric NW-dipping crustal-scale thrust systems (Wyche et al., 2013). These structures are thought to be responsible for shortening across the region (Wyche et al., 2013) and likely correspond to the D₃ and D₄ deformation events described above.

The fifth phase of deformation, D₅, consisted of NE-SW shortening and resulted in the development of a series of ENE-trending, sinistral faults offsetting the two major D₄ shear zones in the area, the RSZ and the ESZ, as well as all pre-existing folds (Fig. 57f). Supracrustal units are deformed towards these structures, consistent with fault drag. This event may also be responsible for the development of some oblique late-stage fabrics near these structures that are not consistent with S₁ or S₃ orientations. Felsic pegmatite dykes cross cutting the supracrustal stratigraphy are also ENE-trending, parallel to the D₅ faults, and also crosscut earlier folding and D₄ shearing (Fig. 57f). Further, emplacement of these ENE-striking dykes is consistent with NE-SW shortening and an approximate NW-SE σ_3 direction. For these reasons, it is suggested that pegmatites were intruded during D₅ deformation, and by extension, the emplacement of the Seeligson Monzogranite with which pegmatites are directly associated. The intrusion of the 50 x 25 km Seeligson Monzogranite dissected the greenstone belt and may have caused minor tilting of units and structures in the study area to the northwest, enhancing the plunge of S₂ and S₃ folds.

A minor subsequent deformation event, D₆, involved NNE-oriented dextral faulting that cross cuts the RSZ (Fig. 57g). The lack of folding associated with this fault suggests it occurred during late-stage deformation in the brittle regime. Unfortunately, the subsurface orientation of this fault is not constrained, however, the board continuity of the stratigraphy on either side tentatively suggests the lack of a significant vertical component of movement. Furthermore, other minor N-S to NNW-SSE trending faults in the north of the study area with similar offsets to the major D₆ fault, likely represent minor D₆ faults developed during this episode.

Finally, a period of regional extension resulted in the intrusion of several orientations of near-vertical dolerite dykes. These dykes crosscut all lithologies and structures, are principally orientated NW-SE but also NE-SW and mark the final stage of the lithological and structural development of the area (Fig. 57h). These dykes are prevalent across much of the Murchison Domain and wider Yilgarn Craton and are widely regarded to be Proterozoic in age (e.g., Watkins and Hickman, 1990; Ivanic et al., 2010; Ivanic, 2019).

9. Synthesis

The geology of the Rothsay Fold area consists of a ~6.8 km-thick stratigraphic succession, which can be divided into 4.2 km of supracrustal rocks and 2.6 km of mafic-ultramafic intrusive sills. The supracrustal stratigraphy comprises a bimodal sequence of felsic volcaniclastic rocks accompanied by metasedimentary rocks, and mafic-ultramafic volcanic rocks. Components of two bimodal sequences are present: a lower felsic association, an overlying mafic-ultramafic association, and an uppermost felsic association. Many units have been recognised that have not previously been identified by larger-scale regional mapping (Baxter and Lipple, 1985). Supracrustal rocks have been divided into the Chulaar Group, which comprises the lowermost Macs Well Clastics, Two Peaks Volcanics, Beryl West Volcanics and Mulga Volcanics, in addition to the stratigraphically uppermost Willowbank Clastics. Although structural measurements indicate that the basal contact of the Willowbank Clastics does not appear to represent an angular unconformity as previously suggested (e.g., Ivanic, 2019), a lack of exposure prevents the true nature of the contact from being fully established. A suite of four mafic-ultramafic layered intrusive sills have intruded the supracrustal stratigraphy. Each sill complex is distinct; lower sills represent multiple overprinting episodes of magmatism whereas upper sills document a single pulse of magma. Most of these sills show remarkable lateral continuity over distances in excess of 20 km, signifying rapid emplacement of magma, followed by in-situ differentiation. A granitic pluton, the Seeligson Monzogranite, intruded the succession in the southwest and is directly related to a set of parallel ENE-striking pegmatite dykes. These pegmatite dykes have locally been identified as Li-bearing, in addition to the previously known B-enrichment (Fetherston et al., 2017).

A deformational model is proposed to account for the structural development of the Rothsay area. The model invokes an early phase of granite diapirism (D_1) as responsible for the domal architecture of the area. This is consistent with previous structural studies of neighbouring areas (e.g., Clos et al., 2019; Zibra et al., 2020) and suggests the coeval formation of the Rothsay Dome alongside the adjacent Mt. Mulgine Dome and Yalgoor Dome. However, unlike the Yalgoor and Mt. Mulgine Domes that have been unroofed via erosion to reveal their granitic cores, the Rothsay dome is interpreted as not unroofed. Diapirism was followed by subsequent NE-SW shortening (D_2) and E-W shortening (D_3), which caused refolding of the dome in multiple orientations and the latter imparted a regional N-S tectonic grain across the area. Diapiric doming and fold interference are typically considered to be exclusive processes, however, this study demonstrates an example of a diapiric

dome that has been subjected to fold interference on a similar scale to that of the original dome. With ongoing E-W shortening, strain became localised and resulted in the development of two major NNE to NNW-striking shear zones (D_4). The shear zones, one of which is host to lode-gold mineralisation and the other largely unexposed, consistently display a reverse component of shear, consistent with shortening. A subsequent episode of NE-SW shortening (D_5) led to further smaller scale faulting/shearing, coeval with the intrusion of the Seeligson Monzogranite pluton with associated pegmatitic dykes. followed by a late stage of localised brittle faulting (D_6). The intrusion of cross-cutting doleritic dykes, likely in the Proterozoic, marks the final stages of development in the area.

10. Authorship Contribution

J.J Price: Fieldwork, Digitisation, Petrographic Analysis, Structural Analysis, Writing – original draft.

T.G. Blenkinsop: Structural Analysis, Writing – review and editing.

K.M. Goodenough: Writing – review and editing.

A.C. Kerr: Writing – review and editing.

11. Acknowledgements

J.J. Price is supported by a NERC GW4+ DTP studentship from the Natural Environment Research Council [NE/L002434/1]. Fieldwork was conducted thanks to generous logistical support from Minjar Gold Pty and financial support from the Society of Economic Geologists Canada Foundation. Access to tenements for geological mapping was kindly provided by Minjar Gold Pty and Egan Street Resources. Many thanks to Gavyn Kemp for his insights and observations regarding the prospectivity of the Rothsay area. Conversations and correspondence with Dr. Tim Ivanic at GSWA has been greatly appreciated. The structural section of the study benefitted from valuable conversations with Michael Nugus. Thanks to Tony Oldroyd for preparation of thin sections used in this study.

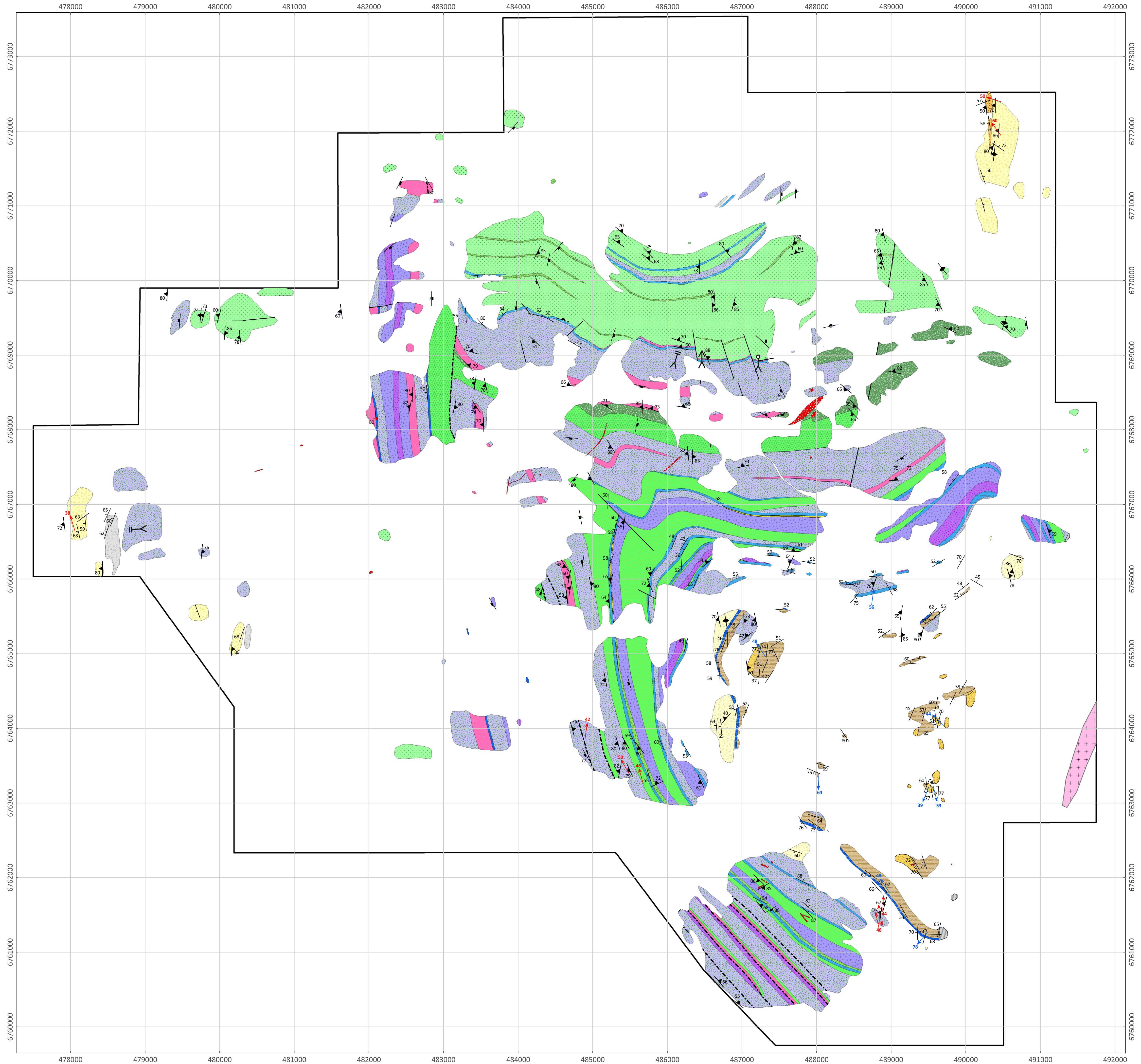
12. References

- Anhaeusser, C.R., 2006. Ultramafic and mafic intrusions of the Kaapvaal Craton, in: Johnson, M.R., Anhaeusser, C.R., Thomas, R.J. (Eds.), *Geology of South Africa*. Geological Society of South Africa, Johannesburg and Council for Geoscience, Pretoria, pp. 95–134.
- Arndt, N. T., Naldrett, A. J. & Pyke, D. R. 1977. Komatiitic and iron-rich tholeiitic lavas of Munro Township, Northeast Ontario. *Journal of Petrology* 18, p. 319–369.
- Arndt, N. T., Lesher, C. M. & Barnes, S. J. 2008. *Komatiite*. Cambridge University Press, 488 pp.
- Baxter, J.L. & Lipple, S.L., 1985. Perenjori, Western Australia. Geological Survey of Western Australia, 1:250,000 Geological Series SH/50-6 Explanatory Notes.
- Blewett, R.S. 2002. Archaean tectonic processes: a case for horizontal shortening in the North Pilbara granite-greenstone terrane, Western Australia. *Precambrian Research*, 113, p. 87–120.
- Blewett, R.S., Shevchenko, S. & Bell, B. 2004. The North Pole Dome: a non-diapiric dome in the Archaean Pilbara Craton, Western Australia. *Precambrian Research* 133, p. 105-120.
- Butt, C.R.M. 1981. The nature and origin of the lateritic weathering mantle, with particular reference to Western Australia. In: Doyle, H.A., Glover, J.E. & Groves, D.I. (eds.), *Geophysical prospecting in deeply weathered terrains*, University of Western Australia, Geology Department and Extension Service, Publication No. 6, p. 11-29.
- Cassidy, K.F., Champion, D.C., Krapez, B., Barley, M.E., Brown, S.J.A., Blewett, R.S., Groenewald, P.B. & Tyler, I.M., 2006. A revised geological framework for the Yilgarn Craton, Western Australia: Geological Survey of Western Australia – Record 2006/8, p. 1–8.
- Champion, D.C. & Cassidy, K.C. 2002. Granites of the northern Murchison Province: their distribution, age, geochemistry, petrogenesis, relationship with mineralisation, and implications for tectonic environment. AMIRA P482/MERIWA M281 - Yilgarn Granitoids. p. 5.1–5.54.
- Clarke, E.D., 1925. The Geology and Mineral Resources of the Yalgoo Goldfield Part II - The Mining Centres of Rothesay and Goodingnow (Payne's Find). Geological Survey of Western Australia, Bulletin 86, 41 pp.
- Clos, F., Weinberg, R.F., Zibra, I. & Schwindinger, M., 2019. Magmatic and anatetic history of a large Archean diapir: Insights from the migmatitic core of the Yalgoo Dome, Yilgarn Craton. *Lithos*, 338–339, p. 18–33.
- Collins, W.J., 1989. Polydiapirism of the Archaean Mt. Edgar Batholith, Pilbara Block, Western Australia. *Precambrian Research*, 43, p. 41–62.
- Collins, W. J., Van Kranendonk, M.J. & Teyssier, C. 1998. Partial convective overturn of Archaean crust in the east Pilbara Craton, Western Australia: Driving mechanisms and tectonic implications. *Journal of Structural Geology*, 20, p. 1405–1424.

- Davis, B.K., Blewett, R.S., Squire, R., Champion, D.C. & Henson, P. A. 2010. Granite-cored domes and gold mineralisation: Architectural and geodynamic controls around the Archaean Scotia-Kanowna Dome, Kalgoorlie Terrane, Western Australia. *Precambrian Research*, 183, p. 316–337.
- de Vries, P.W., 2015. Gold and tectonic evolution of the southern end of the Yalgoo-Singleton greenstone belt , Murchison Domain, Western Australia. Undergraduate BSc thesis, University of New South Wales.
- Dirks, P.H.G.M. & Jelsma, H.A. 1998. Silicic layer-parallel shear zones in a Zimbabwean greenstone sequence: horizontal accretion preceding doming. *Gondwana Research* 1, p. 177–193.
- Fetherston, J.M., Stocklmayer, S.M. & Stocklmayer, V.C., 2017. Gemstones of Western Australia, Second Edition. Geological Survey of Western Australia, Mineral Resources Bulletin 25, 356 pp.
- Gee, R.D., Baxter, J.L., Wilde, S.A. & Williams, I.R. 1981. Crustal development in the Archaean Yilgarn Block, Western Australia. In: Glover, J.E. & Groves, D.I. (eds.) *Archaean Geology, 2nd International Archaean Symposium*, Perth, 1980, Geological Society of Australia Special Publication 7. pp. 43-56.
- Hofmann, A., Dirks, P.H.G.M. & Jelsma, H.A. 2001. Late Archaean foreland basin deposits, Belingwe greenstone belt, Zimbabwe. *Sedimentary Geology*, 141-142. p. 131–168.
- Ivanic, T.J., 2019. Mafic–ultramafic intrusions of the Youanmi Terrane, Yilgarn Craton. Geological Survey of Western Australia, Report 192, 121 pp.
- Ivanic, T.J., 2018. Ninghan, WA Sheet 2339. Geological Survey of Western Australia, 1:100 000 Geological Series.
- Ivanic, T.J., Li, J., Meng, Y., Guo, L., Yu, J., Chen, S. & Zibra, I., 2015. Yalgoo, WA Sheet 2241. Geological Survey of Western Australia, 1:100 000 Geological Series.
- Ivanic, T.J., Van Kranendonk, M.J., Kirkland, C.L., Wyche, S., Wingate, M.T.D. & Belousova, E.A., 2012. Zircon Lu-Hf isotopes and granite geochemistry of the Murchison Domain of the Yilgarn Craton: Evidence for reworking of Eoarchean crust during Meso-Neoarchean plume-driven magmatism. *Lithos*, 148, p. 112–127.
- Ivanic, T.J., Wingate, M.T.D., Kirkland, C.L., Van Kranendonk, M.J. & Wyche, S., 2010. Age and significance of voluminous mafic-ultramafic magmatic events in the Murchison Domain, Yilgarn Craton. *Australian Journal of Earth Science*, 57, p. 597–614.
- Jelsma, H.A., van der Beek, P.A.& Vinyu, M.L., 1993. Tectonic evolution of the Bindura-Shamva greenstone belt (northern Zimbabwe): Progressive deformation around diapiric batholiths. *Journal of Structural Geology*, 15, p. 163–176.
- Kwelwa, S.D., Dirks, P.H.G.M., Sanislav, I.V., Blenkinsop, T.G. & Kolling, S.L. 2018. Archaean gold mineralisation in an extensional setting: The structural history of the Kukuluma and Matandani deposits, Geita greenstone belt, Tanzania. *Minerals* 8 (171), p. 1-33.
- Lowrey, J.R., Ivanic, T.J., Wyman, D.A. & Roberts, M.P., 2017. Platy pyroxene: New insights into spinifex texture. *Journal of Petrology*, 58, p. 1671–1700.

- Lowrey, J.R., Wyman, D.A., Ivanic, T.J., Smithies, R.H. & Maas, R., 2020. Archean Boninite-like Rocks of the Northwestern Youanmi Terrane, Yilgarn Craton: Geochemistry and Genesis. *Journal of Petrology*, 60, p. 2131–2168.
- Myers, J.S. & Watkins, K.P., 1985. Origin of granite- greenstone patterns, Yilgarn Block, Western Australia. *Geology*, 13, p. 778–780.
- Pidgeon, R.T. & Wilde, S.A., 1990. The distribution of 3.0 Ga and 2.7 Ga volcanic episodes in the Yilgarn Craton of Western Australia. *Precambrian Research*, 48, p. 309–325.
- Pidgeon, R. & Hallberg, J., 2000. Age relationships in supracrustal sequences of the northern part of the Murchison Terrane, Archaean Yilgarn Craton, Western Australia: A combined field and zircon U-Pb study. *Australian Journal of Earth Science*, 47, p. 153–165.
- Price, J.J. 2014. Gold exploration in the Yalgoo-Singleton Greenstone Belt, Western Australia. Unpublished BSc thesis, School of Earth & Ocean Sciences, Cardiff University, 123 pp.
- Sanislav, I.V., Brayshaw, M., Kolling, S.L., Dirks, P.H.G.M., Cook, Y.A. & Blenkinsop, T.G. 2017. The structural history and mineralization controls of the world class Geita Hill gold deposit, Geita Greenstone Belt, Tanzania. *Mineralium Deposita* 52(2), pp. 257-279.
- Smithies, R.H., Ivanic, T.J., Lowrey, J.R., Morris, P.A., Barnes, S.J., Wyche, S. & Lu, Y.J., 2018. Two distinct origins for Archean greenstone belts. *Earth & Planetary Science Letters*, 487, p. 106–116.
- Snowden, P. A. & Bickle, M. J. 1976. The Chinamora Batholith: diapiric intrusion or interference fold? *Journal of the Geological Society*, 132 (2). p. 131-137.
- Swager, C., Witt, W.K., Griffin, T.J., Ahmat, A.L., Hunter, W.M., McGoldrick, P.J. & Wyche, S. 1990. A Regional Overview of the Late Archaean Granite Greenstones of the Kalgoorlie Terrane. In: Ho, S.E., Glover, J.E., Myers, J.S. and Muhling, J.R. (eds.) *Third International Archaean Symposium, Perth 1990 - Excursion Guidebook*, University of Western Australia, Perth, Australia, p. 205–303.
- Swager, C. & Griffin, T.J., 1990. An early thrust duplex in the Kalgoorlie-Kambalda greenstone belt, Eastern Goldfields Province, Western Australia. *Precambrian Research*, 48, p. 63–73.
- Van Kranendonk, M.J., Hickman, A.H., Smithies, R.H., Nelson, D. & Pike, G. 2002. Geology and Tectonic Evolution of the Archaean North Pilbara Terrain, Pilbara Craton. *Western Australia. Economic Geology*, 97, p. 695–732.
- Van Kranendonk, M.J., Collins, W.J., Hickman, A. & Pawley, M.J., 2004. Critical tests of vertical vs. horizontal tectonic models for the Archaean East Pilbara Granite-Greenstone Terrane, Pilbara Craton, Western Australia. *Precambrian Research*, 131, p. 173–211.
- Van Kranendonk, M.J. & Ivanic, T.J., 2009. A new lithostratigraphic scheme for the northeastern Murchison Domain, Yilgarn Craton. *GSPA Annual Review 2007-2008, Technical Paper*, p. 35–53.
- Van Kranendonk, M.J., Ivanic, T.J., Wingate, M.T.D., Kirkland, C.L. & Wyche, S., 2013. Long-lived, autochthonous development of the Archean Murchison Domain, and implications for Yilgarn Craton tectonics. *Precambrian Research*, 229, p. 49–92.

- Wang, Q., 1998. Geochronology of the granite-greenstone terranes in the Murchison and Southern Cross Provinces of the Yilgarn Craton, Western Australia. PhD thesis, Australian National University, Canberra, Australia.
- Watkins, K.P. & Hickman, A.H., 1990. Geological evolution and mineralisation of the Murchison Province, Western Australia. Geological Survey of Western Australia, Bulletin 137, 287 pp.
- Wickham, D. 2014. Gold exploration in the Murchison Province, Western Australia with Minjar Gold. Unpublished BSc thesis, School of Earth & Ocean Sciences, Cardiff University, 69pp.
- Wilson, A. H. & Versfeld, J. A. 1994. The early Archaean Nondweni Greenstone Belt, southern Kaapvaal Craton, South Africa, Part II. Characteristics of the volcanic rocks and constraints on magma genesis. Precambrian Research, 67, p. 277–320.
- Zibra, I., Chen, S., Ivanic, T.J., Li, J., Gu, P., Meng, Y., Yu, J. & Wang, C., 2017. Thundelarra, WA Sheet 2340. Geological Survey of Western Australia, 1:100 000 Geological Series.
- Zibra, I., Ivanic, T.J., Chen, S., Clos, F., Li, J., Gu, P., Meng, Y., Yu, J. & Wang, C., 2016. Badja, WA Sheet 2240: Geological Survey of Western Australia, 1:100 000 Geological Series.
- Zibra, I., Peternell, M., Schiller, M., Wingate, M., Lu, Y.-J. & Clos, F., 2018. Tectono-magmatic evolution of the Neoarchean Yalgoo dome (Yilgarn Craton): Diapirism in a pre-orogenic setting. Geological Survey of Western Australia, Report 176, 43 pp.
- Zibra, I., Lu, Y., Clos, F., Weinberg, R.F., Peternell, M., Wingate, M.T.D., Prause, M., Schiller, M. & Tilhac, R., 2020. Regional-scale polydiapirism predating the Neoarchean Yilgarn Orogeny. Tectonophysics, 779, p. 1–26.

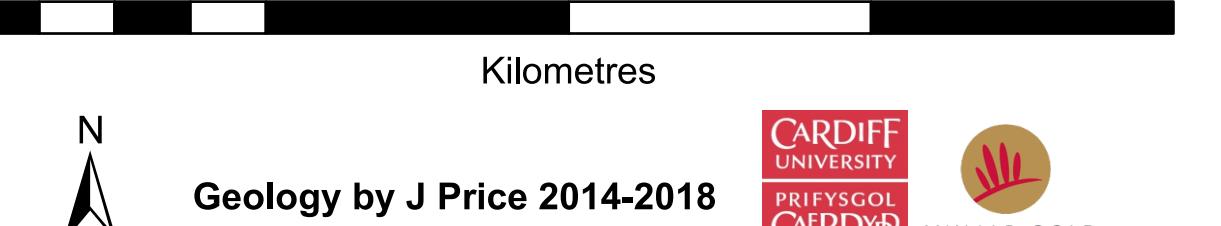


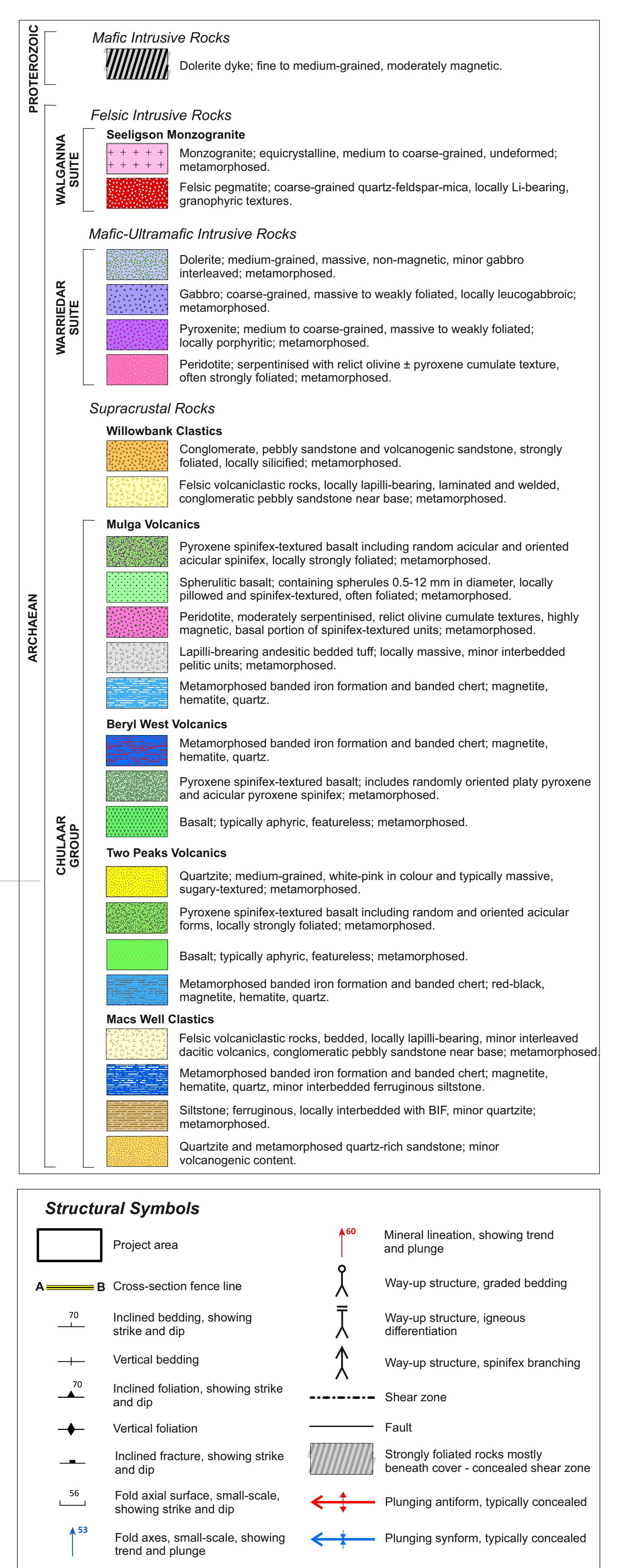
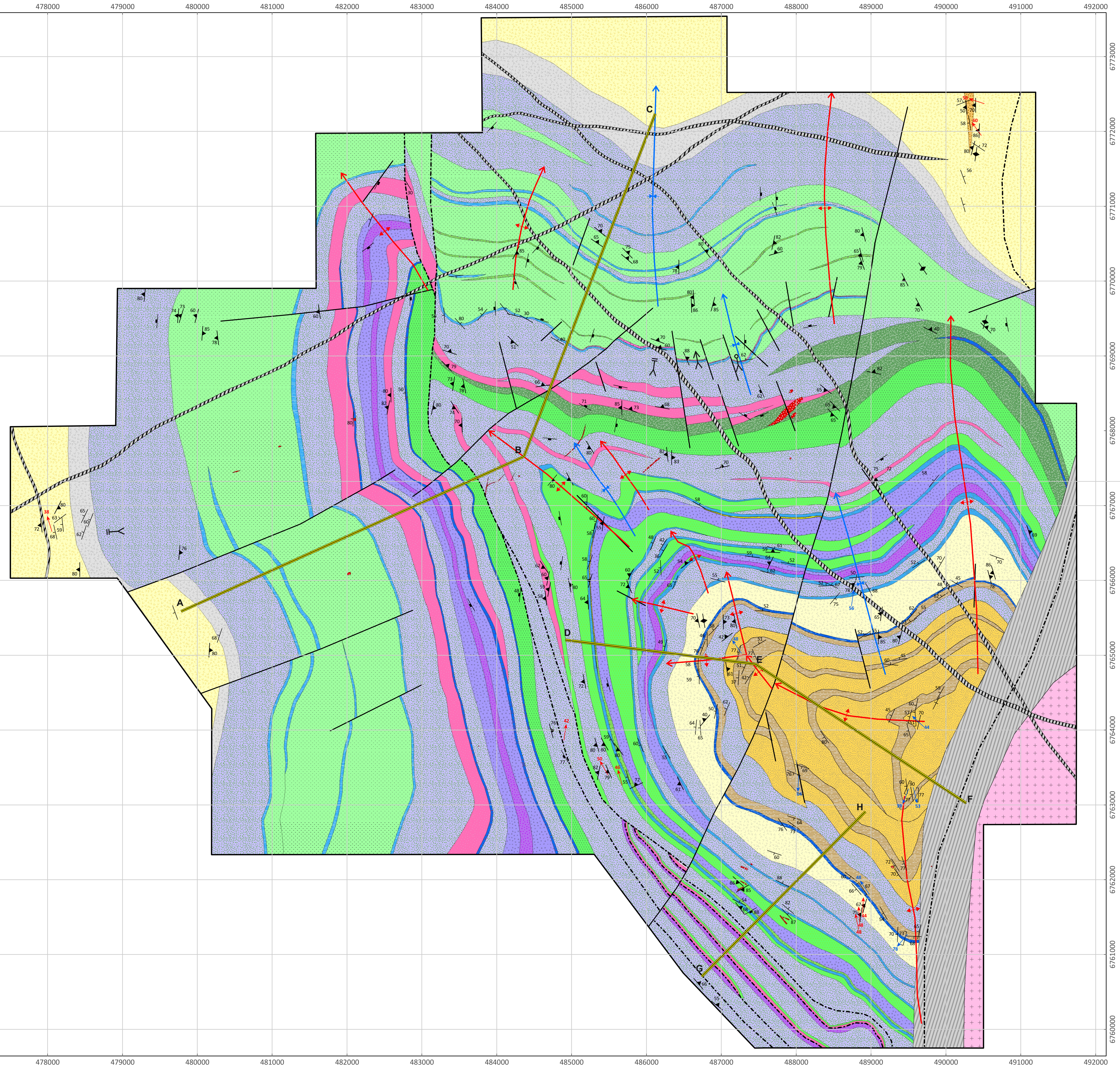
Surface Bedrock Geology of the Rothsay Mining Area, Western Australia

SCALE 1 : 25 000

CO-ORD: GDA_1994_MGA_Zone_50

0.5 1 2 3 4

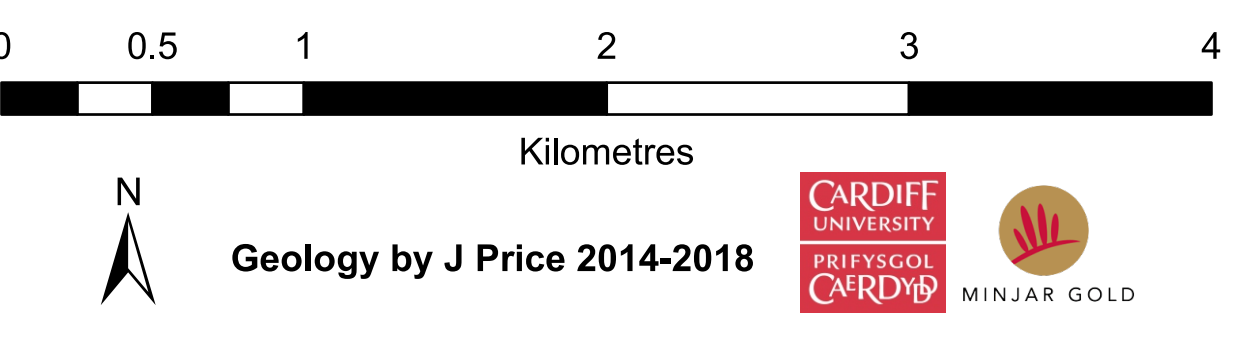




Interpreted Bedrock Geology of the Rothsay Mining Area, Western Australia

SCALE 1 : 25 000

CO-ORD: GDA_1994_MGA_Zone_50



STRATIGRAPHY, PETROGRAPHY AND STRUCTURE
OF ARCHAEN ROCKS IN THE ROTHsay MINING AREA,
WESTERN YILGARN CRATON

This Record is published in digital format (PDF) and is available as a free download from the DMIRS website at <www.dmirswa.gov.au/GSWApublications>.

Further details of geoscience products are available from:

Information Centre
Department of Mines, Industry Regulation and Safety
100 Plain Street
EAST PERTH WESTERN AUSTRALIA 6004
Phone: +61 8 9222 3459 Email: publications@dmirs.wa.gov.au
www.dmirswa.gov.au/GSWApublications

